



Horizontal vs. Vertical Connectivity in Caribbean Reef Corals: Identifying Potential Sources of Recruitment Following Disturbance

Serrano, Xaymara M

https://scholarship.miami.edu/discovery/delivery/01UOML_INST:ResearchRepository/12355363140002976?i#13355513830002976

Serrano, X. M. (2013). Horizontal vs. Vertical Connectivity in Caribbean Reef Corals: Identifying Potential Sources of Recruitment Following Disturbance [University of Miami].
https://scholarship.miami.edu/discovery/fulldisplay/alma991031447679902976/01UOML_INST:ResearchRepository

UNIVERSITY OF MIAMI

HORIZONTAL VS. VERTICAL CONNECTIVITY IN CARIBBEAN REEF CORALS:
IDENTIFYING POTENTIAL SOURCES OF RECRUITMENT FOLLOWING
DISTURBANCE

By

Xaymara M. Serrano

A DISSERTATION

Submitted to the Faculty
of the University of Miami
in partial fulfillment of the requirements for
the degree of Doctor of Philosophy

Coral Gables, Florida

December 2013

©2013
Xaymara M. Serrano
All Rights Reserved

UNIVERSITY OF MIAMI

A dissertation submitted in partial fulfillment of
the requirements for the degree of
Doctor of Philosophy

HORIZONTAL VS. VERTICAL CONNECTIVITY IN CARIBBEAN REEF CORALS:
IDENTIFYING POTENTIAL SOURCES OF RECRUITMENT FOLLOWING
DISTURBANCE

Xaymara M. Serrano

Approved:

Andrew C. Baker, Ph.D.
Associate Professor
Marine Biology and Fisheries

Diego Lirman, Ph.D.
Associate Professor
Marine Biology and Fisheries

Marjorie Oleksiak, Ph.D.
Assistant Professor
Marine Biology and Fisheries

Claire Paris-Limouzy, Ph.D.
Associate Professor
Applied Marine Physics

Margaret Miller, Ph.D.
Adjunct Professor
Marine Biology and Fisheries

M. Brian Blake, Ph.D.
Dean of the Graduate School

Iliana B. Baums, Ph.D.
Assistant Professor
Pennsylvania State University

SERRANO, XAYMARA M.

(Ph.D., Marine Biology and Fisheries)

Horizontal vs. Vertical Connectivity in Caribbean
Reef Corals: Identifying Potential Sources of
Recruitment Following Disturbance

(December 2013)

Abstract of a dissertation at the University of Miami.

Dissertation supervised by Professor Andrew C. Baker.

No. of pages in text. (153)

The extent to which reefs are effectively connected to one another, and their potential to serve as sources of larval replenishment following disturbance, are topics of considerable interest in contemporary reef science. To date, most assessments of reef connectivity have emphasized long-distance horizontal dispersal of propagules from one shallow reef to another. The extent of short-distance vertical connectivity, however, has been largely unquantified. To fill this gap in knowledge, I developed DNA microsatellite loci for two Caribbean depth-generalist coral species with different life-history reproductive strategies (*Montastraea cavernosa* and *Porites astreoides*), and assessed connectivity in >1,200 coral samples collected from 3 depth zones (≤ 10 m, 15-20 m and ≥ 25 m) at sites in Florida (within the Upper Keys, Lower Keys and Dry Tortugas), Bermuda and the U.S. Virgin Islands (USVI). I also tested whether depth zonation in algal symbionts (*Symbiodinium* spp.) could limit effective vertical connectivity (Chapters 2 and 3). Finally, in Chapter 4, I led a collaborative seascape genetics effort to examine coral connectivity between the Flower Garden Banks (FGB) and the Florida Reef Tract at different depth intervals. This is a timely and important investigation because the FGB

are located close to many oil and gas platforms in the Gulf of Mexico (GOM), including the Deepwater Horizon oil rig which exploded in 2010.

Overall, Chapters 2 and 3 revealed significant genetic differentiation by depth in Florida (but not in Bermuda or the USVI) for both species, despite high levels of horizontal connectivity between all three geographic locations (*M. cavernosa*), or between Florida and the USVI (*P. astreoides*) at shallow depths. However, at all sites, and regardless of the extent of vertical connectivity, migration always occurred asymmetrically, with greater downward migration from shallow to deep habitats. Finally, whether or not *M. cavernosa* or *P. astreoides* exhibited depth zonation in algal symbionts did not appear to limit effective connectivity. Together, these findings suggest that: (1) depth is an important population structuring factor for corals, (2) the extent of vertical connectivity varies among and within geographic locations, likely as a consequence of local hydrology, (3) reproductive mode does not necessarily correlate with realized dispersal ability, and (4) shallow reefs are more likely to rely on distant (unimpacted) shallow reefs, rather than nearby deep reefs, to provide a viable source of new recruits following disturbance.

Finally, Chapter 4 revealed high levels of gene flow between the FGB and the shallow Florida population of *M. cavernosa*, but not *P. astreoides*, suggesting limited gene flow among these regions. Results from biophysical modeling were in general agreement, suggesting that differences in reproductive mode and season might be important drivers of reef coral connectivity within the GOM region. Together, these findings suggest that FGB, despite its deep depth, might be an important larval source for shallow coral populations of broadcast spawning taxa in Florida. Furthermore, findings

suggest that an oil spill originating in the GOM: (1) has the potential to impact coral communities in Florida by reducing recruitment from the FGB, (2) is more likely to affect broadcast spawning taxa like *M. cavernosa*, due to high levels of gene flow between FGB and Florida, and (3) regardless of coral reproductive mode, these impacts are more likely to affect shallow habitats, likely sinks for coral larvae produced at FGB. While deep coral populations in Florida may constitute refugia due to their partial isolation from the shallow population (see Chapters 2 and 3), they too might eventually be impacted if shallow populations were slow, or unable to recover.

**To my family and husband,
with love**

ACKNOWLEDGEMENTS

This dissertation was completed thanks to the support, guidance and advice of many people inside and outside the University of Miami. First, I want to thank my advisor, Dr. Andrew Baker, for being a great mentor and friend, and for always encouraging me to do my best. This dissertation would not have been possible without his continuous support and guidance. To the rest of my committee: Iliana Baums, Margaret Miller, Claire Paris, Margie Oleksiak and Diego Lirman, thank you guiding my research in the right direction. Your insight and expertise greatly improved the completion of this degree. I truly hope we can keep collaborating in the future. Finally, I want to thank my two M.S. co-advisors, Drs. Joe Serafy and David Die, for the constant support, encouragement and guidance even during my doctoral degree. You have been a great part of my success in graduate school.

Numerous other people provided field and/or laboratory support. I want to thank M. Durante, N. Polato, D. Ruiz and C. Vera for help with the 454 sequencing data; K. O'Reilly, M. Moon and N. Kurata for volunteering their time in the laboratory to help me complete this dissertation; and to R. Gomez (RSMAS DSO), T. Thyberg, S. Manley, H. Wirshing, R. Cunning, P. Jones, S. Grey, T. Smith, J. Calnan and the crew at BIOS (R. Jones, C. Eddy, T. Noyes and A. Chequer) for helping collect samples. Sampling in the Lower Keys and Dry Tortugas would not have been possible without the amazing help of International SeaKeepers Society: D. Klevan, B. Stockman, J. Jacoby and the crew of Miss Phebe II. Samples from the Florida Keys were collected under research permits FKNMS-2010-030A1, FKNMS-2011-087, SAL-11-1182-SRP, and DRTO-2012-SCI-0009. Samples from the USVI were collected under permits F/SER28:BT and STT-021-

10, and samples from Bermuda were collected and exported under permits SP09060 and CITES 09BM0021.

I also want to thank D. Holstein and C. Paris for providing the modeling data used in Chapter 4; M. Estevanez and A. Palacio for help with the GIS maps; D. Swanson for providing coral cover data used to target our sampling efforts; F. Nunes, T. Shearer and G. Goodbody-Gringley for providing a subset of the samples used in Chapters 2-4; C. Kenkel and the Matz laboratory (UC Austin) for providing primers used in Chapter 3; P. Beerli for statistical assistance with the program MIGRATE; and PSU's Genomics Core Facility, UM's Molecular Core Facility and Cornell's Life Sciences Core Laboratories Center for the genotyping and sequencing. This research was supported with funds from MOTE (Protect Our Reefs grants 2009-2012) and NOAA's Center for Sponsored Coastal Ocean Research under award NA11NOS4780045 to the University of Miami. X. Serrano was supported by a McKnight Doctoral Fellowship, a fellowship from NOAA's Living Marine Resource Science Center, a BIOS Grant in Aid (2009), a RSMAS Alumni Award and small boat funding from RSMAS.

Finally, I want to thank "CR2" laboratory members H. Wirshing, R. Boonstra, A. Correa, P. Jones, R. Silverstein, R. Cuning, R. Winter, A. Palacio and P. Kushlan. Thank you for making the laboratory a very special place to be. To many other special friends made at RSMAS over the years, thank you for making my life so much sweeter. You know who you are. To my family, thank you for always believing in me and never letting me give up. This dissertation is dedicated to you. And to my loving husband, Alexis Torres, there are no words to describe how grateful I am to have you in my life. I really don't think I would have come this far without your support. You are my soulmate.

TABLE OF CONTENTS

	Page
LIST OF TABLES	vii
LIST OF FIGURES	x
 Chapter	
1 GENERAL INTRODUCTION	1
2 LOW VERTICAL CONNECTIVITY IN THE BROADCAST SPAWNING CORAL <i>MONTASTRAEA CAVERNOSA</i> SUGGESTS LIMITED “SEED BANK” POTENTIAL FOR CARIBBEAN DEEP REEFS	8
3 LONG-DISTANCE DISPERSAL AND VERTICAL GENE FLOW IN THE CARIBBEAN CORAL <i>PORITES ASTREOIDES</i> DESPITE BROODING REPRODUCTIVE MODE AND DEPTH ZONATION IN ALGAL SYMBIONTS	39
4 SEASCAPE GENETICS REVEALS DEPTH-RELATED PATTERNS OF REEF CORAL CONNECTIVITY BETWEEN THE FLOWER GARDEN BANKS (GULF OF MEXICO) AND THE FLORIDA REEF TRACT	72
5 SUMMARY, IMPLICATIONS AND RECOMMENDATIONS	116
LITERATURE CITED	126
APPENDICES	137

LIST OF TABLES

Table 2.1.	Nine microsatellite loci developed for <i>Montastraea cavernosa</i> , amplified in four multiplexes (plex A-D) and one singleplex reaction. Given are the locus name, primer sequences, motif type, and the size range of the alleles amplified in base pairs (bp). Locus-specific primer concentrations are also given. All reactions had the same annealing temperature (57°C). Forward primers were fluorescently labeled with one of three dyes (6FAM, VIC or NED).....29
Table 2.2.	<i>Montastraea cavernosa</i> samples (N= 583). Given are total sample size (N), number of unique multi-locus genotypes (Ng) and ratio of genets over samples collected (Ng/N). GPS locations are in decimal degrees (WGS84)..... 30
Table 2.3.	<i>Montastraea cavernosa</i> pairwise F_{ST} values for each population. Statistically significant values ($p < 0.05$) after FDR correction are highlighted in bold.....32
Table 2.4.	<i>Montastraea cavernosa</i> (A) Comparison of log Bayes factors (marginal log-likelihood differences, LBF) approximated by thermodynamic integration for four different gene flow models (A= full, B= shallow to mid/deep, C= mid/deep to shallow and D= panmixia). (B) Estimated mutation-scaled population sizes (θ), mutation-scaled migration rates (M) and number of migrants per generation ($Nm = \theta * M / 4$) between source and receiving populations for model best supported (B= shallow to mid/deep). Numbers in parenthesis indicate the 95% confidence interval (CI) for parameters θ and M.....33
Table 3.1.	Microsatellite loci for <i>Porites astreoides</i> . Given are the locus name, primer sequences, repeat type followed by the number of repeats and the size range of the alleles amplified in base pairs (bp). All reactions had the same annealing temperature (57°C). Forward primers were fluorescently labeled with one of three dyes (6FAM, VIC or NED). Loci were amplified in two multiplex reactions (plex A and B) or as described in Kenkel et al. (2013).....60
Table 3.2.	<i>Porites astreoides</i> samples (N= 660). Given are total sample size (N), number of unique multi-locus genotypes (Ng) and ratio of genets over samples collected (Ng/N). GPS locations are in decimal degrees (WGS84).....61
Table 3.3.	<i>Porites astreoides</i> pairwise F_{ST} values for each population. Statistically significant values ($p < 0.05$) after FDR correction are highlighted in bold.....63

Table 3.4.	<p><i>Porites astreoides</i> (A) Comparison of log Bayes factors (marginal log-likelihood differences, LBF) approximated by thermodynamic integration for four different gene flow models (A= full, B= shallow to mid/deep, C= mid/deep to shallow and D= panmixia) in the Upper Keys, Lower Keys, Bermuda and the U.S. Virgin Islands. In the case of Dry Tortugas, we compared the following four different gene flow models: (A= full, B= shallow/mid to deep, C= deep to shallow/mid and D= panmixia). (B) Estimated mutation-scaled population sizes (θ), mutation-scaled migration rates (M) and number of migrants per generation ($Nm = \theta * M / 4$) between source and receiving populations for model best supported (B = shallow to mid/deep). Numbers in parenthesis indicate the 95% CI for parameters θ and M.....64</p>
Table 4.1.	<p><i>Montastraea cavernosa</i> (n = 363) and <i>Porites astreoides</i> (n = 484) sampling locations. Given per species are total sample size (N), the number of unique multi-locus genotypes (Ng) and the ratio of genets over samples collected (Ng/N). GPS locations are in decimal degrees (WGS84).....91</p>
Table 4.2.	<p>Pairwise F_{ST} values for each <i>Montastraea cavernosa</i> (upper table) and <i>Porites astreoides</i> (lower table) population. Statistically significant values ($p < 0.05$) are highlighted in bold.....93</p>
Table 4.3.	<p>Average membership probability for each <i>Montastraea cavernosa</i> cluster (A) and potential migrants with inferred ancestry (B), regarded as an individual being an immigrant itself or as having a parent or grandparent from that population. Individuals were assigned to the cluster (1= shallow or 2= deep) with the highest probability of assignment in a previous STRUCTURE run (Figure 4.1A). Potential migrants were identified as having a ≥ 0.1 probability of being or having an ancestor from another population.....94</p>
Table 4.4.	<p>Average membership probability for each <i>Porites astreoides</i> cluster (A) and potential migrants with inferred ancestry (B), regarded as an individual being an immigrant itself or as having a parent or grandparent from that population. Individuals were assigned to the cluster (1= shallow, 2= deep and 3= FGB) with the highest probability of assignment in a previous STRUCTURE run (Figure 4.1B). Potential migrants were identified as having a ≥ 0.1 probability of being or having an ancestor from another population. There are no potential migrants in cluster 3 (FGB).....96</p>
Table 4.5.	<p>Direction of gene flow and number of migrants per generation for <i>Montastraea cavernosa</i> and <i>Porites astreoides</i>. (A) Comparison of log Bayes factors (marginal log-likelihood differences, LBF) approximated by</p>

thermodynamic integration for three different gene flow models (*M. cavernosa*: A= FGB to shallow, B= FGB to mid/deep and C= panmixia; *P. astreoides*: A= FGB to shallow, B= FGB to mid/deep and C= panmixia in the Upper Keys and Lower Keys and A= FGB to shallow/mid, B= FGB to deep and C= panmixia in the Dry Tortugas). (B) Estimated mutation-scaled population sizes (θ) between source and receiving populations for model best supported (C). Numbers in parenthesis indicate the 95% CI for parameter θ97

LIST OF FIGURES

Figure 2.1.	Sampling locations in the Caribbean and western Atlantic. Individual sites are labeled as designated in Table 2.2. White circles denote shallow (≤ 10 m) sites, gray circles denote intermediate (15-20 m) sites, and black circles denote deep (≥ 25 m) sites.....34
Figure 2.2.	<i>Montastraea cavernosa</i> population structure across regions [Upper Keys, Lower Keys and Dry Tortugas (within Florida), Bermuda and the U.S. Virgin Islands] and depths [shallow (≤ 10 m), mid (15-20 m) and deep (≥ 25 m)]. Bar graphs show the average probability of membership (y-axis) of individuals (n= 577, x-axis) in K= 2 clusters as identified by STRUCTURE. Samples were arranged in order of increasing depth within region.....35
Figure 2.3.	Mean log-likelihood LN of (A) K (hypothesized number of populations) and delta K (B) values for STRUCTURE analysis of <i>Montastraea cavernosa</i> samples. Values of K= 1 – 20 were tested by running 3 replicate simulations for each K (error bars in upper figure indicate variance among replicates).....36
Figure 2.4.	Principal Component Analysis (PCA) of allele frequency covariance in <i>Montastraea cavernosa</i> Florida populations. 8 of 163 axes were retained, explaining 100% of the cumulative variance. Plotted are the first and second axes explaining 50.29% (p < 0.01) and 13.07% (p > 0.05) of the variance, respectively. Axes cross at 0. The different shapes denote each of the 3 regions sampled in this study (Upper Keys, Lower Keys and Dry Tortugas), whereas the different colors denote each of the 3 depths under comparison [shallow (≤ 10 m), mid (15-20 m) and deep (≥ 25 m)]......37
Figure 2.5.	<i>Symbiodinium</i> types detected in a subset of <i>Montastraea cavernosa</i> samples from each depth and geographic location, using either Denaturing Gradient Gel Electrophoresis (upper column per depth category) or quantitative PCR (lower column per depth category). The numbers of individual coral colonies sampled for each depth are indicated. Colonies hosting mixed symbiont communities (i.e., more than 1 type) were partitioned into each appropriate category.....38
Figure 3.1.	Sampling locations in the Caribbean and western Atlantic. Individual sites are labeled as designated in Table 3.2. White circles denote shallow (≤ 10 m) sites, gray circles denote intermediate (15-20 m) sites, and black circles denote deep (≥ 25 m) sites.....65
Figure 3.2.	<i>Porites astreoides</i> population structure across regions [Upper Keys, Lower Keys and Dry Tortugas (within Florida), Bermuda and the U.S. Virgin

- Islands] and depths [shallow (≤ 10 m), mid (15-20 m) and deep (≥ 25 m)]. Bar graphs show the average probability of membership (y-axis) of individuals ($n = 590$, x-axis) in $K = 3$ clusters as identified by STRUCTURE. Samples were arranged in order of increasing depth within region.....66
- Figure 3.3. Mean log-likelihood of K (A) and Delta K (B) values for STRUCTURE analysis of *Porites astreoides* samples. Values of $K = 1 - 20$ were tested by running 3 replicate simulations for each K (error bars in upper figure indicate variance among replicates).....67
- Figure 3.4. Principal Component Analysis (PCA) of allele frequency covariance in *Porites astreoides* populations. 14 of 79 axes were retained, explaining 100% of the cumulative variance. Plotted are the first and second axes explaining 38.59% ($p < 0.01$) and 21.28% ($p < 0.05$) of the variance, respectively. Axes cross at 0. The different shapes denote each of the 3 geographic locations sampled in this study (Florida, Bermuda and U.S. Virgin Islands), whereas different colors denote each of the 3 depths under comparison [shallow (≤ 10 m), mid (15-20 m) and deep (≥ 25 m)].68
- Figure 3.5. Isolation-by-distance patterns in *Porites astreoides*. Geographic distance explained 17% of the variation in genetic distance (F_{ST}) when all sites with ≥ 10 individuals were included (A), 39% when the U.S. Virgin Islands sites were excluded (B), and none when Bermuda sites were excluded (C).....69
- Figure 3.6. *Symbiodinium* types detected in a subset of *Porites astreoides* corals from shallow (≤ 10 m), intermediate (15-20 m) or deep (≥ 25 m) depths, using denaturing gradient gel electrophoresis (A) versus high-sensitivity quantitative PCR (B, C). In (C), migrants were identified in STRUCTURE as having a probability of membership >0.70 to the deep cluster (shallow migrants), or as having a probability of membership >0.70 to the shallow cluster (deep migrants). Note that there are no deep migrants in shallow habitats in the U.S. Virgin Islands. Numbers in parenthesis indicate number of colonies assessed.....70
- Figure 4.1. *Montastraea cavernosa* (A) and *Porites astreoides* (B) population structure across regions (Flower Garden Banks, Dry Tortugas, Lower Keys and Upper Keys) and depths [shallow (≤ 10 m), mid (15-20 m) and deep (≥ 25 m)]. Bar graphs show the average probability of membership (y-axis) of individuals (x-axis) in $K = 2$ (*M. cavernosa*) and $K = 3$ (*P. astreoides*) clusters as identified by STRUCTURE. Within regions, samples were arranged in order of increasing depth.....98

Figure 4.2.	Principal Component Analysis (PCA) of allele frequency covariance in <i>Montastraea cavernosa</i> (A) and <i>Porites astreoides</i> (B) populations. For <i>M. cavernosa</i> , 9 of 163 axes were retained, explaining 100% of the cumulative variance. Plotted are the first and second axes explaining 42.36% ($P < 0.01$) and 15.76% ($P > 0.05$) of the variance, respectively. For <i>P. astreoides</i> , 9 of 72 axes were retained, explaining 100% of the cumulative variance. Plotted are the first and second axes explaining 35.50% ($P < 0.05$) and 26.35% ($P < 0.01$) of the variance, respectively. Axes cross at 0. The different shapes denote each of the 4 regions sampled in this study (Upper Keys, Lower Keys, Dry Tortugas and Flower Garden Banks), whereas the different colors denote each of the 3 depths under comparison [shallow (≤ 10 m), mid (15-20 m) and deep (≥ 25 m in Florida or 20-30 in Flower Garden Banks)]......99
Figure 4.3.	<i>Montastraea cavernosa</i> backtracking (depicted in blue) from the Upper Keys (A), Lower Keys (B) or Dry Tortugas (C) at shallow sites, and forward tracking (depicted in red) from Flower Garden Banks sites. Green areas show the overlap of backtracking and forward tracking. Sites are listed in Table 4.1.....100
Figure 4.4.	<i>Porites astreoides</i> backtracking (depicted in blue) from the Upper Keys (A), Lower Keys (B), or Dry Tortugas (C) at shallow sites, and forward tracking (depicted in red) from Flower Garden Banks sites. Sites are listed in Table 4.1.....101
Figure 4.5.	<i>Montastraea cavernosa</i> backtracking from shallow sites (≤ 10 m) in the Upper Keys. Sites are listed in Table 4.1. Colors represent the probability density function of particles after 30 days of release for five different depth layers (10, 20, 30, 40 and 50 m).....102
Figure 4.6.	<i>Montastraea cavernosa</i> backtracking from intermediate (15-20 m) and deep sites (≥ 25 m) in the Upper Keys. Sites are listed in Table 4.1. Colors represent the probability density function of particles after 30 days of release for five different depth layers (10, 20, 30, 40 and 50 m).....103
Figure 4.7.	<i>Montastraea cavernosa</i> backtracking from shallow sites (≤ 10 m) in the Lower Keys. Sites are listed in Table 4.1. Colors represent the probability density function of particles after 30 days of release for five different depth layers (10, 20, 30, 40 and 50 m).....104
Figure 4.8.	<i>Montastraea cavernosa</i> backtracking from intermediate (15-20 m) and deep sites (≥ 25 m) in the Lower Keys. Sites are listed in Table 4.1. Colors represent the probability density function of particles after 30 days of release for five different depth layers (10, 20, 30, 40 and 50 m).....105

Figure 4.9.	<i>Montastraea cavernosa</i> backtracking from shallow sites (≤ 10 m) in the Dry Tortugas. Sites are listed in Table 4.1. Colors represent the probability density function of particles after 30 days of release for five different depth layers (10, 20, 30, 40 and 50 m).....	106
Figure 4.10.	<i>Montastraea cavernosa</i> backtracking from intermediate (15-20 m) and deep sites (≥ 25 m) in the Dry Tortugas. Sites are listed in Table 4.1. Colors represent the probability density function of particles after 30 days of release for five different depth layers (10, 20, 30, 40 and 50 m).....	107
Figure 4.11.	<i>Montastraea cavernosa</i> forward tracking from intermediate/deep sites (20-30 m) in the Flower Garden Banks. Sites are listed in Table 4.1. Colors represent the probability density function of particles after 30 days of release for five different depth layers (10, 20, 30, 40 and 50 m).....	108
Figure 4.12.	<i>Porites astreoides</i> backtracking from shallow sites (≤ 10 m) in the Upper Keys. Sites are listed in Table 4.1. Colors represent the probability density function of particles after 10 days of release for five different depth layers (10, 20, 30, 40 and 50 m).....	109
Figure 4.13.	<i>Porites astreoides</i> backtracking from intermediate (15-20 m) and deep sites (≥ 25 m) in the Upper Keys. Sites are listed in Table 4.1. Colors represent the probability density function of particles after 10 days of release for five different depth layers (10, 20, 30, 40 and 50 m).....	110
Figure 4.14.	<i>Porites astreoides</i> backtracking from shallow sites (≤ 10 m) in the Lower Keys. Sites are listed in Table 4.1. Colors represent the probability density function of particles after 10 days of release for five different depth layers (10, 20, 30, 40 and 50 m).....	111
Figure 4.15.	<i>Porites astreoides</i> backtracking from intermediate (15-20 m) and deep sites (≥ 25 m) in the Lower Keys. Sites are listed in Table 4.1. Colors represent the probability density function of particles after 10 days of release for five different depth layers (10, 20, 30, 40 and 50 m).....	112
Figure 4.16.	<i>Porites astreoides</i> backtracking from shallow sites (≤ 10 m) in the Dry Tortugas. Sites are listed in Table 4.1. Colors represent the probability density function of particles after 10 days of release for five different depth layers (10, 20, 30, 40 and 50 m).....	113
Figure 4.17.	<i>Porites astreoides</i> backtracking from intermediate (15-20 m) and deep sites (≥ 25 m) in the Dry Tortugas. Sites are listed in Table 4.1. Colors represent the probability density function of particles after 10 days of release for five different depth layers (10, 20, 30, 40 and 50 m).....	114

Figure 4.18. *Porites astreoides* forward tracking from intermediate/deep sites (23-25 m) in the Flower Garden Banks. Sites are listed in Table 4.1. Colors represent the probability density function of particles after 10 days of release for five different depth layers (10, 20, 30, 40 and 50 m).....115

CHAPTER 1

General introduction

Problem statement

The decline of coral reefs in the Caribbean has been well documented (e.g., Gardner et al. 2003). Multiple bleaching episodes over the past 15 years, a recent severe bleaching episode in Florida and the U.S. Caribbean (2005), and the projected future impacts of climate change on shallow reefs worldwide (Hughes et al. 2003, Hoegh-Guldberg et al. 2007) pose serious problems for a long-term management strategy. Current thinking (Marshall and Schuttenberg, 2006) emphasizes maximizing ecosystem resilience, the ability of reefs to return to their previous state of diversity and abundance following disturbance, as a critical management goal. For corals, resilience depends on the ability of individual colonies to recover from disturbances such as bleaching, as well as colonize disturbed areas that experience mortality (Nystrom and Folke, 2001). Successful recruitment of corals to impacted areas relies on a reliable supply of coral larvae from a relatively unimpacted area. For these processes to maintain ecosystem function despite temporary loss of coral, they must operate over ecologically significant timescales. However, in an era of climate change, there is considerable doubt as to how much reef-to-reef connectivity will exist if shallow reefs are being impacted over regional scales by episodes of high-temperature bleaching. Since connectivity tends to decrease with distance (the “isolation by distance” theory of island biogeography), recruitment to reefs may be very low if large geographic areas are affected and the distance between source and sink effectively increases.

Understanding patterns of coral connectivity, sources of recruitment, and recovery timelines, are critical needs for managers who are increasingly operating under the implicit assumption that climate change and other impacts to reefs are unlikely to improve in the short term. Consequently, a need is emerging for an ecosystem-based management approach that prioritizes the conservation of reef resources of maximum importance (West and Salm, 2003). In this context, deep and mesophotic coral ecosystems (≥ 30 m) have been under-investigated. Logistical difficulties and safety issues related to working at or below the depth limits of SCUBA have left these ecosystems poorly understood, despite their close proximity to well-studied shallow reefs (Menza et al. 2008; Kahng et al. 2010). However, recent advances in technical diving methods and other instrumentation (e.g., mapping) are providing easier access to these coral ecosystems (Hinderstein et al 2010), resulting in an increased scientific and management interest (e.g., 2010 Coral Reefs issue dedicated to mesophotic reefs, and launch of website www.mesophotic.org).

Larval dispersal and marine connectivity

The degree to which marine populations are connected has important consequences for how coral reef populations persist, how they respond to stressors and how they can be managed (Sale et al. 2005; Jones et al. 2007). The scale of population connectivity also helps managers and policymakers determine the optimal size and spacing of Marine Protected Areas (MPAs). While genetic exchange over large spatial scales might allow distant populations to rescue impacted reefs, restricted gene flow indicates that populations rely on local recruitment and thus local management is needed (Hemond and Vollmer, 2010). Furthermore, high connectivity among populations is

assumed to confer resilience against perturbations, while habitat fragmentation can threaten populations with extinction (Hughes et al. 2005; Jones et al. 2009).

The degree of connectivity among marine populations highly depends on the scale of larval dispersal, which varies greatly among marine organisms. Some larvae may disperse just a few meters from where they were spawned, while others may disperse ten to hundreds of km to distant reefs (Gaines et al. 2007). Some of the factors known to influence the scale of dispersal include the pelagic larval duration, larval behavior and the number of larvae that survive to settlement (reviewed in Cowen and Sponaugle, 2009). Corals exhibit a variety of reproductive strategies that may also affect the potential for dispersal (Magalon et al. 2005). The general expectation is that coral brooding species will exhibit limited dispersal capabilities compared to broadcast spawning species, presumably due to shorter larval pre-competency periods. The main limitation for studies of larval dispersal, however, is that small propagule size and potentially lengthy planktonic dispersal phases limit the ability to directly measure larval dispersal distance. Therefore, the understanding of “connectivity” relies heavily (but not exclusively, e.g., Cowen et al. 2006) on estimates of gene flow as proxies for organismal dispersal (Miller and Howard, 2004).

The study of marine connectivity via larval dispersal is also complicated by surface current patterns (e.g., Paris et al. 2007). The use of coupled biophysical modeling has thus been a major topic of interest in recent years, in an attempt to further understand the degree of connectivity between marine populations (reviewed by Werner et al. 2007). Biophysical models can directly calculate dispersal matrices and assess their dependence on circulation patterns and larval behavior (Botsford et al. 2009). However, models need

to be validated with empirical methods in order to test predictions, and to better parameterize and strengthen the model capabilities. For example, the multidisciplinary field of “seascape genetics”, or the combination of genetic approaches with other tools to test hypotheses of marine connectivity, has already begun to reveal important insights and has helped guide new approaches in management (Selkoe et al. 2008).

Tools for assessing genetic variation in corals

Until recently, the understanding of the evolution and population ecology of scleractinian corals had been greatly limited by the scarcity of suitable population genetic makers capable of detecting genetic differentiation (van Oppen et al. 2000; Baums et al. 2005a). For corals, slow evolutionary rates for mitochondrial DNA left allozymes as the only markers available to investigate patterns of coral genetic variation (Shearer and Coffroth, 2004). However, microsatellite-based analyses have been shown to be more powerful than those based on allozymes (Waser and Strobeck, 1998), as they can sample a larger portion of the total genomic variation with relatively lower costs, and are more practical and useful due to their high degree of polymorphism (Baums et al. 2005a). Furthermore, microsatellites are particularly useful for genotyping reproductively complex organisms such as corals because unique genets can be usually identified with a high degree of accuracy and precision (Severance and Karl, 2006).

Developing microsatellites for coral species with algal symbionts can be particularly difficult, as DNA extraction protocols typically extract both host and symbiont DNA. Therefore, caution must be used to ensure that markers developed are host-specific (Shearer et al. 2005). Unless the DNA template is from asymbiotic tissue (not possible for brooders, which acquire symbionts directly from the parent colony),

steps should be taken to: (1) minimize the contamination of symbiont DNA in the template; and (2) verify that the molecular markers developed are derived from the coral host and not its algal symbionts. Otherwise, including markers from the algal symbionts in analyses for corals can lead to inappropriate conclusions, as biogeographic patterns do not necessarily correlate for both organisms (Shearer et al. 2005).

In this study, “next generation” 454 DNA sequencing was used to more effectively develop microsatellite loci for the two focal species, *Montastraea cavernosa* and *Porites astreoides*. Some of the advantages of this technique is that it provides thousands of DNA sequence reads within one 4-hour run, increasing throughput and speed and significantly reducing the overall costs compared to traditional sequencing methods (Margulies et al. 2005; Wheat, 2008), while still maintaining a very high level of accuracy (> 99%). Furthermore, with a greater depth and coverage, 454 sequencing has been shown to outperform traditional methods in molecular marker identification (Wheat, 2008; Vera et al. 2008).

Coral-algal symbiosis and depth zonation in algal symbionts

Scleractinian corals depend critically on a mutualistic association with dinoflagellate endosymbiotic algae (*Symbiodinium* spp.) for metabolism, calcification and growth (e.g., Muscatine, 1990). *Symbiodinium* spp. are genetically diverse, consisting of at least 9 phylogenetically distinct clades (A-I; Pochon and Gates, 2010). Coral-algal symbioses thus exhibit significant diversity in their *Symbiodinium*, and many coral species examined to date have been found to associate with more than one symbiont type, sometimes within the same coral colony (e.g., Rowan and Knowlton, 1995, Baker and Romanski, 2007; Silverstein et al. 2012). In some cases, the limits of vertical distribution

of coral species have been correlated with the photophysiological capacity of the symbionts hosted (Iglesias-Prieto et al. 2004). For example, it has been suggested that corals that host only one type of symbiont will have limited vertical distribution patterns as a result of the photophysiological constraints of its symbionts (Rowan and Knowlton, 1995, Iglesias-Prieto et al. 2004). Alternatively, corals that host more than one symbiont type can potentially extend their depth range by hosting symbionts adapted to different light regimes (e.g., Iglesias-Prieto et al. 2004; Sampayo et al. 2007; Frade et al. 2008).

Overall, the coral-symbiont interaction implies that studies of larval dispersal and connectivity in corals need to be supplemented by investigations of symbiont dispersal (Baums, 2008), because processes of symbiont transfer may impose limitations on the colonization and post-settlement survival of coral offspring (Bongaerts et al. 2010). For example, brooding coral species may be limited in their ability to settle outside the direct parental range if depth-specific symbionts are transferred to the offspring. On the other hand, such limitations are not expected for broadcasting corals, since they acquire algal symbionts from the water column. To date, the vast majority of depth-generalist Caribbean coral species studied have been found to exhibit marked zonation of *Symbiodinium* over depth (Bongaerts et al. 2010). Intraspecific variation also tends to be greatest in shallower reefs (1-8 m), where some species have been shown to host up to five distinctive symbionts (e.g., *Montastraea faveolata*; Warner et al. 2006). Conversely, at deeper depths (15-25 m), variation from colony to colony tends to decrease significantly, as one algal type tends to be associated with most or all the colonies (Warner et al. 2006). However, to date, *Symbiodinium* communities hosted by depth-generalists on deep reefs (≥ 30 m) have been relatively understudied (Bak et al. 2005).

Research overview

To date, most assessments of reef connectivity have emphasized long-distance horizontal dispersal of propagules from one shallow reef to another. The extent of short-distance vertical connectivity, however, has been largely unquantified. This dissertation used a multidisciplinary approach to investigate, for the first time, the connectivity of Caribbean reef coral populations at both horizontal (long-distance dispersal) and vertical (depth) scales. A combination of published and newly-developed DNA microsatellite loci were applied to >1,200 colonies of two important depth-generalist coral species with different life-history reproductive strategies (*Montastraea cavernosa* and *Porites astreoides*), to estimate gene flow in these species between different depths (≤ 10 m, 15-20 m and ≥ 25 m) and localities [Upper Keys, Lower Keys and Dry Tortugas (within Florida), Bermuda, and the U.S. Virgin Islands]. Algal symbiont (*Symbiodinium* spp.) diversity was also assessed in a subset of corals to determine the functional potential to colonize shallow vs. deep environments, determine patterns of depth zonation (if any), and assess the extent to which these corals might respond to ongoing climate change by hosting heat-tolerant symbionts (Chapters 2 and 3). Finally, genetic results were coupled with biophysical modeling (Chapter 4) to assess connectivity between the Flower Garden Banks (Gulf of Mexico) and the Florida Reef Tract, and determine whether the Flower Garden Banks might act as an important larval source for Florida's shallow vs. deep coral populations. Overall, this study has potential relevance for a variety of coral reef conservation applications, will contribute to inform a management strategy to help protect critical reef resources and also aid in ecologically effective sizing and placement of MPAs.

CHAPTER 2

Low vertical connectivity in the broadcast spawning coral *Montastraea cavernosa* suggests limited “seed bank” potential for Caribbean deep reefs

SUMMARY

The The Deep Reef Refugia Hypothesis suggests that deep reefs can act as local recruitment sources for shallow reefs following disturbance. To test this hypothesis, nine polymorphic DNA microsatellite loci were developed for the Caribbean depth-generalist coral *Montastraea cavernosa*. Vertical connectivity was assessed in ~600 coral colonies collected from 3 depth zones (≤ 10 m, 15-20 m and ≥ 25 m) at sites in Florida (Upper Keys, Lower Keys and Dry Tortugas), Bermuda, and the U.S. Virgin Islands. Migration rates were estimated to determine the probability of coral larval migration from shallow to deep, deep to shallow, or in both directions symmetrically. Algal symbiont (*Symbiodinium* spp.) diversity and distribution was also assessed to test whether symbiont depth zonation might limit vertical connectivity. Contrary to expectations, analyses revealed significant genetic differentiation by depth in Florida (but not in Bermuda or the U.S. Virgin Islands), despite high levels of horizontal connectivity between all three of these geographic locations at shallow depths. Within Florida, greater vertical connectivity was observed in the Dry Tortugas compared to the Lower or Upper Keys. At all sites, and regardless of the extent of vertical connectivity, migration always occurred asymmetrically, with greater downward migration from shallow to intermediate/deep habitats. Finally, most colonies hosted a single *Symbiodinium* type (C3), excluding symbiont availability as a structuring factor. Together, these findings suggest that the

potential for shallow reefs to recover from deep water refugia is generally limited, but varies among geographic locations likely as a consequence of local hydrology.

BACKGROUND

The most devastating impacts of climate change on coral reef ecosystems have occurred at shallow depths (e.g., Glynn et al. 2001; West and Salm, 2003; Bak et al. 2005), where the interacting stress of high light and high temperature has resulted in the most severe episodes of mass coral “bleaching” (loss of symbionts from corals and other reef invertebrates) and mortality. Recent evidence has suggested that deep reefs and light-dependent mesophotic coral ecosystems (MCEs) that form at depths between 30-150 m have fared better than their shallow water counterparts, due to lower heat-induced photoinhibition in these low light environments (Glynn, 1996; Glynn et al. 2001; Baker et al. 2008; van Oppen et al. 2011; Smith et al., unpublished data), less severe storm impacts, and reduced loss of major herbivores (Bongaerts et al. 2010; van Oppen et al. 2011), as well as diseases (Bongaerts et al. 2010). These observations support the Deep Reef Refugia Hypothesis (Bongaerts et al. 2010) that deep reefs and MCEs may serve as refugia for shallow reefs, but whether they can provide a viable larval supply for shallow reefs following disturbance has not yet been established.

One way to determine the capacity of deep coral populations to replenish shallow reefs following disturbance is to measure the extent and direction of gene flow among these habitats. The brooding coral *Seriatopora hystrix* (Dana, 1846) exhibits different patterns of vertical connectivity depending on location: at Scott Reef (northwest Australia), recruitment of deep water larvae into shallow habitats was inferred from

cluster-based analyses, but migration rates and direction of gene flow (shallow to deep vs. deep to shallow) were not assessed (van Oppen et al. 2011). Conversely, at Yonge Reef (northeast Australia) there was little connectivity among these habitats, which was later suggested to be the result of strong selective pressures along the depth gradient (Bongaerts et al. 2011a). Prada and Hellberg (2013) measured survivorship in reciprocally transplanted colonies of the Caribbean octocoral *Eunicea flexuosa* (Lamouroux, 1821) and showed that native colonies (i.e., colonies transplanted to the same depth of origin) had a selective advantage over non-native colonies that originated from a different depth. In addition, genetic differentiation supported the presence of two depth-segregated lineages, providing the first evidence of higher migration rates from shallow to deep habitats for a coral species. Together, these studies suggest that genetic structure with depth originates from local adaptation of corals to the different environmental conditions in shallow vs. deep habitats.

Montastraea cavernosa (Linnaeus, 1767) is a gonochoric broadcast spawner considered an “extreme” depth-generalist (Bongaerts et al. 2010), as it inhabits depths from 3-100 m (Reed, 1985; Lesser et al. 2010). In addition, this species is found throughout the Atlantic region, extending from Bermuda to Brazil to the West African coast (Veron, 2000; Nunes et al. 2009; Goodbody-Gringley et al. 2011). Spawning takes place approximately one week after the full moon during the months of August through October (Nunes et al. 2009), and recent observations have shown that deep and shallow colonies can spawn in synchrony (Vize et al. 2006). The large eggs of *M. cavernosa* are thought to increase larval survival time and dispersal capability, as well as increase post-settlement survival (Nunes et al. 2009). In addition, algal symbionts are not present in the

eggs, which suggest that corals might be capable of colonizing habitats over a broad depth range by acquiring the appropriate local symbionts from the water column. Overall, these characteristics might facilitate wide-scale dispersal, as evidenced by the moderate to high gene flow documented among shallow sites in the Caribbean-North Atlantic (Nunes et al. 2009; Goodbody-Gringley et al. 2011) and within the region of Brazil (Nunes et al. 2009). However, whether *M. cavernosa* comprises a single panmictic population across its depth distribution remains poorly understood.

In the present study, we determine the role of deep reefs in shallow reef recovery for *M. cavernosa*. Using high throughput (454) sequencing, we developed nine DNA microsatellite loci and used these to assess vertical connectivity in 583 coral colonies collected from 3 depth zones (shallow ≤ 10 m, mid 15-20 m and deep ≥ 25 m) at sites in Florida (within the Upper Keys, Lower Keys, and Dry Tortugas), Bermuda, and the U.S. Virgin Islands (USVI). We evaluated patterns of connectivity at three levels: among geographic locations (long distance *horizontal* connectivity), among reefs within a geographic location (intra-regional comparisons in the Florida Reef Tract), and among depths at each region (short distance *vertical* connectivity). Migration rates were estimated among depths at each region to determine whether migration is more likely to occur from deep to shallow reefs, from shallow to deep reefs, or in both directions symmetrically. Finally, we assessed algal symbiont (*Symbiodinium* spp.) diversity in a subset of corals to determine the functional potential to colonize shallow vs. deep environments and determine patterns of depth zonation, if any.

METHODS

Sample collection

Field activities were focused on shallow (≤ 10 m), intermediate (15-20 m) and deep (≥ 25 m) coral communities along the (1) Florida Reef Tract (within sites in the Upper Keys, Lower Keys and Dry Tortugas), (2) Bermuda, and (3) USVI (Table 2.1, Figure 2.1). These different locations provided an opportunity to assess geographic differences in vertical connectivity. In addition, the comprehensive sampling design along the Florida Reef Tract (~400 km) allowed for intra-regional scale comparisons of patterns of connectivity observed among reefs within a geographic location.

At each geographic location, corals were sampled using SCUBA along depth transects. A haphazard approach was used to collect samples from colonies at least 1 m apart to minimize the likelihood of sampling clones. Two different sampling methods were used, per the requirements of the respective permitting agencies. Where allowed, samples were removed from colonies as small tissue biopsies (0.25 cm^2) using a 4 mm internal diameter hollow steel punch, and preserved in 95% ethanol. When destructive sampling was not permitted, small polyp biopsies were collected using a modification of the syringe method described in Correa et al. (2009a). Briefly, a 60 mL syringe (without a needle) was held flush with the upper rim of a corallite and the plunger of the syringe was pulled out, sucking the polyp tissue into the syringe. The syringe was then stored in an individual numbered zip lock bag attached to a slate. After each dive, the contents of each syringe were expelled into a 15 mL Falcon tube and centrifuged for 5 min at 500 g. The supernatant was then removed and the pellet transferred to a 2 mL tube with 500 μL of DNAB + 1% SDS (Rowan and Powers, 1991) and heated to 65°C for 1.5-2 hrs.

Microsatellite development

Cnidarians with algal symbionts are particularly difficult candidates for microsatellite development because DNA extraction protocols typically extract both host and symbiont DNA (Shearer et al. 2005). Therefore, to minimize contamination by symbiont DNA in the template used for host microsatellite development, *M. cavernosa* tissue was bleached using the photosynthetic inhibitor DCMU as described in Jones (2004). Sampling occurred when the colony appeared visibly pale and genomic DNA was extracted using a modified organic extraction (Baker et al. 1997), prior to 454 sequencing on a Roche GS 454 FLX+ sequencer, and subsequent library construction (Genomics Core Facility, Penn State University).

A total of 47,968 single sequence reads (i.e., not assembled into contigs) generated from the 454 sequencing were searched for the presence of microsatellite repeats using the computer program Tandem Repeat Finder (Gelfand et al. 2006). Primers were designed for a subset of sequences with a minimum of six tri-, tetra-, penta- or hexanucleotide repeats (n= 104) using the web-based program Primer 3 (Untergrasser et al. 2012). Primers were screened and optimized by visually inspecting bands on 2% agarose gels. Candidate markers (n= 14) were then screened against the algal symbionts isolated from the colony used for microsatellite development (identified as *Symbiodinium* type C3) and other preexisting algal cultures in clades B, C and D isolated from the coral species *Orbicella faveolata* (Ellis and Solander, 1786), to confirm specificity to host DNA. Primers that amplified any of the cultured *Symbiodinium* (n= 4) were considered to be derived from the symbiont and thus were excluded from further development.

Microsatellite genotyping

A total of 9 microsatellite loci were developed for scoring on an ABI 3730 automated sequencer. Forward primers were fluorescently labeled with NED, VIC or 6FAM (Applied Biosystems, CA). PCR reactions were performed in four multiplex reactions (11 μ L total volume) and one singleplex reaction (10 μ L total volume) using 1 μ L of 50-100 ng of template DNA (Table 2.1). Reactions were performed using primer concentrations specific to each locus (Table 2.1), 5 \times PCR Reaction Buffer (Promega), 2.75 mM of MgCl₂ (Promega), 0.8 mM of dNTPs, and 0.5 U of Taq polymerase (Promega). Thermal cycling for all reactions was performed with an initial denaturation step of 94°C for 3 min, followed by 35 cycles of 94°C for 1 min; 57°C (annealing temperature) for 1 min; 74°C for 1 min; and a final extension at 74°C for 7 mins. PCR products were visualized with an automated sequencer (ABI 3730) using an internal size standard (Genescan LIZ-500, Applied Biosystems, CA). Electropherograms were visualized and alleles scored using the software GeneMapper 4.0 (Applied Biosystems, CA). Samples that failed to amplify more than two of the nine loci were excluded from further analysis (n= 160). In this dataset, there was a per locus failure rate of <10% (except for marker MC49 which had a failure rate of 13.7%), and a per sample failure rate of 2.7%.

Analysis of multi-locus genotype data

Identical *multi-locus genotypes* (MLGs) were identified in GenAlEx v.6.41 (Peakall and Smouse, 2006) by requiring complete matches at all loci. The same number of unique MLGs (n= 577) were found whether missing data were considered or not. Unique MLGs were then used for subsequent analyses. Tests for conformation to Hardy

Weinberg Equilibrium (HWE) expectations were performed using the program Genepop (Raymond and Rousset, 1995). The R-package FDRtool was then used to adjust p-values for multiple testing (Strimmer, 2008). Since large heterozygote deficits are common in marine invertebrates (Addison and Hart, 2005; Baums, 2008), the program INEST (Chybicki and Burczyk, 2009) was used to distinguish among some of the possible causes for departures for HWE by estimating null allele frequencies while accounting for inbreeding. Population level pairwise F_{ST} comparisons were performed in GenAIEx v.6.41. Finally, principal component analysis (PCA) was performed on a matrix of covariance values calculated from population allele frequencies in the program GenoDive v.2.20 (Meirmans and Van Tienderen, 2004).

Population structure was investigated using a Bayesian clustering approach performed in STRUCTURE v.2.3.3 (Pritchard et al. 2000), on the web-based Bioportal server from the University of Oslo. Correlated allele frequencies and admixed populations were assumed. Because sampling location information set as prior information can assist clustering for data sets with weak structure (Hubisz et al. 2009), the LOCPRIOR option was used. Values of K (i.e., hypothesized number of populations) from 1 – 20 were tested by running 3 replicate simulations per K with 10^6 Markov Chain-Monte Carlo repetitions and 10^3 burn-in iterations. The most likely value for K based on the STRUCTURE output was then determined by plotting the log probability [L(K)] of the data over multiple runs and comparing that with delta K (Evanno et al. 2005), as implemented in the web-based program STRUCTURE HARVESTER (Earl, 2009). Results of the three STRUCTURE runs assuming K= 2 were merged with CLUMPP (Jakobsson and Rosenberg, 2007) and visualized with DISTRUCT (Rosenberg, 2004).

Migration patterns were estimated using MIGRATE v.3.4.2 (Beerli and Felsenstein, 2001). MIGRATE uses a Bayesian approach to estimate the likelihood of alternative population genetic models using coalescence theory. In the present study, we used the results of STRUCTURE (Figure 2.2) as prior information to compare four different gene flow models at each geographic location: (A) a full model with three populations (shallow, mid and deep) and symmetrical gene flow; (B) a model with two populations (shallow and mid/deep pooled) and one migration rate from shallow to mid/deep; (C) a model with two populations (shallow and mid/deep pooled) and one migration rate from mid/deep to shallow; and (D) a model where all three populations (shallow, mid and deep) were considered part of the same panmictic population. The most complex model (A) was used to experiment with run conditions until convergence was achieved and posterior distributions were acceptable [final parameter settings: long-inc 100, long-sample 15,000, replicates 20, burn-in 20,000, and 4 heated chains (1, 1.5, 3, 100,000)]. Models A - D were then compared and ranked using the thermodynamic integration framework as described in Beerli and Palczewski (2010).

Algal symbiont characterization

A subset of the corals used for microsatellite analyses was selected haphazardly to assess the diversity of symbiont populations and potential patterns of depth zonation. *Symbiodinium* types were identified by denaturing gradient gel electrophoresis (DGGE) and sequencing of ITS-2 rDNA. This gene region was amplified using the primers ITSintfor2 and ITS2clamp (LaJeunesse and Trench, 2000) and amplification products were separated by DGGE using a 35-75% gradient. Dominant bands on the gel were excised, re-amplified, and sequenced using the BigDye Terminator v3.1 cycle sequencing

kit and an automated sequencer (ABI 3730). Sequences were then identified via BLAST in GenBank (accession numbers are given in Appendix 2.3).

Quantitative PCR (qPCR) assays were used in addition to DGGE to better understand patterns of zonation with depth and detect the presence of background symbiont types not detectable by DGGE (e.g., Mieog et al. 2009). The assay for *Symbiodinium* clade B targeted the large subunit of the nuclear rDNA, and was carried out as described in Correa et al. (2009b). Assays targeting specific actin loci in *Symbiodinium* clades C and D, however, were carried out in multiplex as described in Cunning and Baker (2013). All qPCR reactions were performed using a StepOnePlus Real-Time PCR System (Applied Biosystems, CA) and reaction volumes were 10 μ l, using 1 μ l of genomic DNA template. Two replicates per sample were used per clade assayed.

RESULTS

Multi-locus genotyping and tests of Hardy-Weinberg Equilibrium

Our analysis of 583 samples yielded 577 unique MLGs (Table 2.1), suggesting virtually no asexual reproduction in this species at sampling distances >1 m. Repeated MLGs were always confined to a single sampling location (within <1 km). Tests of HWE for each of the 15 combinations of region/depth (Table 2.1, population column) individually revealed that all 9 loci were largely in HWE, as only 3.7% of 135 tests showed significant deviations from HWE after FDR correction (Appendix 2.1). Individual inbreeding values were generally low (F_i mean= 0.01; 95% confidence

interval= 0-0.07), as well as null allele frequencies (ranging between 0.04-0.12 across loci and populations, Appendix 2.2).

Assessment of vertical vs. horizontal connectivity

Overall, patterns of genetic subdivision showed strong support for two clusters that correlate closely with depth (Figure 2.2). Across all 5 regions, shallow colonies were assigned to a “shallow” cluster (depicted in blue), while colonies from intermediate and deep depths were either assigned to the shallow cluster or to a “deep” cluster (depicted in yellow), with high probabilities of membership to either cluster (>80%). Fifty three individuals (9%) had similar probabilities of membership to both clusters (50-79%), probably as a result of admixture (i.e., interbreeding between shallow and deep colonies). This pattern of colonies showing predominant membership to only one genetic cluster also held when higher values of K were explored (results not shown). Finally, plots of mean log-likelihood of K and delta K suggested that the most likely number of population clusters present in the full dataset is two (Figures 2.3A and 2.3B).

The degree of genetic differentiation with depth varied among regions (Figure 2.2). The Upper and Lower Keys displayed the most genetic structure with depth, with ~57% and ~90% of all colonies at deep depths (≥ 25 m) assigned to the deep population, respectively. Conversely, Dry Tortugas samples consisted of a single panmictic population, with 81-99% of all colonies assigned to the common shallow cluster, despite being collected at depths from 8-25 m. Similarly, the USVI and Bermuda were dominated by one cluster across all depths (67-98% in the USVI and 95-98% in Bermuda, respectively).

When restricting comparisons to the shallow depth category across regions, no genetic structure was evident (Figure 2.2), suggesting a high degree of horizontal connectivity among sites separated by up to 1,992 km. These findings were also supported by pairwise F_{ST} comparisons (Table 2.3), where the greatest F_{ST} values were observed among locations separated by depth rather than horizontal distance (Table 2.3). For example, shallow and deep sites in the Lower Keys showed one of the largest F_{ST} values (0.07, Table 2.3), even though the distance between these sites is only ~20 km. Congruently, PCA on allele frequency differences among sites in Florida (Figure 2.4), separated sites by depth (PC1= 50% of variance) rather than region.

Migration rates among shallow and deep habitats

Preliminary runs were performed to determine which (if any) depth intervals could be pooled to reduce the parameters estimated in the gene flow models under comparison. MIGRATE was thus performed (1) pooling shallow and intermediate depths or (2) pooling intermediate and deep depths. MIGRATE runs consistently ranked the gene flow model in which intermediate and deep depths were pooled as the best (data not shown). Therefore, all analyses were performed pooling individuals from intermediate and deep depths. Table 2.4A summarizes the marginal log-likelihood differences (log Bayes factors) and ranking of each of the 4 gene flow models compared (A= full, B= shallow to mid/deep, C= mid/deep to shallow and D= panmixia) using the thermodynamic integration approximation as described in Beerli and Palczewski (2010). Overall, this method consistently ranked the gene flow model with migration from shallow to mid/deep as the best model across all regions. This ranking occurred even for regions where STRUCTURE suggested panmixia (Dry Tortugas, Bermuda and the

USVI). Furthermore, in regions with the largest degree of genetic differentiation with depth (Florida's Upper and Lower Keys, Figure 2.2), the panmictic gene flow model was ranked third, suggesting it was less likely. Consistently, there was a larger number of migrants per generation (N_m) from shallow to deep in regions where the panmixia model was ranked second (Dry Tortugas and Bermuda, respectively, Table 2.4B).

Algal symbiont characterization

M. cavernosa samples predominantly housed *Symbiodinium* type C3 across depths and regions, as shown via ITS-2 DGGE (n= 109, upper column in each depth category in figure 2.5). Interestingly, two other *Symbiodinium* types were identified (D1a and B1, Figure 2.5) in 11% of the shallow colonies assessed from Florida, but not in any other location (Bermuda or the USVI) or depth (intermediate or deep colonies). Further analysis with qPCR (lower column in each depth category in figure 2.5) detected additional background symbiont types in clade D in only 4 of the samples previously assessed with DGGE, suggesting that the conclusions drawn from DGGE were valid.

DISCUSSION

We developed 9 new microsatellite loci to undertake the most comprehensive analysis of population genetic structure for the Caribbean reef-building coral species *Montastraea cavernosa* in horizontal (long-distance) and vertical (short-distance) directions. We show that this species: (1) consists of two genetic clusters separated by depth; (2) exhibits panmixia across shallow sites separated by >1,700 km, (3) varies by region in its degree of vertical (depth) connectivity; (4) exhibits migration rates that are higher from shallow to intermediate/deep habitats; and (5) predominantly hosts the same

symbiont type across regions and depths. These findings suggest that deep reefs have limited potential to aid in shallow reef recovery as predicted by the Deep Reef Refugia Hypothesis (*sensu* Bongaerts et al. 2010).

Two genetic clusters separated by depth

The small percent of admixed individuals observed (<10%) suggests that migration between deep and shallow habitats has occurred but that little interbreeding among colonies has taken place. These findings are consistent with observations from van Oppen et al. (2011) and Prada and Hellberg (2013) for *S. hystrix* and *E. flexuosa*, respectively. Van Oppen et al. (2011) suggested that one possible explanation for the lack of interbreeding among shallow and deep individuals is reproductive isolation. This might result if, for example, populations at different depths become locally adapted, and immigration to the “wrong” habitats results in poor performance (immigrant inviability, *sensu* Prada and Hellberg, 2013). Interestingly, Budd et al. (2012) showed no significant genetic differentiation between two different *M. cavernosa* morphotypes present at depths of 10-30 m, suggesting a high degree of polymorphism and phenotypic plasticity in this species. It is possible however, that the two nuclear loci used in Budd et al. (2012) had insufficient resolution to detect differentiation by depth in the colonies assessed.

Alternatively, the potential for interbreeding can be reduced if there are temporal differences in spawning times (Levitan et al. 2004) between shallow and deep habitats (Prada and Hellberg, 2013). Although this is unlikely for *M. cavernosa* since mass spawning of deep water colonies has been observed to be synchronized with their shallow water counterparts (Vize, 2006), little fertilization can occur if deep gametes arrive late to the surface (e.g., Levitan et al. 2004).

High connectivity among shallow sites

There was little evidence for geographic differentiation between shallow sites separated by >1,700 km (Florida, Bermuda and the USVI, Figure 2.2 and Table 2.3). These findings confirm results of Nunes et al. (2009) and Goodbody-Gringley et al. (2011), both of which showed high levels of gene flow within the North Atlantic region for this species, and no significant differentiation between Bermuda and the Caribbean. This suggests that long-distance horizontal connectivity is much greater than short-distance vertical connectivity in this species. Furthermore, based on the patterns of connectivity observed here, it is more likely that shallow reefs rely on more distant, unimpacted shallow reefs to provide a viable source of new recruits following disturbance.

Regional differences in vertical connectivity

Even though there was strong evidence to support the presence of two populations separated by depth, the depth at which different populations make this transition, and the degree of genetic differentiation, vary among regions (Figure 2.2). For example, changes in genetic structure were observed at a shallower depth in the Upper and Lower Keys compared to the Dry Tortugas or the USVI, suggesting that the corresponding deep habitat may be at greater depths than those assessed at these latter two locations. Interestingly, the deep cluster appears to be absent in Bermuda: despite sampling a broad depth gradient (4-58 m), only one individual was found showing signs of admixture. It is possible that this location only receives larvae from the closest upstream shallow population (Florida), due to its high latitude. Regardless, results are consistent with findings from Billingham et al. (1997), which showed no genetic subdivision for this

species in Bermuda from depths of 2-30 m. Furthermore, our findings are in agreement with a recent small-scale study (n= 105, Brazeau et al. 2013), which showed that genetic structure with depth also varies for *M. cavernosa* at two other localities in the Caribbean (Bahamas vs. Cayman Islands).

Surprisingly, the largest genetic differentiation observed in this study occurred between the Lower Keys shallow and deep sites, while the lowest degree of differentiation occurred in the Dry Tortugas, even though these regions are only ~130 km apart. These findings strongly suggest that the potential for shallow reefs to recover from deep refugia may vary between sites as a consequence of local hydrology. Florida represents a unique case for testing the Deep Reef Refugia Hypothesis, as larvae are subject to complex current patterns driven primarily by the inter-annual variability in the Florida Current and associated frontal eddies. The region near Dry Tortugas, however, has a well-established spatial pattern of more mesoscale eddy activity compared to the Lower or Upper Keys (Hitchcock et al. 2005; Kourafalou and Kang, 2012). These mesoscale eddies, extending down to >100 m (Kourafalou and Kang, 2012), can act as important retention mechanisms for larvae spawned in the Dry Tortugas (e.g., Hitchcock et al. 2005; Paris, unpublished data), and may therefore facilitate genetic mixing of individuals from shallow and deep habitats, as evidenced by the lack of genetic structure at this location (Figure 2.2, Table 2.3) and highest number of migrants from shallow to deep (Table 2.4B). Conversely, the general decrease in mesoscale eddies west from the Dry Tortugas (Kourafalou and Kang, 2012) suggests that in the Lower and Upper Keys the strong currents produced by the Florida Current could quickly advect the deep larvae away from adjacent shallow habitat. These reefs however, could be important larval

sources for shallow reefs further downstream (e.g., the northern Florida reef tract). Therefore, future work should aim at elucidating the role of deep reefs as refugia for nearby vs. more distant, downstream shallow reefs.

Higher migration from shallow to deep

Remarkably, the gene flow model with migration from shallow to mid/deep was ranked as the best model in all 5 regions (Table 2.4A). This ranking was consistent even in regions where STRUCTURE suggested panmixia (Dry Tortugas, Bermuda and the USVI). Furthermore, in the Dry Tortugas and Bermuda, the gene flow model of migration from mid/deep to shallow was ranked least probable (Table 2.4A). These findings strongly suggest that there is asymmetrical gene flow among shallow and deep habitats. Thus, genetic mixing between shallow and deep populations is likely maintained by the supply of larvae down the slope (from shallow to deep), rather than by migration in both directions. This is further evidenced by the lack of individuals in shallow habitats assigned with high probability to the deep cluster (Figure 2.2). Therefore, although we cannot rule out the possibility that recovery of shallow reefs might be aided by nearby deeper reefs, it is unlikely to be sufficient to promote rapid recovery.

To date, only Prada and Hellberg (2013) have estimated migration rates between shallow and deep habitats for a coral species. In the octocoral species studied, the authors also found that migration was higher from shallow to deep, suggesting that this might be a consistent pattern for many coral species. One reason for this might be a higher gamete production in shallow environments, because this is where coral growth rate and coral cover tend to be highest (Riegl and Piller, 2003). Moreover, since rates of photosynthesis and calcification tend to decline significantly with depth (Mass et al. 2007; Slattery et al.

2011), shallow coral colonies tend to grow faster to sexual maturity due to higher light availability. In addition, shallow colonies might be more capable of allocating more energy reserves to gamete production than deep colonies due to a greater translocation of photosynthetic products from algal symbionts (e.g., Muscatine et al. 1989; Mass et al. 2007). Although this deficit is supplemented with heterotrophic feeding in *M. cavernosa* (particularly at depths >45 m, Lesser et al. 2010), total reef accretion is generally considered to be negatively correlated with increasing depth (Grigg, 2006). Furthermore, a higher polyp density per area recorded in shallow (3 m) vs. deep (18 m) sites in *O. faveolata* suggests a significant reduction in fecundity (egg production per cm²) at deep sites, implying a depth-related fecundity cost arising from a change in colony architecture (Villinski, 2003).

Alternatively, deeper reefs may be less environmentally harsh than shallow reefs, promoting higher survivorship of migrants in a downward direction. Finally, higher migration from shallow to deep sites might result if shallow colonies fragment, fall down the slope and subsequently re-attach in deeper habitats (i.e., adult migration). However, this is unlikely for *M. cavernosa*, since fragmentation would result in clone mates and we only observed ~1% clonality in our dataset.

M. cavernosa predominantly hosts one type of symbiont across regions and depths

The coral-symbiont interaction implies that studies of larval dispersal and connectivity in corals need to be supplemented by investigations of symbiont dispersal (Baums, 2008), because processes of symbiont transfer may impose limitations on the colonization and post-settlement survival of coral offspring (Bongaerts et al. 2010). However, such limitations are not expected for species that acquire their *Symbiodinium*

from the environment (i.e., horizontally). These corals are able to acquire locally abundant symbionts and so might be capable of colonizing habitats over a broad depth range.

Overall, we found that *M. cavernosa* predominantly hosts a single *Symbiodinium* type (C3) across all regions and depths assessed, regardless of the method used (DGGE or qPCR). Depth-generalist coral species often harbor a single symbiont type over their entire depth range but can also show a cladal or sub-cladal shift in symbiont types (e.g., Rowan and Knowlton, 1995; Warner et al. 2006; Sampayo et al. 2007; Frade et al. 2008; Bongaerts et al. 2011b). The depth at which the shift occurs varies between species, and for *M. cavernosa* it is suggested to occur well into the mesophotic zone (>60 m) and at the sub-cladal level (Lesser et al. 2010). Furthermore, *Symbiodinium* type C3 is considered a pandemic, host-generalist symbiont (LaJeunesse, 2005), because it occurs in a wide range of Pacific genera at both shallow and intermediate (<20 m) depths (LaJeunesse et al. 2003, 2004), as well as in mesophotic samples of at least 5 of the 10 Pacific species assessed in Bongaerts et al. (2011b). Together, findings suggest that the coral-symbiont association observed in *M. cavernosa* is unlikely to limit the vertical connectivity of the holobiont.

Implications: The role of deep reefs in shallow reef recovery

Overall, our findings were surprising for a broadcast spawning coral with documented high gene flow throughout the Caribbean. *M. cavernosa* is one of the few Caribbean species inhabiting a broad depth range between 3-100 m, making it one of the few candidates for testing the Deep Reef Refugia Hypothesis. Nevertheless, we found genetic structure with depth in this species. Furthermore, findings from this study confirm

new evidence suggesting that depth is an important population structuring factor in corals (Eytan et al. 2009; van Oppen et al. 2011; Prada and Hellberg, 2013; Brazeau et al. 2013). In fact, our findings support those from Caribbean broadcast spawners in the genus *Oculina* (Eytan et al. 2009), the Pacific brooding coral *S. hystrix* (van Oppen et al. 2011) and the Caribbean octocoral *E. flexuosa* (Prada and Hellberg, 2013), despite different study locations, coral species and reproductive strategies. Together, the lack of depth-generalist coral species in the Caribbean region (~25%, Bongaerts et al. 2010; but see Smith et al. 2010), combined with our findings, suggest that the capacity for deep reefs to act as “seed banks” may be limited on Caribbean reef slopes. Furthermore, if these patterns prove consistent over a broad range of species then the expectation that MCEs may be refugia for shallow water taxa appears significantly reduced.

What if we were to lose all shallow reefs?

It has been suggested that, while reefs would suffer badly in a scenario of total coral mortality at depths <10 m, only about 50% of the total area occupied by reef-building corals would actually disappear (Riegl and Piller, 2003). However, loss of the upper 20 m would result in a reduction in area of >80% (Riegl and Piller, 2003). If we assume that coral reefs will still exist in intermediate and deep habitats (≥ 15 m) partly due to lower thermal stress and more stable conditions, then our findings suggest that some locations might be able to recover from nearby deep reefs, even though this process might take multiple generations due to low migration rates from deep to shallow habitats. Conversely, some locations might be unable to recover at all from their deep water counterparts and will have to rely on the recovery of other shallow habitats first, or in the supply of larvae from distant deep reefs. However, even if impacted shallow reefs are re-

colonized by larvae originating from deep water, strong selective forces (e.g., Bongaerts et al. 2011a; Prada and Hellberg, 2013) might result in reduced or little post-settlement survival. Therefore, shallow reefs (<15 m) deserve a high priority for managers and measures should be taken to reduce local and global anthropogenic impacts that might further accelerate their loss rate.

Table 2.1. Nine microsatellite loci developed for *Montastraea cavernosa*, amplified in four multiplexes (plex A-D) and one singleplex reaction. Given are the locus name, primer sequences, motif type, and the size range of the alleles amplified in base pairs (bp). Locus-specific primer concentrations are also given. All reactions had the same annealing temperature (57°C). Forward primers were fluorescently labeled with one of three dyes (6FAM, VIC or NED; Applied Biosystems, CA).

Locus	Primer sequence (5'-3')	Motif type	Allele size range (bp)	Forward primer (μM)	Reverse primer (μM)	Plex
MC4	F: 6FAM-ACGATCAAGACTCCAACGA R: GCTCTTCGTGAACACTGAGG	(TTA)7 T (TTA)2	97-222	0.4	0.4	A
MC18	F: VIC-GGAGAACTGGATACCATGTC R: TATGGTCCTGGGACAACCT	(AAT)2 TAT (AAT)9	218-260	0.4	0.4	A
MC29	F: 6FAM-CTCCTTGGTCACCCTACAA R: GGTGAAGAAGCAGCCATTGG	(AAAC)7	155-194	0.08	0.08	B
MC41	F: 6FAM-AATTACGCAACACTGTGCA R: TCGACTGACCGAAGTACCT	(GGTA) imperfect	344-448	0.4	0.4	B
MC46	F: VIC-CGGTGTAGCTCTAGCAGGA R: ACTGAGTCGCAGCATTGG	(TTTTGT) imperfect	124-163	0.08	0.08	C
MC49	F: VIC-ATTCCTCCAGTGATGTACCT R: CTGAGTTCCTGCCATTAGG	(TGT)10	192-384	0.5	0.5	D
MC65	F: NED-TTTGTGATTGGCCAGGGTG R: TTGTGCTGTGAAGCATGAT	(TTTGGT)6	112-172	0.35	0.35	D
MC97	F: 6FAM-ACATGTGGCCTTGTTACCA R: CGAACATCAGTGACAACCT	(ACAA)6 ACAG (ACAA)	163-187	0.08	0.08	C
MC114	F: VIC-ACTGTAGATCGAGGCGTTTC R: TCTGTTCTCTGACTCTTTCG	(TTG)10 [15bp insert] (TTG)6	152-230	0.55	0.55	single

Table 2.2. *Montastraea cavernosa* samples (N= 583). Given are total sample size (N), number of unique multi-locus genotypes (Ng) and ratio of genets over samples collected (Ng/N). GPS locations are in decimal degrees (WGS84). USVI= U.S. Virgin Islands

Region	Subregion	Population	Site name	Site in map	Estimated depth (m)	N	Ng	Ng/N	Latitude	Longitude
Florida	Upper Keys	UK shallow	Conch reef	UK1	5	13	13	1.00	24.9465	-80.50207
			DL patch	UK2	5	6	6	1.00	25.0136833	-80.41387
			Little Conch reef	UK3	5	11	11	1.00	24.9511167	-80.4614
			Marker 39	UK4	5	12	12	1.00	25.0094333	-80.45792
			Sand island	UK5	5	12	12	1.00	25.0178667	-80.36823
			Tavernier Rocks	UK6	5	3	3	1.00	24.9389833	-80.56272
			Hens and Chickens	UK7	5	4	4	1.00	24.9341333	-80.54952
			Wolf reef	UK8	5	9	9	1.00	25.02185	-80.39623
			Behind Conch reef	UK9	5	6	6	1.00	24.9575833	-80.45603
	UK mid	SW of Molasses reef	UK10	16	14	14	1.00	25.0042333	-80.38757	
		NE of Conch reef SPA	UK11	17	16	16	1.00	24.9465333	-80.45687	
		UK deep	Pickles deep	UK12	25	7	7	1.00	24.97095	-80.43075
			Conch reef	UK13	29	12	12	1.00	24.9580667	-80.45243
	Lower Keys	LK shallow	N of Molasses reef	UK14	37	4	4	1.00	25.0041333	-80.37987
			Western Sambo reef	LK1	8	6	6	1.00	24.4784833	-81.7302
			Marker 32	LK2	8	10	10	1.00	24.4741667	-81.74268
		LK mid	Near Key West	LK3	9	11	11	1.00	24.4687667	-81.82217
			American Shoal mid1	LK4	14	20	20	1.00	24.5158167	-81.54248
			American Shoal mid2	LK5	16	21	19	0.91	24.5138167	-81.54315
	LK deep	American Shoal	LK6	25	30	30	1.00	24.5042167	-81.58197	
	Dry Tortugas	DT shallow	Dry Tortugas National Park	DT1	8	38	38	1.00	24.6107833	-82.87133
Near Dry Tortugas			DT2	15	31	31	1.00	24.72225	-82.78715	
Outside Dry Tortugas			DT3	25	44	44	1.00	24.62875	-83.10167	

Bermuda	BDA shallow	Castle Harbour 4m inshore	BDA1	4	25	23	0.92	32.3598833	-64.69243
		Castle Harbour 4m offshore	BDA2	4	25	25	1.00	32.3367167	-64.65738
	BDA mid	Castle Harbour 18 m	BDA3	18	43	43	1.00	32.3354167	-64.65405
	BDA deep	Castle Harbour 26 m	BDA4	26	16	15	0.94	32.3252667	-64.65423
		Castle Harbour 35 m	BDA5	35	1	1	1.00	32.3253667	-64.65287
		Castle Harbour 40 m	BDA6	40	9	9	1.00	32.3246167	-64.65308
		Castle Harbour 44 m	BDA7	44	7	7	1.00	32.3255833	-64.6661
		Castle Harbour 49 m	BDA8	49	4	4	1.00	32.3251833	-64.65173
		Castle Harbour 53-58 m	BDA9	53-58	9	9	1.00	32.3253167	-64.6623
USVI	USVI shallow	Flat Cay	USVI1	7	42	42	1.00	18.5303667	-65.65172
	USVI mid	Buck Island	USVI2	20	12	12	1.00	18.4647167	-65.49722
	USVI deep	College Shoal	USVI3	30-33	50	49	0.98	18.3098167	-65.12772
TOTAL				583	577	0.99			

Table 2.3. *Montastraea cavernosa* pairwise F_{ST} values for each population. Statistically significant values ($p < 0.05$) after FDR correction are highlighted in bold. UK= Upper Keys, LK= Lower Keys, DT= Dry Tortugas, Bermuda= Bermuda and USVI= U.S. Virgin Islands.

Population	UK shallow	UK mid	UK deep	LK shallow	LK mid	LK deep	DT shallow	DT mid	DT deep	BDA shallow	BDA mid	BDA deep	USVI shallow	USVI mid
UK mid	0.016													
UK deep	0.035	0.005												
LK shallow	0.007	0.025	0.045											
LK mid	0.033	0.009	0.015	0.041										
LK deep	0.064	0.022	0.015	0.070	0.011									
DT shallow	0.000	0.020	0.040	0.003	0.034	0.063								
DT mid	0.020	0.006	0.027	0.012	0.025	0.042	0.017							
DT deep	0.012	0.005	0.008	0.017	0.024	0.035	0.013	0.009						
BDA shallow	0.013	0.019	0.028	0.029	0.037	0.070	0.017	0.035	0.020					
BDA mid	0.013	0.019	0.025	0.032	0.036	0.066	0.016	0.039	0.021	0.003				
BDA deep	0.013	0.018	0.031	0.018	0.038	0.071	0.018	0.023	0.018	0.000	0.003			
USVI shallow	0.014	0.026	0.046	0.007	0.048	0.079	0.012	0.022	0.020	0.028	0.032	0.019		
USVI mid	0.035	0.037	0.047	0.026	0.037	0.060	0.019	0.031	0.026	0.029	0.035	0.022	0.032	
USVI deep	0.015	0.016	0.022	0.013	0.025	0.043	0.011	0.021	0.004	0.020	0.019	0.017	0.017	0.007

Table 2.4. *Montastraea cavernosa* (A) Comparison of log Bayes factors (marginal log-likelihood differences, LBF) approximated by thermodynamic integration for four different gene flow models (A= full, B= shallow to mid/deep, C= mid/deep to shallow and D= panmixia). (B) Estimated mutation-scaled population sizes (θ), mutation-scaled migration rates (M) and number of migrants per generation ($Nm = \theta * M / 4$) between source and receiving populations for model best supported (B= shallow to mid/deep). Numbers in parenthesis indicate the 95% confidence interval (CI) for parameters θ and M. UK= Upper Keys, LK= Lower Keys, DT= Dry Tortugas, Bermuda= Bermuda and USVI= U.S. Virgin Islands.

(A)

Region	LBF for model				Rank of model			
	A	B	C	D	A	B	C	D
Upper Keys	-409905	0	-3845	-13985	4	1	2	3
Lower Keys	-20701	0	-765	-6320	4	1	2	3
Dry Tortugas	-25438	0	-219775	-8971	3	1	4	2
Bermuda	-26545	0	-214437	-13043	3	1	4	2
USVI	-29678	0	-800	-4121	4	1	2	3

(B)

Source population	Receiving population	Parameter and 95% CI		
		θ	M	Nm
UK shallow	UK mid/deep	3.87 (0.60-7.40)	14.77 (6.40-24.26)	14.28
LK shallow	LK mid/deep	6.82 (2.60-11.2)	2.40 (0.13-4.60)	3.81
DT shallow	DT mid/deep	25.01 (4.40-67.27)	7.49 (2.73-12.53)	46.83
BDA shallow	BDA mid/deep	13.30 (2.40-40.27)	11.65 (4.33-20.47)	38.73
USVI shallow	USVI mid/deep	6.16 (0.80-11.33)	9.68 (4.40-15.33)	14.90

Figure 2.1. Sampling locations in the Caribbean and western Atlantic. Individual sites are labeled as designated in Table 2.1. White circles denote shallow (≤ 10 m) sites, gray circles denote intermediate (15-20 m) sites, and black circles denote deep (≥ 25 m) sites.

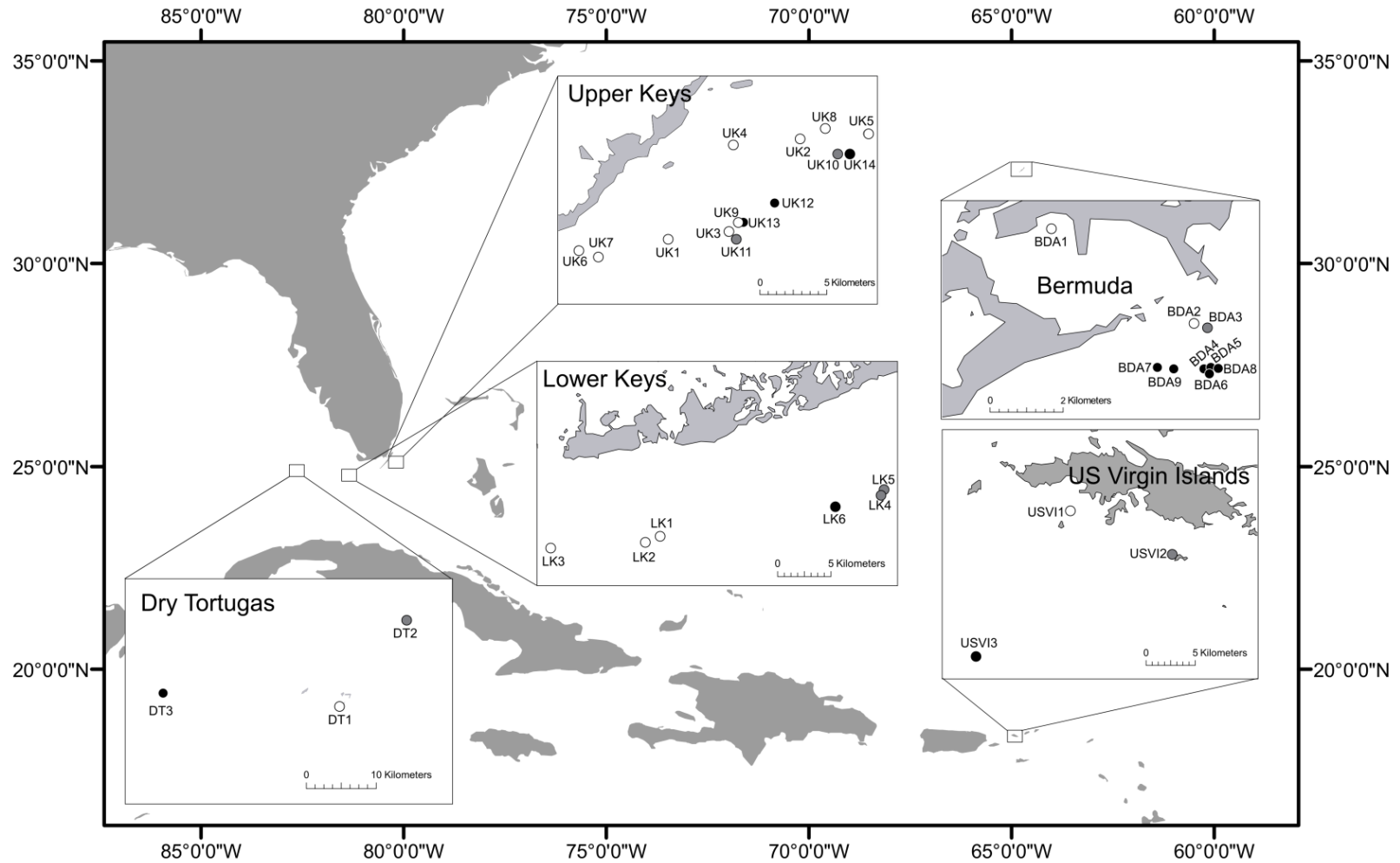


Figure 2.2. *Montastraea cavernosa* population structure across regions [Upper Keys, Lower Keys and Dry Tortugas (within Florida), Bermuda and the U.S. Virgin Islands] and depths [shallow (≤ 10 m), mid (15-20 m) and deep (≥ 25 m)]. Bar graphs show the average probability of membership (y-axis) of individuals (n= 577, x-axis) in K= 2 clusters as identified by STRUCTURE. Samples were arranged in order of increasing depth within region.

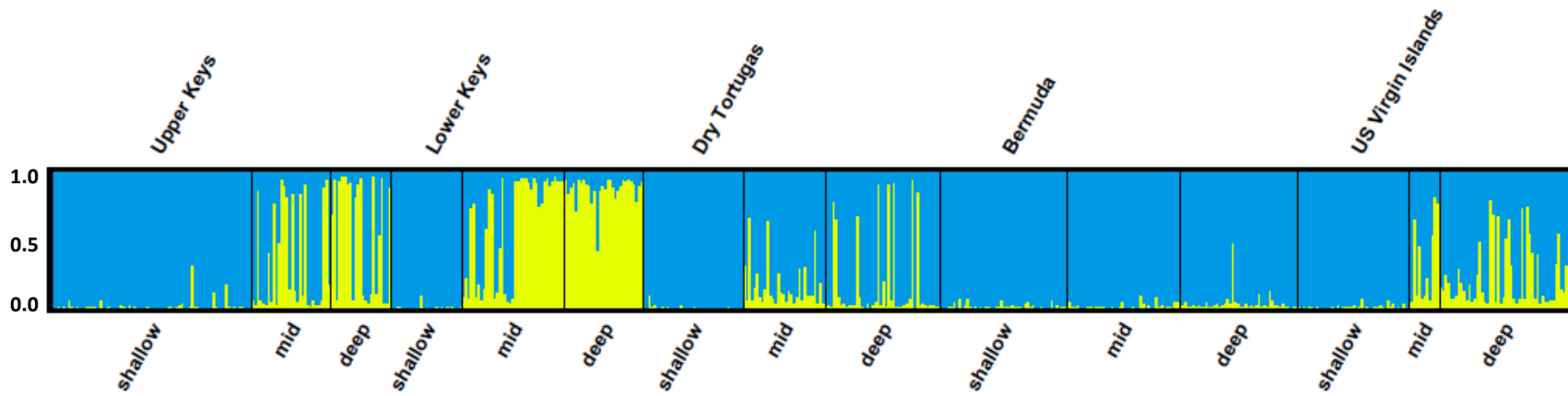


Figure 2.3. Mean log-likelihood LN of (A) K (hypothesized number of populations) and delta K (B) values for STRUCTURE analysis of *Montastraea cavernosa* samples. Values of K= 1 – 20 were tested by running 3 replicate simulations for each K (error bars in upper figure indicate variance among replicates).

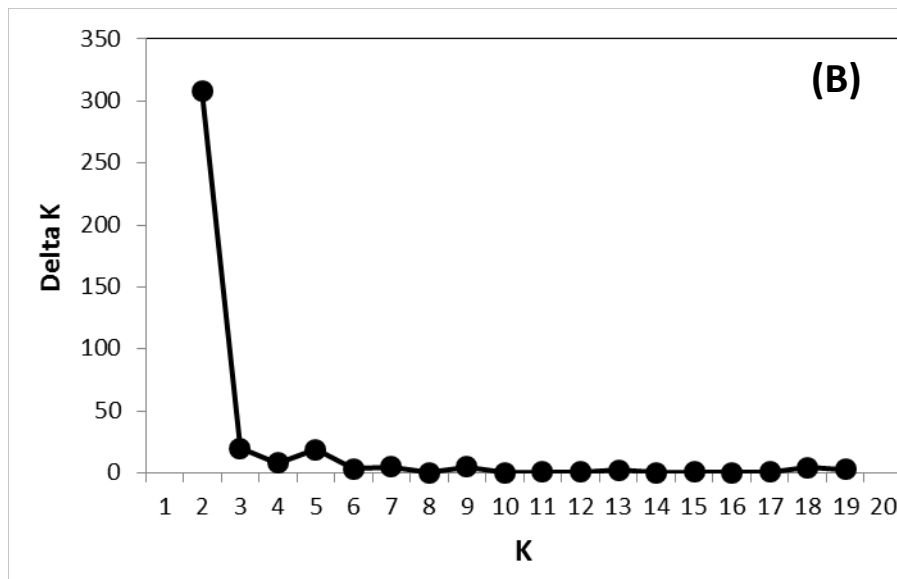
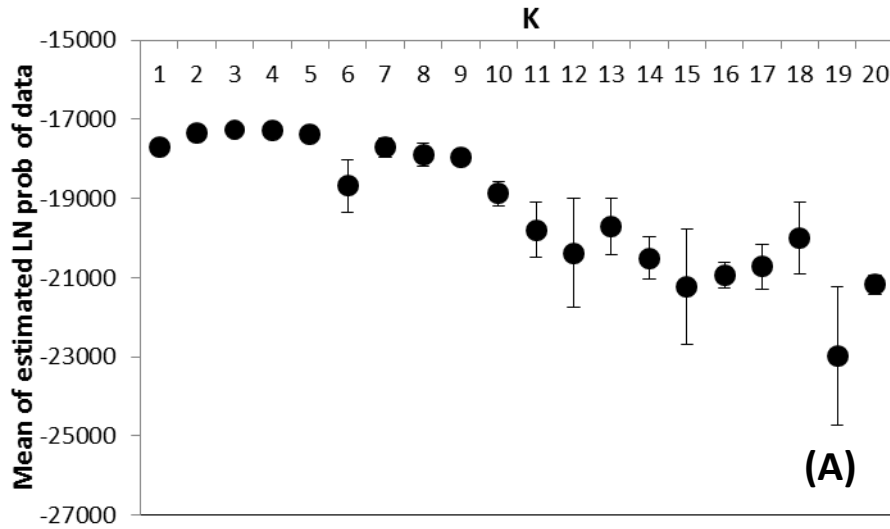


Figure 2.4. Principal Component Analysis (PCA) of allele frequency covariance in *Montastraea cavernosa* Florida populations. 8 of 163 axes were retained, explaining 100% of the cumulative variance. Plotted are the first and second axes explaining 50.29% ($p < 0.01$) and 13.07% ($p > 0.05$) of the variance, respectively. Axes cross at 0. The different shapes denote each of the 3 regions sampled in this study (Upper Keys, Lower Keys and Dry Tortugas), whereas the different colors denote each of the 3 depths under comparison [shallow (≤ 10 m), mid (15-20 m) and deep (≥ 25 m)]. UK= Upper Keys, LK= Lower Keys, DT= Dry Tortugas

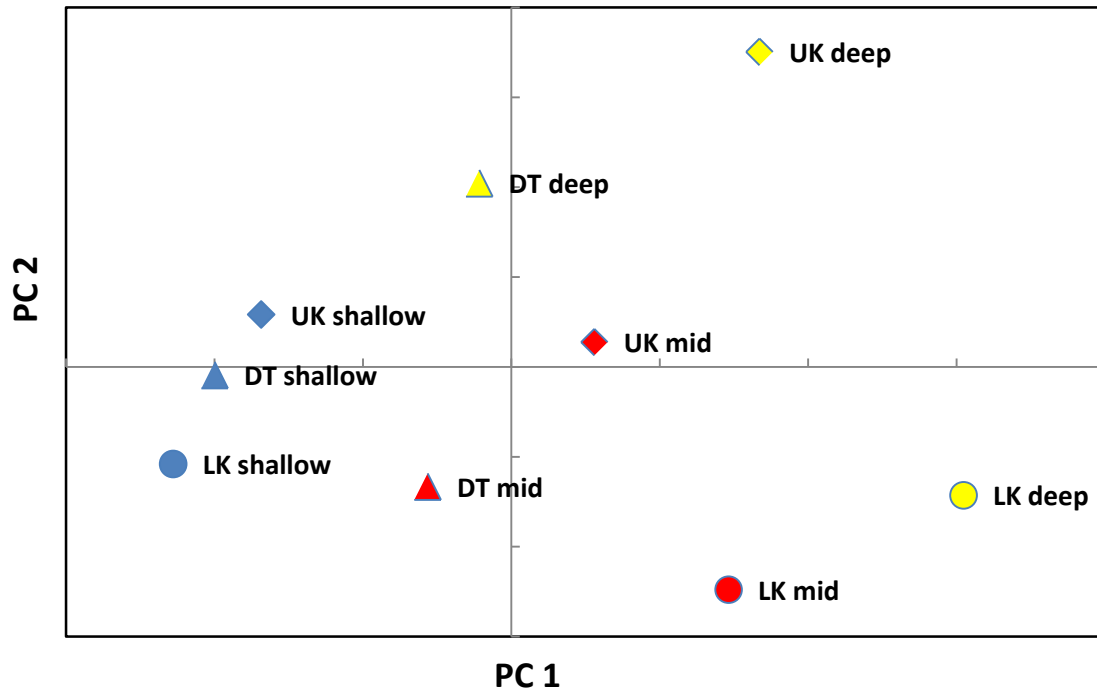
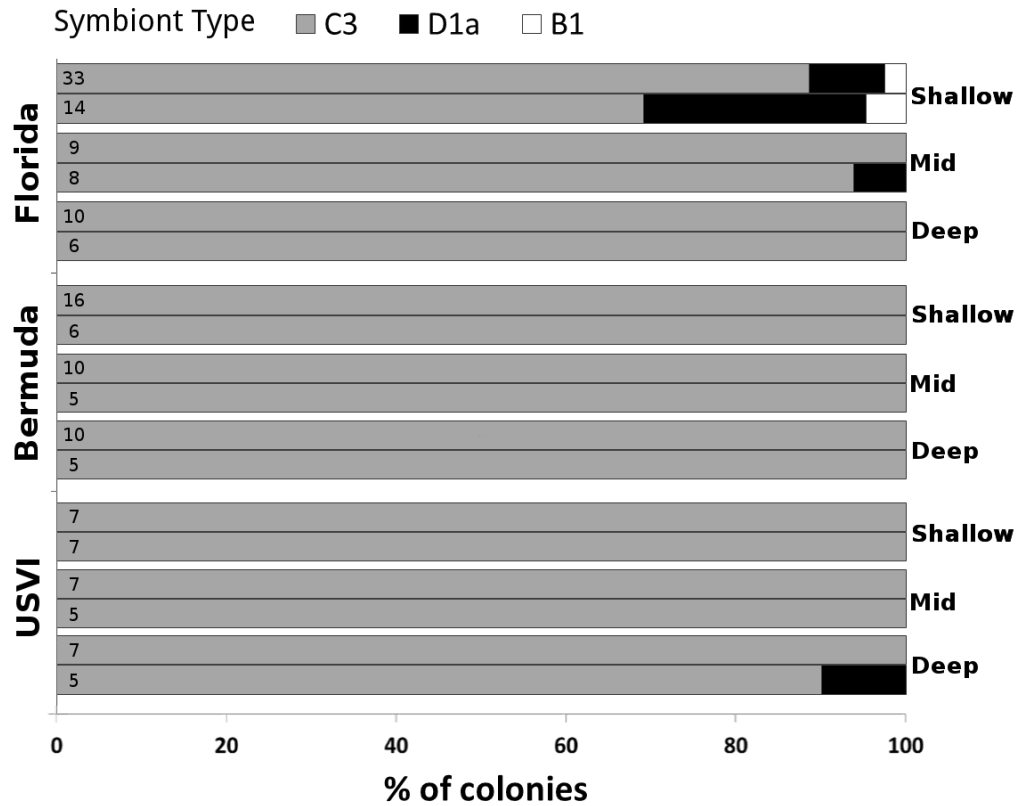


Figure 2.5. *Symbiodinium* types detected in a subset of *Montastraea cavernosa* samples from each depth and geographic location, using either Denaturing Gradient Gel Electrophoresis (upper column per depth category) or quantitative PCR (lower column per depth category). The numbers of individual coral colonies sampled for each depth are indicated. Colonies hosting mixed symbiont communities (i.e., more than 1 type) were partitioned into each appropriate category. USVI= U.S. Virgin Islands



CHAPTER 3

Long-distance dispersal and vertical gene flow in the Caribbean coral *Porites astreoides* despite brooding reproductive mode and depth zonation of algal symbionts

SUMMARY

The variation in life-history and reproductive strategies has often been used to predict patterns of larval dispersal and connectivity in marine invertebrates. For corals, the general expectation is that brooding species exhibit limited dispersal capabilities and lower genetic connectivity compared to broadcast spawning species, presumably as a result of shorter pre-competency periods. In this study, we assessed patterns of genetic connectivity for the brooding Caribbean coral *Porites astreoides* in both horizontal (long-distance) and vertical (short-distance) directions. We also tested whether depth zonation of algal symbionts (*Symbiodinium* spp.) might limit effective connectivity due to maternal transmission of symbionts from parent colonies to larvae. Contrary to expectations, *P. astreoides* exhibited high levels of gene flow between the U.S. Virgin Islands and Florida (despite low levels of gene flow between the Caribbean and Bermuda), suggesting this species has similar or greater long-distance dispersal compared to other Caribbean broadcast spawning taxa studied to date. Similarly, high levels of gene flow were observed among depths in two of the three geographic locations examined (Bermuda and the U.S. Virgin Islands), as has been reported recently for the Caribbean broadcast spawner *Montastraea cavernosa* (Chapter 2). Finally, depth zonation in the algal symbionts of *P. astreoides* did not appear to limit effective connectivity. Together,

these findings suggest that brooding reproductive mode and/or maternal transmission of algal symbionts do not necessarily result in low dispersal ability, and instead suggest that extrinsic factors (e.g., oceanographic features) are more likely to drive connectivity in corals, at least in the Caribbean region.

BACKGROUND

Variation in life-history characteristics, such as reproductive mode and larval type, has often been used to predict patterns of larval dispersal and connectivity in marine invertebrates (Miller and Ayre, 2008). Scleractinian corals are excellent study models, as they exhibit a variety of life-history and reproductive strategies that can directly influence their potential for dispersal (Magalon et al. 2005). For example, corals can reproduce by internal fertilization (brooding), or by external fertilization (broadcast spawning) [Fadlallah, 1983; Szmant, 1986; Harrison and Wallace, 1990]. Brooded larvae are more advanced in their development when released, and therefore are competent to settle within hours (Fadlallah, 1983; Szmant, 1986). In addition, algal symbionts (*Symbiodinium* spp.) are usually transmitted directly to the offspring (Fadlallah, 1983), which may impose limitations on the colonization and post-settlement survival of the holobiont. Conversely, larvae produced from broadcast spawners usually require 5–7 days of development in the water column before achieving competency (reviewed in Harrison and Wallace, 1990). Algal symbionts are not generally present in the eggs and must be acquired *de novo* from the water column, usually several days after settlement (e.g., Coffroth et al. 2001). Together, these characteristics are thought to facilitate long-distance dispersal in broadcast spawners compared to brooding species. However, no studies have yet examined the potential for long (horizontal) vs. short (vertical) distance

dispersal for brooding vs. broadcast spawning coral species using comparable empirical datasets.

Porites astreoides (Lamarck, 1816) is a common coral species found throughout the Caribbean, occurring over a wide range of depths and habitats (Goreau, 1959; Goreau and Wells, 1967) down to 70 m (Bongaerts et al. 2010). It occurs as two color morphs, with a yellow/green morph generally observed in shallower waters than a brown morph, although both are often found side by side (Gleason 1993; McGuire, 1998). In addition, *P. astreoides* is a brooding coral that undergoes internal fertilization, releasing semi-mature planulae monthly from January to September (Szmant, 1986; Goodbody-Gringley et al. 2013) and having an unusual mixed breeding system, where half of the colonies are hermaphroditic and the other half are female (Chornesky and Peters, 1987). Finally, algal symbionts are present in brooded larvae when released (Chornesky and Peters, 1987) and reportedly follow strong patterns of depth zonation in the range of 2-25 m (Warner et al. 2006).

Montastraea cavernosa (Linnaeus, 1767) is an important reef-building Caribbean coral which also inhabits a wide depth range between 3-100 m (Reed, 1985; Lesser et al. 2010). However, *M. cavernosa* is a broadcast spawner that requires external fertilization, releasing gametes in synchrony (Vize, 2006) during the months of August through October (Nunes et al. 2009). In addition, algal symbionts are not present in the eggs and thus be acquired from the water column. In a previous study (see Chapter 2), we undertook the most comprehensive analysis of population genetic structure for *M. cavernosa* in both horizontal (long-distance) and vertical (short-distance) directions. Overall, we showed that this species exhibits significant genetic differentiation with

depth in Florida (Upper and Lower Keys), but not in Bermuda or the U.S. Virgin Islands (USVI), despite high levels of horizontal connectivity between all three of these geographic locations at shallow depths. These observations strongly suggest that long-distance horizontal connectivity is much greater than short-distance vertical connectivity for *M. cavernosa*. However, whether these patterns were driven by intrinsic factors (e.g., reproductive mode) or extrinsic factors (e.g., local hydrology) remains unknown.

The main goal of the present study was to examine to what extent the contrasting life-history and reproductive strategies of *P. astreoides* and *M. cavernosa* can influence larval dispersal and levels of gene flow at both horizontal (long-distance) and vertical (short-distance) scales. First, we expanded the empirical dataset from our previous study (Chapter 2) to include samples from *P. astreoides* from the same geographic locations [Upper Keys, Lower Keys and Dry Tortugas (within Florida), Bermuda and the USVI] and depths (shallow ≤ 10 m, mid 15-20 m and deep ≥ 25 m) as those from *M. cavernosa*. Then, we used a combination of newly-developed and existing DNA microsatellite loci for *P. astreoides* to evaluate patterns of connectivity at three levels: among geographic locations (long-distance dispersal), among reefs within a geographic location (within Florida), and among depths in each region (short-distance dispersal). Migration rates were estimated among depths in each region to determine whether coral larval migration was more likely to occur from shallow to deep, from deep to shallow, or in both directions symmetrically. Finally, we tested whether depth zonation in algal symbionts (*Symbiodinium* spp.) might limit effective vertical connectivity for *P. astreoides* due to maternal transmission of symbionts from parent colonies to larvae.

METHODS

Sample collection

Field activities were focused on shallow (≤ 10 m), intermediate (15-20 m) and deep (≥ 25 m) coral communities along the (1) Florida Reef Tract (within sites in the Upper Keys, Lower Keys and Dry Tortugas), (2) Bermuda, and (3) the USVI (Table 3.2, Figure 3.1). At each site, a haphazard approach was used to collect samples from colonies at least 1 m apart to minimize the likelihood of sampling clones. Two different sampling methods were used, per the requirements of the respective permitting agencies. When permitted, samples were removed from colonies as small tissue biopsies (0.25 cm^2) using a 4 mm internal diameter hollow steel punch, and preserved in 95% ethanol. When destructive sampling was not permitted, tissue biopsies were collected using a razor blade, transferred at the surface to a 2 mL tube with 500 μL of DNAB + 1% SDS (Rowan and Powers, 1991), and heated to 65°C for 1.5-2 hrs. Finally, since *P. astreoides* is known to occur as two color morphs (yellow/green and brown), we recorded this information as often as possible ($n = 200$).

Microsatellite development

To minimize contamination by symbiont DNA in the template used for host microsatellite development, *P. astreoides* tissue was bleached using the photosynthetic inhibitor DCMU as described in Jones (2004). Sampling occurred when the colony appeared visibly pale and genomic DNA was extracted using a modified organic extraction (Baker et al. 1997), prior to 454 sequencing on a Roche GS 454 FLX+ sequencer, and subsequent library construction (Genomics Core Facility, Penn State University).

A total of 30,770 single sequence reads (i.e., not assembled into contigs) generated from the 454 sequencing were searched for the presence of microsatellite repeats using the computer program Tandem Repeat Finder (Gelfand et al. 2006). Primers were designed for a subset of sequences with a minimum of six tri-, tetra-, penta- or hexanucleotide repeats (n = 40) using the web-based program Primer 3 (Untergrasser et al. 2012). Primers were screened for variability and optimized by visually inspecting bands on 2% agarose gels. Candidate markers (n = 6) were then screened against the algal symbionts isolated from the colony used for microsatellite development (identified as *Symbiodinium* type A4) and other preexisting algal cultures in clades A, B, C and D isolated from this species or the coral species *Orbicella faveolata*, to confirm specificity to host DNA. None of the candidate markers amplified any of the cultured *Symbiodinium*. Therefore, they were determined to be derived from the host and thus useful for proposed analyses.

Microsatellite genotyping

Four microsatellite loci were further developed for scoring on an ABI 3730 automated sequencer. Forward primers were fluorescently labeled with NED, VIC or 6FAM (Applied Biosystems, CA). PCR reactions were performed in two multiplex reactions (11 μ L total volume, consisting of 2 primer pairs each) using 1 μ L of 50-100 ng of template DNA (Table 3.1). Reactions were performed using primer concentrations specific to each locus (Table 3.1), 5 \times PCR Reaction Buffer (Promega), 2.75 mM of MgCl₂ (Promega), 0.8 mM of dNTPs, and 0.5 U of Taq polymerase (Promega).

P. astreoides samples were amplified with a total of 8 microsatellite loci (Table 3.1): four as described above and four as described in Kenkel et al. (2013). Thermal

cycling for all reactions was performed with an initial denaturation step of 94°C for 3 min, followed by 35 cycles of 94°C for 1 min; 57°C (annealing temperature) for 1 min; 74°C for 1 min; and a final extension at 74°C for 7 mins. PCR products were visualized with an automated sequencer (ABI 3730) using an internal size standard (Genescan LIZ-500, Applied Biosystems, CA). Electropherograms were visualized and alleles scored using the software GeneMapper 4.0 (Applied Biosystems, CA). Samples that failed to amplify more than two of the eight loci ($n = 190$), or samples which exhibited triallelic genotypes ($n = 12$) at any of the markers from Kenkel et al. (2013) were excluded from further analysis. In this dataset, there was a per locus failure rate of <10% (except for marker Past_3 which had a failure rate of 13.7%), and a per sample failure rate of 0.51%.

Analysis of multi-locus genotype (MLG) data

Identical MLGs (clones) were identified in GenAlEx v.6.41 (Peakall and Smouse, 2006) by requiring complete matches at all loci. The same number of unique MLGs ($n = 590$) were found whether missing data were considered or not. Unique MLGs were then used for subsequent analyses. Tests for conformation to Hardy Weinberg Equilibrium (HWE) expectations were performed using the program Genepop (Raymond and Rousset, 1995). The R-package FDRtool was then used to adjust p-values for multiple testing (Strimmer, 2008). Since large heterozygote deficits are common in marine invertebrates (Addison and Hart, 2005; Baums, 2008), the program INEST (Chybicki and Burczyk, 2009) was used to distinguish among some of the possible causes for departures for HWE by estimating null allele frequencies while accounting for inbreeding. Population level pairwise F_{ST} comparisons were performed in GenAlEx v.6.41. Finally, principal component analysis (PCA) was performed on a matrix of covariance values

calculated from population allele frequencies in the program GenoDive v.2.20 (Meirmans and Van Tienderen, 2004).

Population structure was investigated using a Bayesian clustering approach performed in STRUCTURE v.2.3.3 (Pritchard et al. 2000), on the web-based Bioportal server from the University of Oslo. Correlated allele frequencies and admixed populations were assumed. Values of $K = 1-20$ were tested by running three replicate simulations with 10^6 Markov Chain-Monte Carlo repetitions each and a burn-in of 10^3 iterations. The most likely value for K based on the STRUCTURE output was determined by plotting the log probability $[L(K)]$ of the data over multiple runs and comparing that with delta K (Evanno et al. 2005), as implemented in the web-based program STRUCTURE HARVESTER (Earl, 2009). Results of the three STRUCTURE runs for the most likely K were then merged with CLUMPP (Jakobsson and Rosenberg, 2007) and visualized with DISTRUCT (Rosenberg, 2004).

Migration patterns were estimated using MIGRATE v.3.4.2 (Beerli and Felsenstein, 2001). We used the results of STRUCTURE (Figure 3.2) as prior information to compare four different gene flow models at each geographic location (except Dry Tortugas, see below): (A) a full model with three populations (shallow, mid and deep) and symmetrical gene flow; (B) a model with two populations (shallow and mid/deep pooled) and one migration rate from shallow to mid/deep; (C) a model with two populations (shallow and mid/deep pooled) and one migration rate from mid/deep to shallow; and (D) a model where all three populations (shallow, mid and deep) were considered part of the same panmictic population. In the case of Dry Tortugas, we used the results of STRUCTURE as prior information to pool individuals from shallow and

intermediate depths instead of intermediate and deep depths. Finally, the most complex model (A) was used to experiment with run conditions until convergence was achieved and posterior distributions were acceptable [final parameter settings: long-inc 100, long-sample 15,000, replicates 20, burn-in 20,000, and 4 heated chains (1, 1.5, 3, 100,000)]. Models A – D were then compared and ranked using the thermodynamic integration framework as described in Beerli and Palczewski (2010).

Algal symbiont characterization

A subset of the corals used for microsatellite analyses was selected haphazardly to assess the diversity of symbiont populations and potential patterns of depth zonation. *Symbiodinium* types were identified by denaturing gradient gel electrophoresis (DGGE) and sequencing of ITS-2 rDNA. This gene region was amplified using the primers ITSintfor2 and ITS2clamp (LaJeunesse and Trench, 2000) and amplification products were separated by DGGE using a 35-75% gradient. Dominant bands on the gel were excised, re-amplified, and sequenced using the BigDye Terminator v3.1 cycle sequencing kit and an automated sequencer (ABI 3730). Sequences were then identified via BLAST in GenBank (accession numbers are given in Appendix 3.4).

Quantitative PCR (qPCR) assays were used in addition to DGGE to better understand patterns of zonation with depth and detect the presence of background symbiont types not detectable by DGGE (e.g., Mieog et al. 2009). The assay for *Symbiodinium* clade A targeted the ITS1-5.8S-ITS2 of the large subunit of the nuclear rDNA, and was carried out as described in Correa et al. (2009b). Assays targeting specific actin loci in *Symbiodinium* clades C and D, however, were carried out in multiplex as described in Cunning and Baker (2013). All qPCR reactions were performed

using a StepOnePlus Real-Time PCR System (Applied Biosystems, CA) and reaction volumes were 10 μ l, using 1 μ l of genomic DNA template. Two replicates per sample were used per clade assayed.

RESULTS

Multi-locus genotyping and tests of Hardy Weinberg Equilibrium

Our genetic analysis of 660 *P. astreoides* samples yielded 590 unique MLGs (Table 3.2), suggesting 10% clonality, either as result of asexual reproduction and/or fragmentation. Most clones were confined to a single sampling location (within <1 km) except in two cases, both at two different mid-depth sites within the Upper or Lower Keys. Tests of HWE for each of the 15 combinations of region/depth (Table 3.2, population column) individually revealed that all 8 loci are largely in HWE, as only 5.8% of 120 tests showed significant deviations from HWE after FDR correction (Appendix 3.1). Individual inbreeding values were generally low (F_i mean = 0.01; 95% confidence interval = 0 - 0.04), as well as null allele frequencies (which ranged between 0.03 - 0.06 across loci and populations, Appendix 3.2).

Assessment of vertical vs. horizontal connectivity

Patterns of genetic subdivision for *P. astreoides* showed strong support for three clusters (Figures 3.2, 3.3A and 3.3B) that correlate with depth in Florida (shallow vs. deep), and with geographic distance (Bermuda vs. Florida or the USVI). Within Florida, significant differentiation with depth was observed in all three regions. The largest differentiation occurred in the Upper Keys, with 79% of the individual colonies at intermediate and deep depths (≥ 15 m) assigned with high probabilities of membership ($>70\%$) to the deep cluster (depicted in orange, Figure 3.2). Conversely, the Dry Tortugas

exhibited significant differentiation with depth, but at depths ≥ 25 m, and with only 59% of the colonies at this depth assigned with high probabilities of membership to the deep cluster. Finally, 17% of all the Florida individuals showed signs of admixture (i.e., individuals with probabilities of membership $< 70\%$ to either cluster), suggesting some degree of interbreeding between shallow and deep colonies. In addition, we identified a large number of individuals as migrants (i.e., originated from a different depth than the one they were collected from), particularly in the Lower Keys. Specifically, 13% of the individuals in the Lower Keys shallow habitats exhibited high probabilities of membership to the deep cluster, while 16% of the individuals in deep habitats exhibited high probabilities of membership to the shallow cluster. Finally, despite significant structure with depth in Florida, high levels of gene flow were observed among depths in the USVI and Bermuda. The USVI shared the common shallow cluster present in Florida at all depths (42-81%). Conversely, the “local” Bermudan cluster (depicted in green, Figure 3.2) dominated across all depths (46-95%) within this geographic location.

Overall, no genetic structure was observed among shallow sites of Florida and the USVI (Figure 3.2), suggesting a high degree of horizontal connectivity among sites separated by $> 1,700$ km within the Caribbean. Conversely, Bermuda appears isolated from the rest of the Caribbean, but there are a few individuals who appear to share the same shallow population present in Florida and the USVI at the 4 m (shallow) offshore site (Figure 3.2). Isolation-by-distance analyses confirmed these results (Figures 3.5A, 3.5B and 3.5C), as 39% of the variation in genetic distance is explained by geographic distance between Florida and Bermuda, while none of the variation was explained by geographic distance between Florida and the USVI. Pairwise F_{ST} were also in agreement

(Table 3.1B). The largest F_{ST} values occurred when Bermudan populations are compared to any of the populations from Florida or the USVI, regardless of depth. Finally, PCA analyses (Figure 3.2B) also suggested that populations from Bermuda were reproductively isolated from Florida or the USVI (PC1, explaining 39% of the variance) and that habitats clustered together by depth within Florida (PC2, explaining 21% of the variance). All populations within the USVI (regardless of depth) clustered together with the common shallow population present in Florida.

Genetic variation due to differences in color morph

Our findings show that genetic subdivision was not associated with color morph type (Appendix 3.6), suggesting that both color morphs (yellow/green or brown) constitute a single species.

Migration rates among shallow and deep habitats

Table 3.4A summarizes the marginal log-likelihood differences (LBFs) and ranking of each of the 4 gene flow models compared (A= full, B= shallow to mid/deep, C= mid/deep to shallow and D= panmixia) using the thermodynamic integration approximation as described in Beerli and Palczewski (2010). Overall, this method consistently ranked the gene flow model with migration from shallow to mid/deep (or shallow/mid to deep in Dry Tortugas) as the best model across all regions. This ranking occurred even for regions where STRUCTURE suggested panmixia (Bermuda and the USVI). Furthermore, the ranking of all the other 3 gene flow models under comparison (A, C and D; Table 3.4A) occurred similarly in all 5 regions. Finally, the largest significant differentiation between the Upper Keys shallow and deep sites observed in

Figure 3.2 is confirmed by the smallest number of migrants per generation (N_m) from shallow to mid/deep compared to any other region (Table 3.4B).

Algal symbiont characterization

DGGE showed evidence for strong depth zonation in algal symbionts in both Florida and the USVI, but not in Bermuda (Figure 3.6A). In Florida and the USVI, most shallow and mid-depth colonies only hosted *Symbiodinium* types A4 or A4a. However, most deep colonies only hosted *Symbiodinium* type C1. The shift appears to occur quite deep, as colonies in the range of 20-30 m hosted either A4/A4a or C1, whereas all colonies deeper than 30 m only hosted C1. In Bermuda, on the other hand, all colonies hosted *Symbiodinium* type A4 or A4a across all depths (Figure 3.6A). Mixed symbiont communities (A4 + B1) were detected at this location, but only in samples from the 4 m inshore (shallow) site.

Further analyses with qPCR (Figures 3.6B and 3.6C) revealed mixed symbiont communities (A+C, A+D, C+D or A+C+D) in shallow and deep corals from Florida, but not from Bermuda or the USVI. Fifty percent of the shallow and 14% of the deep corals assessed from Florida had background D not previously detected with DGGE (Figure 3.6B). Colonies identified as “migrants” (Figure 3.6C) also hosted mixed symbiont communities in Florida, but not in the USVI (which only hosted A or C). Furthermore, “migrant” colonies hosted symbionts most commonly found in the habitat they settled in, rather than the symbionts most commonly found in their depth of origin (Figure 3.6C). For example, 33% of the “migrant” colonies from deep water origin that settled in shallow habitats in Florida hosted background D not previously detected with DGGE.

DISCUSSION

Horizontal (long-distance) connectivity

This study represents the first assessment of connectivity for the coral species *Porites astreoides* within the Caribbean region. Overall, very little differentiation was found between shallow sites in Florida and the USVI, despite being separated by >1,700 km (Figures 3.2, 3.4 and 3.5B, Table 3.3). These findings suggest that this coral species has the ability to disperse over large distances within the Caribbean region. Furthermore, these findings suggest genetic exchange between the eastern and western Caribbean (even though we only sampled one location at each), despite the lack of genetic exchange among these regions observed for broadcast spawning coral species such as *Acropora palmata* (Baums et al. 2005b) and *Orbicella annularis* (Foster et al. 2012).

The high gene flow observed for *P. astreoides* within the Caribbean region did not translate into high levels of connectivity between the Caribbean and Bermuda. Findings strongly suggest that, in contrast to *M. cavernosa* (Chapter 2), *P. astreoides* from Bermuda are generally isolated from the rest of the Caribbean (Figures 3.2, 3.4 and 3.5B, Table 3.3). However, the presence of a few individuals at the offshore shallow (4 m) site which share the same common population from Florida and the USVI (Figure 3.2) suggests that larvae originating from the Caribbean can occasionally disperse and settle in Bermuda. In agreement with these findings, Nunes et al. (2011) showed that, out of 6 coral species, the only one which showed no significant differentiation between Brazil and the Caribbean was *P. astreoides*, suggesting that this species also has the potential to disperse as far south as Brazil. The authors concluded that the long-distance dispersal

observed in this species could be due to its ability to raft and/or its tolerance to freshwater and high sedimentation.

Vertical (short-distance) connectivity

The degree of vertical connectivity varied among and within geographic locations (Figure 3.2). Within Florida, significant structure with depth was observed at all 3 regions. Patterns weakened from east to west, with the largest differentiation occurring in the Upper Keys and the lowest in the Dry Tortugas (Figure 3.2). In addition, the depths at which this transition occurred were quite shallow and varied regionally: in the Upper and Lower Keys the transition occurred at ≥ 15 m, while in the Dry Tortugas it occurred at ≥ 25 m. Bermuda and the USVI, on the other hand, appeared to be highly panmictic, although it is possible that at these two locations the corresponding deep habitat may be at greater depths than those assessed (>33 m). Alternatively, no genetic barriers may exist with respect to depth, suggesting that at these locations deep reefs may act as important recruitment sources for their shallow water counterparts, as predicted by the Deep Reef Refugia Hypothesis (*sensu* Bongaerts et al. 2010).

Overall, the patterns observed in this study for *P. astreoides* are remarkably similar to those found for the broadcast spawning coral *M. cavernosa* (Chapter 2), despite different life-history reproductive strategies. In fact, both species exhibited similar patterns of genetic differentiation with depth in 4 of the 5 regions assessed (Upper Keys, Lower Keys, Bermuda and the USVI); strongly suggesting that extrinsic factors are more likely to influence patterns of vertical connectivity in Caribbean corals. For example, since light is regarded as the primary factor limiting the maximum depth of hermatypic coral growth (Falkowski et al. 1990; Mundy and Babcock, 1998), the absolute depths

defining the degree of genetic structure may vary as a result of site-specific variability in parameters such as water clarity and/or light intensity, which in turn result in different light regimes with depth. In addition, we hypothesized in Chapter 2 that variation in local hydrology could drive differences in patterns of genetic structure within Florida, such that strong currents near the Dry Tortugas might facilitate genetic mixing between shallow and deep colonies compared to the Lower and Upper Keys.

Inshore vs. offshore differences?

Interestingly, findings suggest little genetic mixing between the Bermuda offshore shallow (4 m) site and all other Bermuda sites – including the inshore shallow (4 m) site – despite similar depths and close proximity (~3.5 km). Kenkel et al. (2013) had similar findings among individuals in inshore vs. offshore shallow sites (2-3 m) in the lower Florida Keys. The authors suggested that *P. astreoides* coral populations inhabiting reefs <10 km apart within the same depth range can exhibit substantial genetic differences as well as physiological differences in response to thermal stress. However, our analyses comparing inshore vs. offshore shallow sites in the Upper Keys do not appear to support these conclusions, as there was little evidence for genetic differentiation among shallow inshore or offshore sites (Appendix 3.5). Instead, the presence of a few individuals at offshore shallow sites with high probabilities of membership to the deep cluster suggests that it is possible that some of the genetic differences observed in Kenkel et al. (2013) might be due to whether these individuals originated in shallow vs. deep water. In other words, genetically different individuals observed in offshore shallow sites in Kenkel et al. (2013) could be of deep water origin, as a result of their closer proximity to deep reefs compared to inshore shallow sites.

Is genetic variation due to differences in color morph?

More than two decades ago, Potts and Garthwaite (1991) suggested that the two *P. astreoides* color morphs (yellow/green and brown) could be in fact two different species. To test this hypothesis, we assessed whether patterns of genetic structure (Figure 3.2) were driven by differences in color morph. Our findings clearly show that genetic subdivision is not associated with color morph type (Appendix 3.6), suggesting that both color morphs constitute a single species (i.e., are not reproductively isolated). These findings are in agreement with Weil (1993), who failed to detect any significant genetic differences between the two color morphs. The author thus concluded that differences in color among *P. astreoides* colonies might be more related to depth and habitat. Gleason (1993) further showed that morph-specific variation in *P. astreoides* appears to correspond to differences in UV tolerance.

Migration rates among shallow and deep habitats

The gene flow model with migration from shallow to mid/deep (or shallow/mid to deep in Dry Tortugas) was ranked as the best model in all 5 regions (Table 3.4A). These findings strongly suggest that there is an asymmetry in gene flow, with greater downward migration from shallow to deep habitats. Overall, these findings agree with those for the broadcast spawning species *M. cavernosa* (Chapter 2) and octocoral *Eunicea flexuosa* (Prada and Hellberg, 2013). Taken together, these findings strongly suggest that this asymmetry in gene flow might be more common than appreciated in corals. We hypothesized in Chapter 2 that one reason for this asymmetry is higher gamete production in shallow environments, as a result of higher growth rates, coral cover, and polyp density per area, as well as a faster growth to sexual maturity compared to deeper

environments (e.g., Riegl and Piller, 2003; Villinski, 2003; Mass et al. 2007; Slattery et al. 2011; Prada and Hellberg, 2013). In addition, we hypothesized that shallow colonies might be more capable of allocating more energy reserves to gamete production compared to deep colonies due to a greater translocation of photosynthetic products from algal symbionts (e.g., Muscatine et al. 1989; Mass et al. 2007). Finally, we hypothesized that deeper reefs may be less environmentally harsh than shallow reefs, promoting higher survivorship of migrants in a downward direction.

Alternatively, fragmentation of shallow colonies and subsequent gravity-driven re-attachment in deeper habitats (i.e., adult migration) would result in a higher migration from shallow to deep. However, this is unlikely since all repeated MLGs observed were confined to the same sampling location (within 1 km) and/or depth interval.

Algal symbiont characterization

Using DGGE, we found that most shallow corals in Florida and USVI only associated with *Symbiodinium* types A4 or A4a, while most deep colonies (particularly ≥ 30 m) only associated with *Symbiodinium* type C1 (Figure 3.6A). Similar results were found by Baker (1999) in Panamá and Bahamas, and Warner et al. (2006) along a depth gradient in Belize (2-25 m). The only main difference between this study and Warner's study is that the depth at which we observed all colonies to host type C1 was slightly deeper (≥ 30 m vs. ≤ 25 m). Further analyses with qPCR (Figures 3.6B and 3.6C) however, revealed mixed symbiont communities (i.e., those hosting multiple *Symbiodinium* types) in shallow, deep, and "migrant" colonies from Florida, but not from the USVI. Since *P. astreoides* acquires algal symbionts via maternal transmission, these findings strongly suggest that a large portion of colonies from Florida acquire new

symbionts after settlement either through “switching” or “shuffling” (*sensu* Baker, 2003). In fact, colonies identified as migrants were more likely to contain algal symbionts that matched those found in the habitats they settled in, rather than remaining with the type they inherited from their parents (Figure 3.6C). This is not entirely surprising, as van Oppen et al. (2011) observed similar patterns for the brooding coral *Seriatopora hystrix* at Scott Reef (Australia), where shallow colonies identified as having originated from deep water also hosted the same *Symbiodinium* type most commonly found in shallow habitats.

While patterns of depth zonation were observed in Florida and the USVI, corals in Bermuda hosted only *Symbiodinium* type A4 or A4a regardless of depth. The lack of depth zonation in this location may be the result of this site’s isolated high latitude location. However, the mixed symbiont communities observed at the inshore shallow site could be the result of this site’s continuous exposure to anthropogenic stressors and high sedimentation rates (Flood et al. 2005), compared to offshore sites. Alternatively, habitat differences (e.g., inshore vs. offshore), could be driving both host (Figure 3.2) and algal symbiont differences (Figure 3.6A).

In summary, contrary to expectations, depth zonation in the algal symbionts of *P. astreoides*, when it occurred, did not appear to affect the ability of this coral to disperse. Instead, we hypothesize that possessing or acquiring the appropriate symbionts (“high light” vs. “low light”) might be an important mechanism used to increase post-settlement survival across a wide range of habitats and depths. This might be particularly important for deep migrants that settle in shallow habitats (Figure 3.6C), as symbionts in clade A are considered “shallow water specialists” (Rowan and Knowlton, 1995; LaJeunesse,

2002). These symbionts are the only known to produce compounds that provide protection from UV (Banaszak et al. 2000), offering a competitive advantage under conditions of high irradiance (LaJeunesse, 2002).

Implications

The Caribbean coral *P. astreoides*, with a brooding reproductive mode and maternal transmission of algal symbionts, was expected to show low levels of gene flow in both horizontal (long-distance) and vertical (depth) directions. However, we found that *P. astreoides* exhibits high levels of horizontal gene flow between the USVI and Florida (>1,700 km), suggesting that *P. astreoides* has similar or greater dispersal potential compared to other Caribbean broadcast spawning taxa [similar: *O. faveolata* (Severance and Karl, 2006) and *M. cavernosa* (Chapter 2); greater: *A. palmata* (Baums et al. 2005b), *A. cervicornis* (Vollmer and Palumbi, 2007) and *O. annularis* (Severance and Karl, 2006)], as well as other Caribbean brooding taxa shown to recruit in close proximity to the parent population (*Siderastraea radians*, Vermeij 2005; *Agaricia agaricites*, Brazeau et al. 2005). Interestingly, Severance and Karl (2006) showed a significant difference in dispersal ability for sister species *O. annularis* and *O. faveolata*, despite their similar reproductive traits. Together, these findings suggest that reproductive mode does not necessarily correlate with dispersal ability, at least in the Caribbean region. These findings contrast with those of Nunes et al. (2011), which found that the extent of gene flow within populations in Brazil was correlated with the reproductive traits of the species studied.

Our findings also suggest that *P. astreoides* exhibits relatively higher levels of vertical (short-distance) connectivity compared to the broadcast spawning species *M. cavernosa* (Chapter 2), as a result of higher interbreeding among shallow and deep

colonies (up to 17% in Florida), and higher survival across depths. In fact, 5% of all *P. astreoides* individuals from shallow habitats in Florida had high probabilities of membership to the deep cluster (compared to 0.3% in *M. cavernosa*, see Chapter 2), suggesting that these deep migrants were able to successfully recruit in shallow habitats (Figure 3.2). One possible explanation is that *P. astreoides* is more competitive in high irradiance (shallow) habitats because it possesses the appropriate symbionts in clade A, whereas *M. cavernosa* hosts the same *Symbiodinium* type (in clade C) across depths (Chapter 2). Alternatively, higher survival of *P. astreoides* might result from availability of maternal (energy) reserves (Szmant, 1986) plus input from algal symbionts (Richmond, 1987) compared to broadcast spawned larvae. This may provide an explanation for why brooding corals might fare better in sub-optimal and/or marginal environments (e.g., Lirman and Manzello, 2009). Finally, *P. astreoides* planulae, competent to settle a few hours after released, might be more capable of controlling their swimming and/or vertical position in the water column compared to broadcast spawned larvae, which might be important for selecting an optimal substratum and increasing post-settlement survival.

Alternatively, a higher degree of vertical connectivity in *P. astreoides* could be the result of increased chances of genetic mixing due to multiple reproductive events per year. Regardless, our findings suggest that *P. astreoides* is effective at dispersing over both long and short distances. Therefore, neither the mode of reproduction or algal transmission is necessarily a good predictor of dispersal ability, at least for coral species within the Caribbean region. Instead, other extrinsic factors (pre- or post-settlement) appear to be more important drivers of connectivity.

Table 3.1. Microsatellite loci for *Porites astreoides*. Given are the locus name, primer sequences, repeat type followed by the number of repeats and the size range of the alleles amplified in base pairs (bp). All reactions had the same annealing temperature (57°C). Forward primers were fluorescently labeled with one of three dyes (6FAM, VIC or NED). Loci were amplified in two multiplex reactions (plex A and B) or as described in Kenkel et al. (2013).

Reference	Locus	Primer sequence (5'-3')	Motif type	Allele size range (bp)	Forward primer (μM)	Reverse primer (μM)	Plex
Current study	PA3	F: VIC-CATTAACCGACTACAGTCCGT R: ACGTAAATCGCAGGACCTC	(TTCTT) imperfect	328-368	0.08	0.08	A
Current study	PA7	F: 6FAM-TTACAGTGGTCAAGCCTGG R: TTACAGGCTCCCACTAGC	(CGTC) ₂ CATC (CGTC) ₆	244-268	0.4	0.4	B
Current study	PA13	F: NED-AGATCCGCCAAGGCGAGTT R: GAGCGACGTAGGCGCAAAGAT	(ATT) ₂ ATG (ATT) ₉	162-219	0.4	0.4	B
Current study	PA69	F: 6FAM-GCCTACCATGTTAAATCCTTG R: TGGTGTAAGTGAAGGTCACA	(ATT) imperfect	157-196	0.08	0.08	A
Kenkel et al. 2013	Past_3	F: FAM-CAGTTGTTCTAAGCTCGCCC R: GGGTTTTGAAGTGCCAGAAA	(CAT) _x	427-460			
Kenkel et al. 2013	Past_16	F: NED-GGTCGGTATGGTCGAAGAAA R: CCTTGGCCTCCGTTAAGATA	(CAT) _x	262-280			
Kenkel et al. 2013	Past_17	F: FAM-ACCAAAATGCTTCCTCGTTG R: AGCGGCCACTTTCTTCTGTA	(ATTG) _x	269-313			
Kenkel et al. 2013	Past_21	F: FAM-TTGGAGATCAGTCGCACAAA R: TCTCTCACTTGCGGGTTCTT	(ATG _x) _x	164-230			

Table 3.2. *Porites astreoides* samples (N= 660). Given are total sample size (N), number of unique multi-locus genotypes (Ng) and ratio of genets over samples collected (Ng/N). GPS locations are in decimal degrees (WGS84). USVI= U.S. Virgin Islands

Region	Sub region	Population	Site name	Site in map	Estimated depth (m)	N	Ng	Ng/N	Latitude	Longitude
Florida	Upper Keys	UK shallow	Conch reef	UK1	5	7	6	0.86	24.9465	-80.50207
			DL patch	UK2	5	10	10	1.00	25.0136833	-80.41387
			Little Conch reef	UK3	5	17	13	0.76	24.9511167	-80.4614
			Marker 39	UK4	5	11	11	1.00	25.0094333	-80.45792
			Sand island	UK5	5	24	19	0.79	25.0178667	-80.36823
			Tavernier Rocks	UK6	5	3	3	1.00	24.9389833	-80.56272
			Hens and Chickens	UK7	5	19	12	0.63	24.9341333	-80.54952
			Wolf reef	UK8	5	9	9	1.00	25.02185	-80.39623
	UK mid	Behind Conch reef	UK9	5	18	16	0.89	24.9575833	-80.45603	
		SW of Molasses reef	UK10	16	16	14	0.88	25.0042333	-80.38757	
		NE of Conch reef SPA	UK11	17	11	9	0.82	24.9465333	-80.45687	
		Conch reef mid TS	UK12	20	53	42	0.79	24.94621667	-80.45595	
	UK deep	Pickles deep	UK15	25	1	1	1.00	24.97095	-80.43075	
		Conch reef deep1	UK14	29	3	3	1.00	24.9580667	-80.45243	
		Conch reef deep TS	UK13	30	18	15	0.83	24.94698333	-80.455617	
		N of Molasses reef	UK16	37	6	5	0.83	25.0041333	-80.37987	
Lower Keys	LK shallow	Western Sambo reef	LK1	8	8	8	1.00	24.4784833	-81.7302	
		Marker 32	LK2	8	18	15	0.83	24.4741667	-81.74268	
		Near Key West	LK3	9	21	21	1.00	24.4687667	-81.82217	
	LK mid	American shoal mid TS	LK4	14	13	10	0.77	24.5158167	-81.54248	
		American shoal mid	LK5	16	22	22	1.00	24.5138167	-81.54315	
	LK deep	American shoal	LK6	25	36	35	0.97	24.5042167	-81.58197	
Dry Tortugas	DT shallow	Dry Tortugas National Park	DT1	8	44	40	0.91	24.6107833	-82.87133	

	DT mid	Near Dry Tortugas	DT2	15	26	26	1.00	24.72225	-82.78715
	DT deep	Outside Dry Tortugas	DT3	25	48	39	0.81	24.62875	-83.10167
Bermuda	BDA shallow	Castle harbour 4m inshore	BDA1	4	26	19	0.73	32.3598833	-64.69243
		Castle harbour 4m offshore	BDA2	4	22	22	1.00	32.3367167	-64.65738
	BDA mid	Castle harbour 18 m	BDA3	18	32	31	0.97	32.3354167	-64.65405
	BDA deep	Castle harbour 26 m	BDA4	26	20	18	0.90	32.3252667	-64.65423
USVI	USVI shallow	Flat Cay	USVI1	7	42	40	0.95	18.5303667	-65.65172
	USVI mid	Buck Island	USVI2	20	12	12	1.00	18.4647167	-65.49722
	USVI deep	College shoal	USVI3	30-33	44	44	1.00	18.3098167	-65.12772
TOTAL					660	590	0.90		

Table 3.3. *Porites astreoides* pairwise F_{ST} values for each population. Statistically significant values ($p = 0.05$) after FDR correction are highlighted in bold. UK=Upper Keys, LK= Lower Keys, DT= Dry Tortugas, Bermuda= Bermuda and USVI= U.S. Virgin Islands.

Population	UK shallow	UK mid	UK deep	LK shallow	LK mid	LK deep	DT shallow	DT mid	DT deep	BDA shallow	BDA mid	BDA deep	USVI shallow	USVI mid	USVI deep
UK shallow	0.000														
UK mid	0.041	0.000													
UK deep	0.062	0.012	0.000												
LK shallow	0.020	0.030	0.045	0.000											
LK mid	0.033	0.008	0.032	0.017	0.000										
LK deep	0.058	0.021	0.023	0.028	0.017	0.000									
DT shallow	0.053	0.085	0.085	0.058	0.071	0.085	0.000								
DT mid	0.037	0.076	0.100	0.029	0.049	0.064	0.069	0.000							
DT deep	0.029	0.014	0.021	0.024	0.005	0.018	0.056	0.046	0.000						
BDA shallow	0.070	0.079	0.070	0.057	0.076	0.057	0.096	0.093	0.068	0.000					
BDA mid	0.070	0.100	0.091	0.071	0.100	0.088	0.106	0.095	0.081	0.024	0.000				
BDA deep	0.088	0.117	0.107	0.094	0.127	0.110	0.119	0.126	0.106	0.033	0.001	0.000			
USVI shallow	0.029	0.048	0.071	0.033	0.033	0.068	0.052	0.045	0.031	0.091	0.095	0.111	0.000		
USVI mid	0.037	0.043	0.050	0.030	0.033	0.039	0.048	0.043	0.027	0.077	0.093	0.118	0.025	0.000	
USVI deep	0.032	0.038	0.051	0.020	0.021	0.032	0.054	0.048	0.026	0.069	0.095	0.119	0.032	0.011	0.000

Table 3.4. *Porites astreoides* (A) Comparison of log Bayes factors (marginal log-likelihood differences, LBF) approximated by thermodynamic integration for four different gene flow models (A= full, B= shallow to mid/deep, C= mid/deep to shallow and D= panmixia) in the Upper Keys, Lower Keys, Bermuda and the U.S. Virgin Islands. In the case of Dry Tortugas, we compared the following four different gene flow models: (A= full, B= shallow/mid to deep, C= deep to shallow/mid and D= panmixia). (B) Estimated mutation-scaled population sizes (θ), mutation-scaled migration rates (M) and number of migrants per generation ($Nm = \theta * M / 4$) between source and receiving populations for model best supported (B = shallow to mid/deep). Numbers in parenthesis indicate the 95% CI for parameters θ and M. UK= Upper Keys, LK= Lower Keys, DT= Dry Tortugas, Bermuda= Bermuda and USVI= U.S. Virgin Islands.

(A)

Region	LBF for model				Rank of model			
	A	B	C	D	A	B	C	D
Upper Keys	-32589	0	-13659	-25790	4	1	2	3
Lower Keys	-15067	0	-824	-5887	4	1	2	3
Dry Tortugas	-12680	0	-1099	-6943	4	1	2	3
Bermuda	-13633	0	-341	-2555	4	1	2	3
USVI	-14784	0	-1008	-4819	4	1	2	3

(B)

Source population	Receiving population	Parameter and 95% CI		
		θ	M	Nm
UK shallow	UK mid/deep	1.48 (0.00-3.20)	12.11 (6.40-18.07)	4.49
LK shallow	LK mid/deep	2.95 (0.20-5.67)	24.33 (4.73-48.73)	17.96
DT shallow/mid	DT deep	1.71 (0.00-3.53)	29.19 (14.13-47.00)	12.49
BDA shallow	BDA mid/deep	2.40 (0.00-5.73)	40.92 (5.60-77.73)	24.55
USVI shallow	USVI mid/deep	2.34 (0.07-4.53)	27.02 (4.53-55.80)	15.81

Figure 3.1. Sampling locations in the Caribbean and western Atlantic. Individual sites are labeled as designated in Table 3.2. White circles denote shallow (≤ 10 m) sites, gray circles denote intermediate (15-20 m) sites, and black circles denote deep (≥ 25 m) sites.

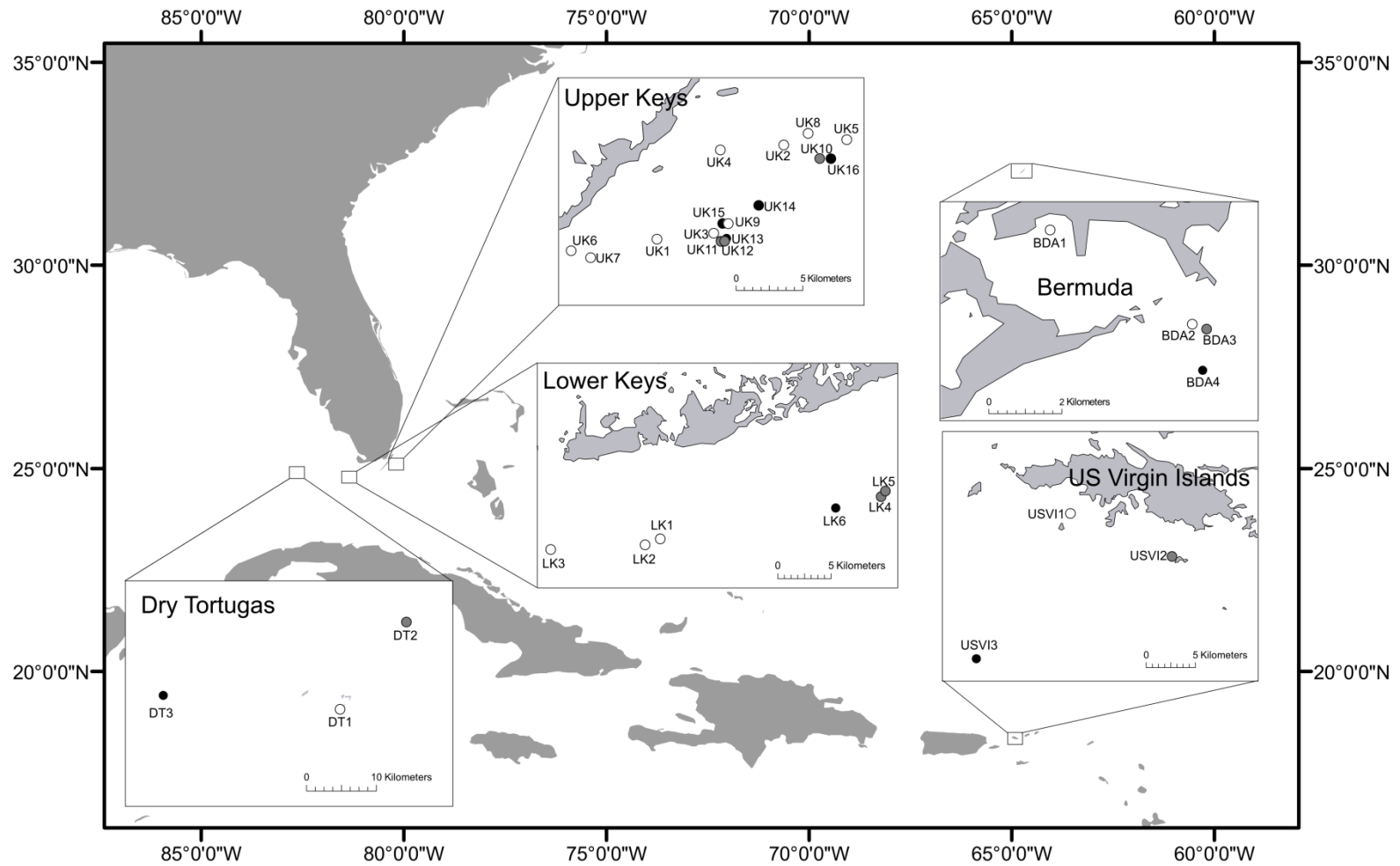


Figure 3.2. *Porites astreoides* population structure across regions [Upper Keys, Lower Keys and Dry Tortugas (within Florida), Bermuda and the U.S. Virgin Islands] and depths [shallow (≤ 10 m), mid (15-20 m) and deep (≥ 25 m)]. Bar graphs show the average probability of membership (y-axis) of individuals ($n = 590$, x-axis) in $K = 3$ clusters as identified by STRUCTURE. Samples were arranged in order of increasing depth within region.

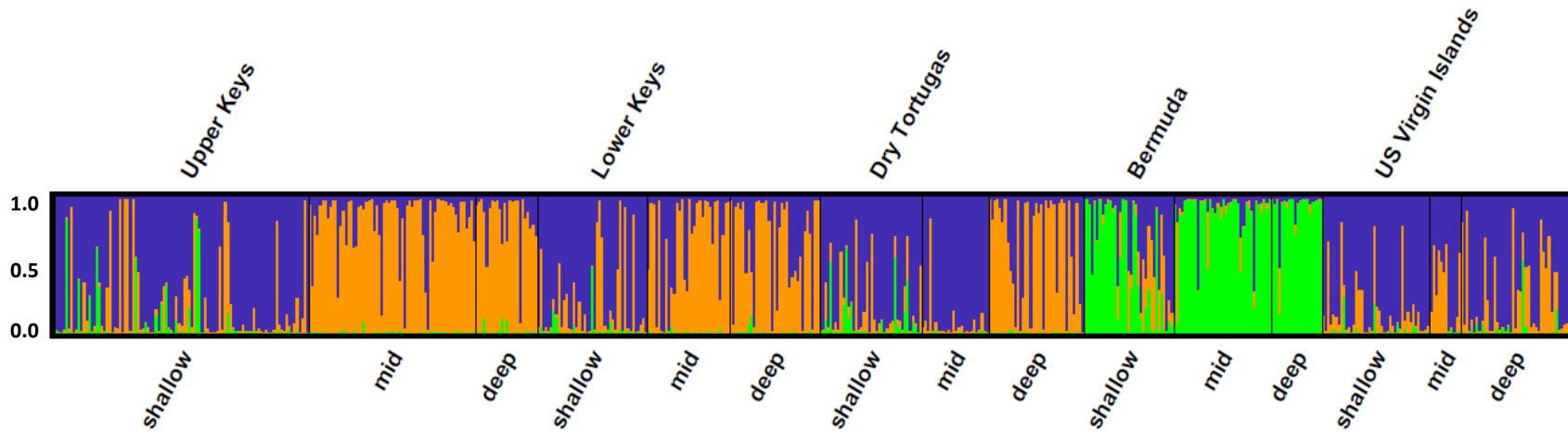


Figure 3.3. Mean log-likelihood of K (A) and Delta K (B) values for STRUCTURE analysis of *Porites astreoides* samples. Values of K = 1 – 20 were tested by running 3 replicate simulations for each K (error bars in upper figure indicate variance among replicates).

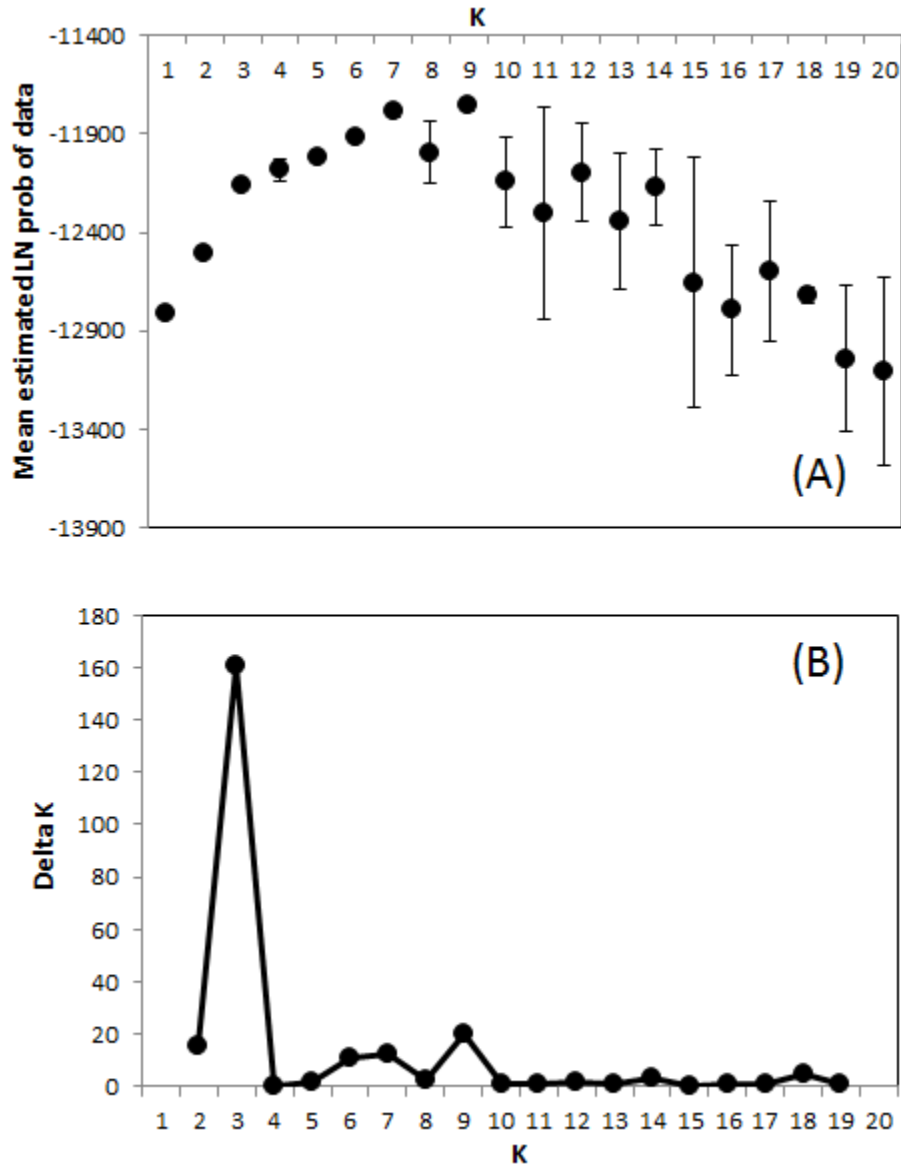


Figure 3.4. Principal Component Analysis (PCA) of allele frequency covariance in *Porites astreoides* populations. 14 of 79 axes were retained, explaining 100% of the cumulative variance. Plotted are the first and second axes explaining 38.59% ($p < 0.01$) and 21.28% ($p < 0.05$) of the variance, respectively. Axes cross at 0. The different shapes denote each of the 3 geographic locations sampled in this study (Florida, Bermuda and U.S. Virgin Islands), whereas different colors denote each of the 3 depths under comparison [shallow (≤ 10 m), mid (15-20 m) and deep (≥ 25 m)]. UK= Upper Keys, LK= Lower Keys, DT= Dry Tortugas, Bermuda= Bermuda and USVI= U.S. Virgin Islands.

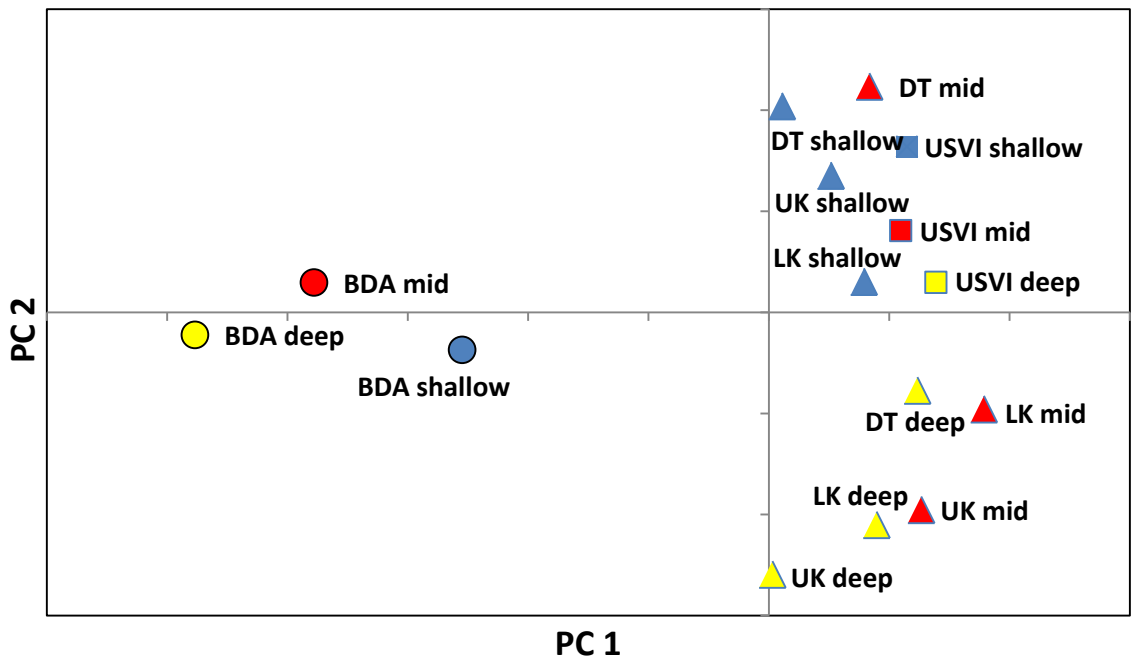


Figure 3.5. Isolation-by-distance patterns in *Porites astreoides*. Geographic distance explained 17% of the variation in genetic distance (F_{ST}) when all sites with ≥ 10 individuals were included (A), 39% when the U.S. Virgin Islands sites were excluded (B), and none when Bermuda sites were excluded (C). USVI= U.S. Virgin Islands

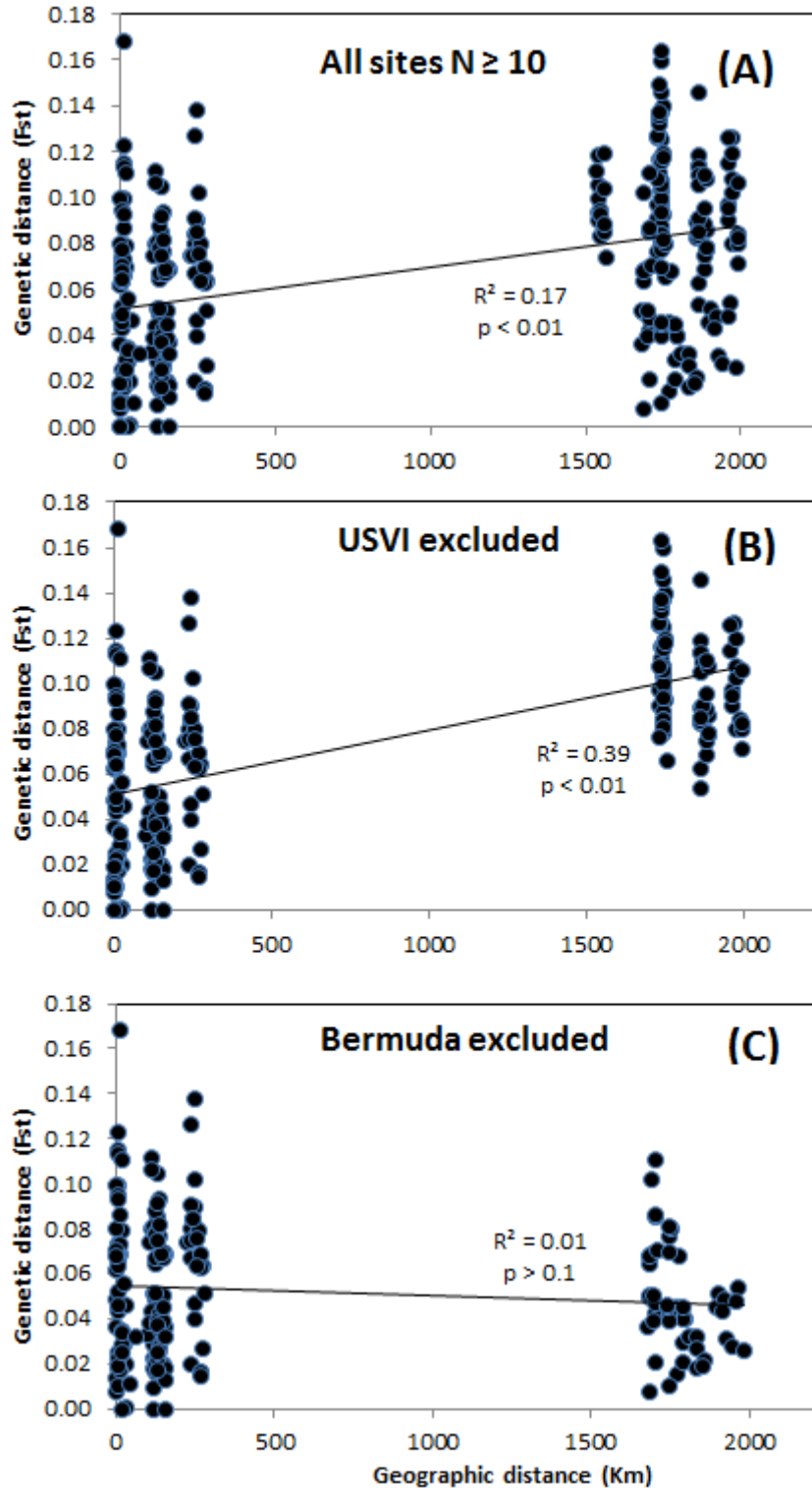
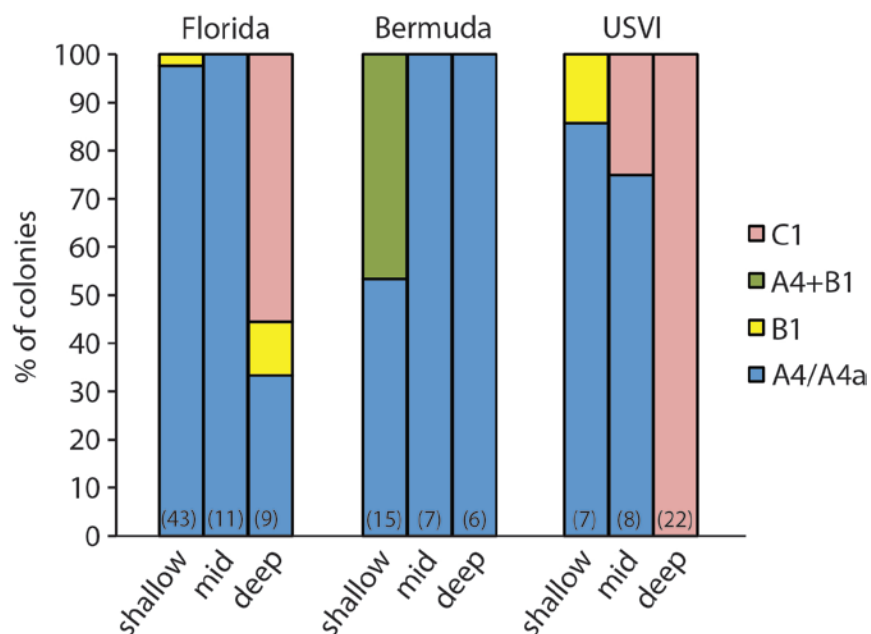
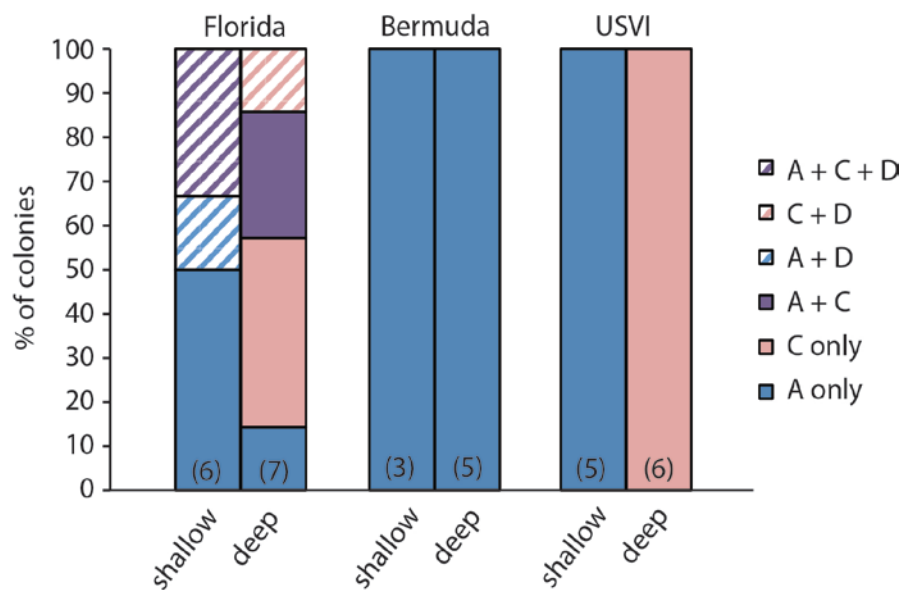


Figure 3.6. *Symbiodinium* types detected in a subset of *Porites astreoides* corals from shallow (≤ 10 m), intermediate (15-20 m) or deep (≥ 25 m) depths, using denaturing gradient gel electrophoresis (A) versus high-sensitivity quantitative PCR (B, C). In (C), migrants were identified in STRUCTURE as having a probability of membership >0.70 to the deep cluster (shallow migrants), or as having a probability of membership >0.70 to the shallow cluster (deep migrants). Note that there are no deep migrants in shallow habitats in the U.S. Virgin Islands. Numbers in parenthesis indicate number of colonies assessed. USVI= U.S. Virgin Islands

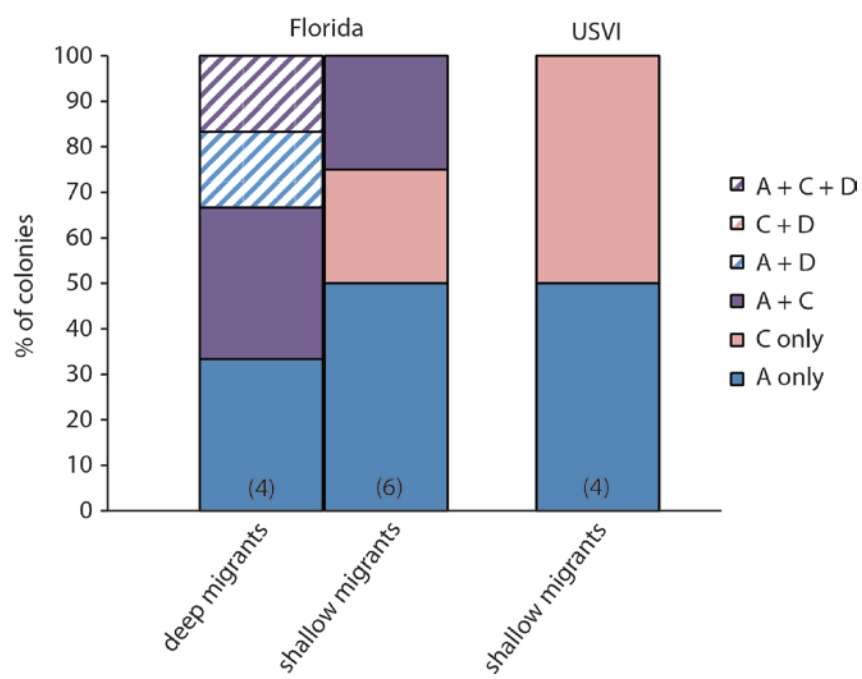
(A)



(B)



(C)



CHAPTER 4

Seascape genetics reveals depth-related patterns of reef coral connectivity between the Flower Garden Banks (Gulf of Mexico) and the Florida Reef Tract

SUMMARY

Since new genetic evidence has shown that coral populations in Florida are isolated by depth (Chapters 2 and 3), we combined the use of genetics and modeling to concurrently examine, for the first time, the degree of connectivity between the Flower Garden Banks (only major coral reefs in the northern Gulf of Mexico) and the Florida Reef Tract at different depth intervals. To achieve this, we expanded our empirical datasets from Florida for the scleractinian coral species *Montastraea cavernosa* (Chapter 2) and *Porites astreoides* (Chapter 3) by including samples from the Flower Garden Banks, and assessed the degree of genetic connectivity between these two regions. Then, we used biophysical modeling to assess whether differences in life-history reproductive strategies among these two species could help explain patterns of connectivity observed. Overall, genetic analyses revealed high levels of gene flow between the Flower Garden Banks (20-30 m) and the shallow (≤ 10 m) Florida population of *M. cavernosa*, but not for *P. astreoides*, suggesting limited gene flow among these regions. These patterns were in general agreement with modeled simulations of larval dispersal, suggesting that (1) Flower Garden Banks might be an important larval source for the shallow Florida population of *M. cavernosa*, and (2) differences in reproductive mode and season might be important drivers of reef coral connectivity within the Gulf of Mexico region.

BACKGROUND

The Flower Garden Banks (FGB) are comprised of two banks (East and West; Rezak et al. 1983; Bright et al. 1984) that rise to about 18 m in depth, and constitute the only two major coral reefs in the northern Gulf of Mexico (GOM) region (Atchison et al. 2008). The closest coral reef system is Lobos-Tuxpan in Mexico (Dokken et al., 2002; Atchison et al. 2008), some 700 km to the south-southwest of the FGB. Although the FGB are located >1,300 km from the Florida Reef Tract (FRT), it could act as important larval source for coral populations in Florida via the Loop and Florida Currents. The Loop Current, which originates in the Caribbean, flows into the GOM and exits through the Florida Straits as the Florida Current (LeHenaff et al. 2012). It is known to transport plankton and fish larvae from the Caribbean into the GOM and the Atlantic (Paris et al., 2005), acting as a major conduit of connectivity between these areas (LeHenaff et al. 2012).

Lugo-Fernandez et al. (2001) investigated coral larval dispersal in the GOM during 6 expected spawning seasons using a combination of satellite-tracked drifters and simulated currents. Observed and simulated tracks showed that coral dispersal in the GOM is primarily driven by 5 circulation modes, one of which is a cross-basin transport that originates near the FGB and arrives near the Florida Keys in 50-60 days. This timeframe is within the expected competency time of broadcast spawned larvae (e.g., Wilson and Harrison, 1998) suggesting that the FGB, once thought to be isolated from the rest of the Caribbean, may function as a source or recruitment stepping stone for coral species in the Florida Keys and points further downstream. Furthermore, Lugo-Fernandez and Gravois (2010) suggested that since mass spawning coincides with hurricane season,

tropical storms might promote coral larval dispersal to and from the FGB by reducing travel times along the basin and increasing the geographic extent of dispersal.

Montastraea cavernosa (Linnaeus, 1767) and *Porites astreoides* (Lamarck, 1816) are common coral species found throughout the Caribbean, including the GOM. *P. astreoides* is considered an early succession species contributing to reef recovery (Goodbody-Gringley et al. 2013), while *M. cavernosa* is an important reef-building coral. Both are considered depth-generalists (Bongaerts et al. 2010) that occur in both shallow and deep water (Goreau, 1959; Goreau and Wells, 1967; Reed, 1985). However, these species differ in their reproductive mode: *P. astreoides* is a brooding coral that undergoes internal fertilization and releases semi-mature planulae from January to September (Szmant, 1986; Goodbody-Gringley et al. 2013), while *M. cavernosa* is a broadcast spawner that releases its gametes in synchrony (Vize et al. 2006) approximately one week after the full moon during the months of August through October (Nunes et al. 2009). *M. cavernosa* thus requires external fertilization, which potentially results in a long pelagic duration (of several days to weeks; Goodbody-Gringley, 2009). Furthermore, its large eggs are thought to increase larval survival time and dispersal capability, as well as increase post-settlement survival (Nunes et al. 2009). Overall, these characteristics are thought to facilitate wide-scale dispersal for *M. cavernosa*, as evidenced by moderate to high gene flow documented in the Caribbean-North Atlantic regions (Nunes et al., 2009; Goodbody-Gringley et al., 2011; see also Chapter 2). However, *P. astreoides* also appear to disperse long distances, as it was shown to exhibit high levels of gene flow between Florida and the USVI (Chapter 3).

In two previous studies (Chapters 2 and 3), we showed that both *M. cavernosa* and *P. astreoides* exhibit significant genetic differentiation with depth within regions in Florida (Upper Keys, Lower Keys and/or Dry Tortugas), despite having very different life-history reproductive strategies. As such, the main goal of this study is to determine whether, and how, the FGB might act as an important larval source for these shallow vs. deep Florida's coral populations, using a multidisciplinary seascape genetics approach. This integrated approach is becoming popular for studying connectivity in reef corals (e.g., Baums et al. 2006; Foster et al. 2012), as it can lead to deeper insight into reef resilience (Selkoe et al. 2008). However, this approach has never been used to explore the mechanisms influencing connectivity at different depths. As a first step, we expanded the empirical datasets from *M. cavernosa* and *P. astreoides* (Chapters 2 and 3) to include samples from the FGB and assess genetic connectivity between the FGB and coral populations in Florida. Then, we estimated migration rates for both species separately in 3 regions within Florida (Upper Keys, Lower Keys and Dry Tortugas) to determine whether migration is more likely to occur (1) from FGB to shallow coral populations in Florida, (2) from FGB to deep coral populations in Florida or (3) whether all three populations consist of one single panmictic unit. Finally, biophysical modeling was used to assess whether connectivity between the FGB and the FRT (if any) is expected to occur through one or multiple generations, and whether differences in reproductive season and pelagic larval duration (PLD) of *M. cavernosa* and *P. astreoides* could affect connectivity between these two locations.

METHODS

I. Empirical genetic data

Sample collection

Within the FRT, corals were sampled using SCUBA at 3 regions (Upper Keys, Lower Keys and Dry Tortugas) in 3 depth zones [shallow (≤ 10 m), intermediate (15-20 m) and deep (≥ 25 m)] (Table 4.1). Three different sampling methods were used, per the requirements of the respective permitting agencies. Where permitted, samples were removed from colonies as small tissue biopsies (0.25 cm^2) using a 4 mm internal diameter hollow steel punch, and preserved in 95% ethanol. When destructive sampling was not permitted, *P. astreoides* tissue biopsies were collected using a razor blade, which was then transferred at the surface to a 2 mL tube with 500 μL of DNAB + 1% SDS (Rowan and Powers, 1991), and heated to 65°C for 1.5-2 hrs. Conversely, *M. cavernosa* samples were collected using a modification of the syringe method described in Correa et al. (2009a). Briefly, a 60 mL syringe (without a needle) was held flush with the upper rim of a corallite and the plunger of the syringe was pulled out, sucking the polyp tissue into the syringe. The syringe was then stored in an individual numbered zip lock bag attached to a slate. After each dive, the contents of each syringe were expelled into a 15 mL Falcon tube and centrifuged for 5 min at 500 g. The supernatant was then removed, and the pellet transferred to a 2 mL tube and heated as described above. Finally, DNA was extracted using a modified organic extraction (Baker et al. 1997).

Collection sites within FGB ranged in depth from 20-30 m (Table 4.1). *P. astreoides* and *M. cavernosa* samples were collected, preserved and extracted as described in Shearer et al. (2005) and Goodbody-Gringley et al. (2011), respectively.

Microsatellite analysis

M. cavernosa samples were amplified with all 9 polymorphic microsatellite loci as described in Chapter 2. *P. astreoides* samples were amplified with all 8 microsatellite loci as described in Chapter 3. For all reactions, 1 µl of 50-100 ng of template DNA was used. PCR products were visualized with an automated sequencer (ABI 3730) using an internal size standard (Genescan LIZ-500, Applied Biosystems, CA). Electropherograms were visualized and alleles scored using the software GeneMapper 4.0 (Applied Biosystems, CA). *P. astreoides* individuals which had triallelic genotypes in any of the markers from Kenkel et al. (2013) were excluded from further analysis. Also, samples that failed to amplify more than two loci were excluded from further analysis (n = 130 for *M. cavernosa*, n = 138 for *P. astreoides*).

Analysis of multi-locus genotype (MLG) data

Identical MLGs (clones) were identified in GenAlEx v.6.41 (Peakall and Smouse, 2006) by requiring complete matches at all loci. Considering missing data in the assignment resulted in the same number of unique MLGs as ignoring missing data (n = 361 for *M. cavernosa* and n = 425 for *P. astreoides*). Unique MLGs were then used for subsequent analyses. Tests for conformation to Hardy Weinberg Equilibrium (HWE) expectations were performed using the program Genepop (Rousset and Raymond, 1995). The R-package FDRtool was then used to adjust p-values for multiple testing (Strimmer, 2008). Tests of pairwise F_{ST} comparisons were done in GenAlEx v.6.41 by comparing each individual population. Finally, principal component analysis (PCA) was performed on a matrix of covariance values calculated from population allele frequencies in the program GenoDive v.2.20.

Population structure was investigated using a Bayesian clustering approach performed in STRUCTURE v.2.3.3 (Pritchard et al. 2000), on the web-based Bioportal server from the University of Oslo. Correlated allele frequencies and admixed populations were assumed. Because sampling location information set as prior information can assist clustering for datasets with weak structure (Hubisz et al. 2009), we used the LOCPRIOR option for *M. cavernosa*. Values of $K = 1-20$ were tested by running replicate simulations (≥ 3) with 10^6 Markov Chain Monte Carlo repetitions each and a burn-in of 10^6 iterations. Finally, results of the three STRUCTURE runs were merged with CLUMPP (Jakobsson and Rosenberg, 2007) and visualized with DISTRUCT (Rosenberg, 2004).

A second approach was used in STRUCTURE to evaluate whether any individuals in the *M. cavernosa* or *P. astreoides* datasets are immigrants to their assumed populations (i.e., STRUCTURE clusters identified in previous runs), or have recent immigrant ancestors. Individuals were pre-assigned to clusters (1= shallow or 2= deep for *M. cavernosa*; 1= shallow, 2= deep or 3= FGB for *P. astreoides*) if they had a probability of membership ≥ 0.70 in previous STRUCTURE runs (without population information). These individuals were used as baseline data (setting USEPOPINFO= 1), by telling STRUCTURE where they originated. STRUCTURE was then run using default values and a value of MIGRPRIOR= 0.08. Finally, potential migrants were identified as those individuals having a ≥ 0.1 probability of being or having an ancestor (parent or grandparent) from another population.

Migration patterns were estimated using MIGRATE v.3.4.2 (Beerli and Felsenstein, 2001). Because we were interested in assessing whether migration is more

likely to go (1) from FGB to shallow coral populations in Florida, (2) from FGB to deep coral populations in Florida or (3) whether all three populations are part of the same panmictic unit, we compared three different gene flow models within each region in Florida: (A) a model with two populations (shallow population of either Upper Keys/Lower Keys/Dry Tortugas and FGB) and one migration rate from FGB to this shallow population, and (B) a model with two populations (deep population of either Upper Keys/Lower Keys/Dry Tortugas and FGB) and one migration rate from FGB to this deep population, and (C) a model where all three populations (shallow and deep populations of either Upper Keys/Lower Keys/Dry Tortugas plus FGB) were considered part of the same panmictic population. To reduce the parameters estimated, we used the results of STRUCTURE (Figures 4.1A and 4.1B) as prior information to decide if we could pool individuals from shallow and intermediate depths or intermediate and deep depths. Consequently, all analyses were performed pooling individuals from intermediate and deep depths, except in the case of *P. astreoides* in the Dry Tortugas, where we pooled individuals from shallow and intermediate depths. Finally, for each region under comparison, different run conditions were tested until convergence was checked and posterior distributions looked acceptable [final parameter settings: long-inc 100, long-sample 15,000, replicates 20, burn-in 20,000, and 4 heated chains (1, 1.5, 3, 100,000)]. The two models described above were then compared and ranked using the thermodynamic integration framework as described in Beerli and Palczewski (2010).

II. Modelling

Two hydrodynamic models, both based on the Hybrid Coordinate Ocean Model (HYCOM; Chassignet et al. 2003), were used to simulate larval dispersal between the

FGB and the FRT. The high resolution (~900 m) Florida Keys/Florida Straits model (FKKeyS-HYCOM; Kourafalou et al. 2009) was nested within the coarser scale (~3.7 km) regional Gulf of Mexico model (GoM-HCOM) for the 5 year period from 2004-2008.

The two hydrodynamic models described above were coupled with the Connectivity Modeling System (CMS) described in Paris et al. (2013). In the Florida Keys, the Backtracking module (Paris et al. 2013) was used to examine possible larval sources in the Gulf of Mexico. However, forward tracking was used to track particles from the FGB after released. Because we were mainly interested in assessing whether differences in reproductive mode of *M. cavernosa* and *P. astreoides* could influence larval dispersal, particles were modeled as neutral (i.e., passive particles). Particle release times were different for each species, depending on the expected reproductive seasons. For *M. cavernosa*, particles were released from August through October, 4-9 days after the full moon, for 5 days each month. Five hundred particles were released from each site (Table 4.1), for a total of 5,250,000. For *P. astreoides*, however, particles were released from April through August around the new moon, for 5 days each month. Five hundred particles were also released from each site (Table 4.1), for a total of 4,875,000. Finally, the Biological module (Paris et al. 2013) was configured to include potential differences in PLD for these species. A maximum PLD of 30 days was chosen for *M. cavernosa*, since broadcast spawned larvae usually require 5–7 days of development in the water column before achieving competency (Harrison and Wallace, 1990). However, a maximum PLD of 10 days was chosen for *P. astreoides*, since brooded larvae are expected to be more advanced in their development when released, and therefore are expected to be competent to settle within hours (Fadllallah, 1983; Szmant, 1986).

RESULTS

I. Empirical genetic data

Multi-locus genotyping and tests of Hardy Weinberg Equilibrium

Our genetic analysis of 363 *M. cavernosa* samples yielded 361 unique multi-locus genotypes (Table 4.1), suggesting virtually no asexual reproduction in this species. The two clones observed were confined to the same sampling location (within <1 km). Tests of HWE were done for each region/depth individually (Table 4.1, population column) and revealed that all 9 loci are largely in HWE, as only 7.8% of 90 tests showed significant deviations from HWE after FDR correction (Appendix 4.1). Locus MC49 had high rates of amplification failure in samples from FGB (78%, Appendix 4.1), but not in any other region or depth.

Our genetic analyses of 484 *P. astreoides* samples yielded 425 unique multi-locus genotypes (Table 4.1), suggesting a ~10% clonality for this species in the regions and depths assessed. Most clones were confined to a single sampling location (within <1 km) with the exception of two cases, both at two different mid-depth sites within the Upper or Lower Keys. Tests of HWE were done for each region/depth individually (Table 4.1, population column) and revealed that all 8 loci are largely in HWE, as only 6.3% of 80 tests showed significant deviations from HWE after FDR correction (Appendix 4.2).

Assessments of genetic connectivity

Patterns of genetic subdivision for *M. cavernosa* (Figure 4.1A) showed strong support for two clusters that correlate closely with depth (within Florida), rather than with geographic distance (FGB vs. FL). The Upper and Lower Keys displayed significant structure with depth, with ~57% and ~90% of the individual colonies at deep depths (≥ 25

m) assigned to the deep cluster (depicted in yellow, Figure 4.1A), respectively. Conversely, Dry Tortugas samples consisted of a single panmictic population across depths, with 81-99% of the colonies assigned to the shallow cluster (depicted in blue, Figure 4.1A). Interestingly, all individuals from FGB were strongly assigned to the shallow cluster present in Florida (>70% probability of membership), despite its depth (20-30 m) and distance (>1,300 km). These patterns were confirmed by pairwise F_{ST} comparisons (Table 4.2A), where the largest F_{ST} values observed were between the shallow and deep sites in the Lower Keys, even though the distance among these sites is only ~20 km. Conversely, no significant differences were found between FGB and shallow sites in Florida. Finally, PCA confirmed the results from STRUCTURE and pairwise F_{ST} comparisons (Figures 4.1A and 4.2A), as 42% of the variance is explained by differences in depth alone, whereas differences due to geographic location (FGB vs. FL) are not significant (second axis, Figure 4.2A).

Patterns of genetic subdivision for *P. astreoides* (Figure 4.1B) however, showed strong support for three clusters, which correlate with depth (shallow vs. deep) in Florida, and with geographic distance (FGB vs. FL) basin-wide. Within Florida, the largest significant differentiation with depth occurred in the Upper Keys, where 79% of the individual colonies at intermediate and deep depths (≥ 15 m) were assigned to the deep cluster (depicted in yellow, Figure 4.1B). FGB appears to be partially isolated from Florida, as most individuals are strongly assigned (>70% probability of membership) to a third cluster (depicted in pink, Figure 4.1B), despite the presence of a few individuals with high probabilities of membership to either the shallow or deep clusters present in Florida. This cluster is confirmed by pairwise F_{ST} comparisons (Table 4.2B), where the

largest F_{ST} values occur between FGB and all other regions in Florida, regardless of depth. PCA further confirmed these results (Figure 4.2B), as habitats clustered together by depth within Florida, and by geographic location (FGB vs. FL). Indeed, >35% of the variance is explained by differences in depth within Florida, whereas >26% of the variance is explained by differences due to geographic distance (FGB vs. FL). Interestingly, PCA also suggests that FGB tends to cluster with shallow habitats in Florida, despite its deeper depth.

Assessment of immigrants using STRUCTURE

Overall, most individuals were correctly assigned to the cluster from which they were sampled (Table 4.3A for *M. cavernosa* and Table 4.4A for *P. astreoides*). For *M. cavernosa*, STRUCTURE identified a total of 30 individuals (8.2%; Table 4.3B) with likely immigrant ancestry in the shallow ($n = 23$) and deep ($n = 7$) clusters. For *P. astreoides* however, this number was much smaller, as only 9 individuals (2.1%; Table 4.4B) were identified by STRUCTURE as having immigrant ancestry in the shallow ($n = 5$) vs. deep ($n = 4$) clusters. No individuals from the FGB cluster were identified as having immigrant ancestry in the shallow vs. deep Florida clusters.

Migration rates among FGB and shallow or deep habitats from Florida

Overall, the thermodynamic integration approximation method described in Beerli and Palczewski (2010) consistently ranked the panmictic gene flow model as the best model across all regions (Table 4.5A). This ranking occurred similarly for both species, even though the *P. astreoides* samples from FGB are significantly different from Florida (Figures 4.1B and 4.2B, Table 4.2B). The model with migration from FGB to shallow populations in Florida was ranked as the second best model across most regions and

species (with the exception of the Lower Keys for *M. cavernosa*, Table 4.5A), despite the relatively deep depth of FGB. Finally, for both species, the largest population sizes (θ) always occurred for the Upper Keys (Table 4.5B), consistent with this region having the largest sample sizes (Table 4.1).

II. Modelling results

Probability density functions per depth interval

For *M. cavernosa*, the backtracking simulations for all three regions in Florida (Upper Keys, Lower Keys and Dry Tortugas) at 5 depth intervals (10, 20, 30, 40 and 50 m) [Figures 4.5-4.10] revealed that the highest concentration of particles occurred at shallow depths (≤ 10 m), even where particles released from intermediate/deep sites (≥ 15 m). In addition, while many of the particles released in the Upper or Lower Keys (regardless of depth) appear to disperse far into the GOM, most of the particles released from the Dry Tortugas appear to be retained within this region even after 30 days of release. Finally, the forward tracking from sites in the FGB (Figure 4.11) showed a similar density of particles across all 5 depth layers. Overall, similar results were found for *P. astreoides* (Figures 4.12-4.18), with the main difference being that the backtracking simulations revealed a higher retention of particles in all three regions in Florida compared to *M. cavernosa*.

Pooled results from backtracking and forward tracking

For *M. cavernosa*, regardless of whether particles were released from the Upper Keys (Figure 4.3A), Lower Keys (Figure 4.3B) or Dry Tortugas (Figure 4.3C) at shallow sites, they appear to disperse far into the GOM region after 30 days in the water column. When juxtaposed with the forward tracking from FGB (Figures 4.3ABC), an area of

overlap was found (depicted in green in Figures 4.3AB) in both simulations for the Upper and Lower Keys, suggesting that habitats within this area could be important stepping stones for multi-generational connectivity between these two locations. Interestingly, no overlap was found among simulations for the Dry Tortugas, even though this area is the closest in distance compared to the Upper or Lower Keys. Finally, none of the three *P. astreoides* backtracking scenarios (Upper Keys, Lower Keys or Dry Tortugas; Figures 4.4ABC) or the forward tracking from FGB (Figures 4.4AB) showed evidence of an overlap among these regions after a maximum PLD of 10 days.

DISCUSSION

Empirical genetic data

Overall, we found strong evidence to support the presence of 2 and 3 genetic clusters for *M. cavernosa* and *P. astreoides*, respectively (Figures 4.1AB, 4.2AB, Tables 4.1AB). Within Florida, differentiation occurred by depth in both species, although at shallower depths in all regions for *P. astreoides*. However, differentiation also occurred with geographic location (FGB vs. FL) for *P. astreoides* (Figures 4.1B and 4.2B, Table 4.2B). These findings suggest that FGB is highly connected to the shallow Florida *M. cavernosa* population, albeit partially isolated from Florida in the case of *P. astreoides*. One possible explanation is that currents favor long-distance dispersal during the expected annual mass spawning season of *M. cavernosa*, but may be less favorable earlier in the year when *P. astreoides* begins its monthly planulation. Lugo-Fernandez et al. (2001) showed that coral dispersal from the GOM to Florida can occur during late summer mass spawning. Lugo-Fernandez and Gravois (2010) further suggested that

hurricanes and tropical storms during spawning season might potentially transport larvae across the basin within a timeframe where larvae are expected to be viable for recruitment. Alternatively, the potentially shorter pelagic duration for brooding species like *P. astreoides* (which release planulae competent for settlement within hours; Harrison and Wallace, 1990) could result in higher recruitment within FGB rather than long-distance dispersal.

The high degree of connectivity observed for *M. cavernosa* across the GOM (Figure 4.1A) confirms the findings of Goodbody-Gringley et al. (2011), who found a high levels of gene flow between shallow sites in the Caribbean (Barbados, Jamaica and Panama) and deep sites in FGB for this species. Conversely, the lack of connectivity between FGB and Florida observed for *P. astreoides* contrasts with the high degree of connectivity observed in Chapter 3 between the USVI and Florida. Therefore, other physical or biological factors localized within the GOM region must be operating to limit effective connectivity between FGB and Florida.

Migration rates and limitations of analyses

The higher degree of connectivity observed for *M. cavernosa* compared to *P. astreoides* (Figures 4.1AB, 4.2AB, Table 4.2AB) was also confirmed by a separate assessment of immigrants using STRUCTURE (Tables 4.2B and 4.3B), where a higher number of *M. cavernosa* individuals were found with likely immigrant ancestry compared to *P. astreoides* (8.2% vs. 2.1%). However, unexpectedly, MIGRATE (Table 4.5A) ranked the panmixia model as best in all three regions for both species. These results support findings for *M. cavernosa*, given that we found no significant genetic differentiation for FGB and the shallow population in Florida for this species. However,

for *P. astreoides*, these findings are not in agreement with all other analyses which suggest significant genetic differentiation for FGB vs. shallow or deep coral populations in Florida (Figures 4.1B and 4.2B, Table 4.2B). It is possible that these findings were driven by insufficient resolution for analyses of MIGRATE, either as result of (1) low sample sizes for FGB, and/or (2) “ghost” or unsampled populations (reviewed in Beerli, 2004) between FGB and Florida. “Ghost” populations are suggested to create the appearance of migration between populations that do not exchange migrants (Slatkin, 2005). In addition, Beerli (2004) explored the effect of having “ghost” populations on gene flow analyses with MIGRATE and found that the biases on the estimation of parameters largely depends on the magnitude of the migration rates from these “ghost” populations. Therefore, it is possible that we were missing “important” populations (i.e., with high immigration rates) between the FGB and FRT for *P. astreoides*. Alternatively, FGB might be simply a “sink” of larvae, having a common upstream population with FRT. We recommend increasing the sample sizes and/or sampling additional populations in the GOM (e.g., sites in the Yucatan peninsula) to get more accurate results.

Modelling results

Overall, the use of backtracking revealed significant differences in the potential for dispersal and connectivity for *M. cavernosa* compared to *P. astreoides*. In all three regions in Florida, a much greater potential for dispersal from the GOM region was observed for *M. cavernosa*. These patterns strongly suggest that reproductive season (and currents associated with this period), as well as potential differences in PLD for this species could be driving the patterns of connectivity observed. Based on these results, it is hypothesized that connectivity between the FGB and the FRT is likely to happen for *M.*

cavernosa directly through the northern GOM region over a few generations. Conversely, the lack of overlap between any of the backtracking or forward tracking trajectories for *P. astreoides* suggest little or no connectivity between the FGB and the FRT. However, it is possible that connectivity among these regions occurs through a different oceanographic mechanism, perhaps east and south in the GOM, along the Yucatan peninsula.

Interestingly, retention within shallow depths in the Dry Tortugas region was observed for both species, and regardless of whether particles were released from shallow or intermediate/deep sites (*M. cavernosa*: Figures 4.9 and 4.10; *P. astreoides*: Figures 4.16 and 4.17). This not surprising, as the Dry Tortugas has a well-established spatial pattern of more mesoscale eddy activity compared to the Lower or Upper Keys (Hitchcock et al. 2005; Kourafalou and Kang, 2012), which has been suggested to be an important retention mechanism for larvae spawned in this area (e.g., Hitchcock et al. 2005; Paris, unpublished data).

Limitations of modeling

Unfortunately, some resolution was lost in the backtracking simulations right in the area where both hydrodynamic models (FKeyS-HYCOM and GoM-HCOM) meet (west of Dry Tortugas). This resulted in an unwanted diagonal line in Figures 4.5-4.10 (*M. cavernosa*) and Figures 4.12-4.17 (*P. astreoides*) in the depth-layered probability density functions. However, since the goal of this study was to assess connectivity between FGB and the FRT (and therefore in the area of overlap between these two regions), we believe that this limitation did not affect the overall outcome of our findings.

A second limitation of the modeling approach used here is that results are based on assuming passive movement of particles, which is likely an unrealistic scenario

(reviewed in Cowen and Sponaugle, 2009). In the future, the CMS can be run using different types of vertical movement, by simulating various behavior and transport processes and giving particles other traits (e.g., buoyancy and vertical migration, see Paris et al. 2013).

Complementary insights from genetics and modeling

Despite some limitations in the analyses, the use of empirical genetic data in conjunction with biophysical modeling led to stronger insights into the factors influencing connectivity between the FGB and the FRT. In general, both methods were in agreement with each other. For example, regardless of the region in Florida, a higher degree of dispersal and connectivity across the GOM was observed for *M. cavernosa* compared to *P. astreoides*. These findings suggest that FGB is more likely to be an important larval source for Florida's shallow populations of broadcast spawning taxa such as *M. cavernosa*, which reproduce later in the year during mass spawning events. Currents during this time might favor long-distance dispersal compared to earlier in the year when brooding species release their monthly planulae. Alternatively, the potentially shorter pelagic duration for brooding species like *P. astreoides* might lead to higher levels of self-recruitment within (or near) Florida and the FGB. Regardless, findings highlight the importance of both intrinsic (e.g., reproductive mode and season) and extrinsic (e.g., oceanographic features) factors when inferring population connectivity.

Implications for the 2010 Gulf of Mexico oil spill

When the Deepwater Horizon (DWH) oil drilling platform exploded, it constituted the largest oil spill in U.S. history (Crone and Tolstoy, 2010; LeHenaff et al. 2012). While the DWH oil spill did not occur close to the Florida Keys, much concern has arisen regarding the potential for oil impacts to reach the FRT via offshore currents (Klemas, 2010; LeHenaff et al. 2012; Goodbody-Gringley et al. 2013). Recently, LeHenaff et al. (2012) used a modeling approach to examine the probability that the Loop Current would entrain oil at the surface of the GOM and direct it towards the Florida Straits. Results suggested that wind plays a major role in pushing the oil toward the coasts along the northern Gulf, preventing the oil from reaching Florida. However, when the wind-induced drift was ignored in the modeling, oil reached the Loop Current and was quickly advected south, reaching the Florida Straits in about 1 month.

Overall, findings from this study suggest that an oil spill originating in the GOM: (1) could have the potential to impact coral communities in Florida by reducing recruitment from the FGB, (2) is more likely to affect broadcast spawning taxa like *M. cavernosa*, due to high levels of gene flow between FGB and the FRT, and (3) regardless of coral reproductive mode, these impacts are more likely to affect shallow habitats, likely sinks for coral larvae produced at FGB. However, although deep coral populations in Florida may constitute refugia due to partial isolation from shallow coral populations, they can still be impacted in the long-term. For example, shallow reefs may be unable to reproduce and/or provide viable recruits down the slope (see Chapters 2 and 3), leaving intermediate and deep coral communities relying entirely on local supply of recruits following catastrophic events.

Table 4.1. *Montastraea cavernosa* (n = 363) and *Porites astreoides* (n = 484) sampling locations. Given per species are total sample size (N), the number of unique multi-locus genotypes (Ng) and the ratio of genets over samples collected (Ng/N). GPS locations are in decimal degrees (WGS84). FL = Florida, FGB = Flower Garden Banks

Region	Sub region	Population	Site name	Estimated depth (m)	<i>M. cavernosa</i>			<i>P. astreoides</i>			Latitude	Longitude
					N	Ng	Ng/N	N	Ng	Ng/N		
FL	Upper Keys	UK shallow	Conch reef	5	13	13	1.00	7	6	0.86	24.9465	-80.5021
			DL patch	5	6	6	1.00	10	10	1.00	25.01368	-80.4139
			Little Conch reef	5	11	11	1.00	17	13	0.76	24.95112	-80.4614
			Marker 39	5	12	12	1.00	11	11	1.00	25.00943	-80.4579
			Sand island	5	12	12	1.00	24	19	0.79	25.01787	-80.3682
			Tavernier Rocks	5	3	3	1.00	3	3	1.00	24.93898	-80.5627
			Hens and Chickens	5	4	4	1.00	19	12	0.63	24.93413	-80.5495
			Wolf reef	5	9	9	1.00	9	9	1.00	25.02185	-80.3962
			Behind Conch reef	5	6	6	1.00	18	16	0.89	24.95758	-80.456
			UK mid	SW of Molasses reef	16	14	14	1.00	16	14	0.88	25.00423
		NE of Conch reef SPA	17	16	16	1.00	11	9	0.82	24.94653	-80.4569	
		Conch reef mid TS	20	N/A		53	42	0.79	24.94622	-80.456		
	UK deep	Pickles deep	25	7	7	1.00	1	1	1.00	24.97095	-80.4308	
		Conch reef deep1	29	12	12	1.00	3	3	1.00	24.95807	-80.4524	
		Conch reef deep TS	30	N/A		18	15	0.83	24.94698	-80.4556		
		N of Molasses reef	37	4	4	1.00	6	5	0.83	25.00413	-80.3799	
	Lower Keys	LK shallow	Western Sambo reef	8	6	6	1.00	8	8	1.00	24.47848	-81.7302
			Marker 32	8	10	10	1.00	18	15	0.83	24.47417	-81.7427
			Near Key West	9	11	11	1.00	21	21	1.00	24.46877	-81.8222
		LK mid	American shoal mid TS	14	20	20	1.00	13	10	0.77	24.51582	-81.5425
		American shoal mid	16	21	19	0.91	22	22	1.00	24.51382	-81.5432	
LK deep		American shoal	25	30	30	1.00	36	35	0.97	24.50422	-81.582	

	Dry Tortugas	DT shallow	Dry Tortugas National Park	8	38	38	1.00	44	40	0.91	24.61078	-82.8713
		DT mid	Near Dry Tortugas	15	31	31	1.00	26	26	1.00	24.72225	-82.7872
		DT deep	Outside Dry Tortugas	25	44	44	1.00	48	39	0.81	24.62875	-83.1017
FGB		FGB	EBN	20-30	3	3	1.00	N/A			27.90665	-93.5926
			EBS	20-30	5	5	1.00	N/A			27.9045	-93.5929
			WBN	20-30	4	4	1.00	N/A			27.87252	-93.809
			WBS	20-30	6	6	1.00	N/A			27.87125	-93.8167
			WBE	20-30	5	5	1.00	N/A			27.87188	-93.8086
			EFGB buoy 2	23-25	N/A			7	7	1.00	27.90532	-93.5915
			WFGB buoy 2	23-25	N/A			7	7	1.00	27.88855	-93.8086
			WFGB buoy 5	23-25	N/A			8	7	0.88	27.88843	-93.809
TOTAL					363	361	1.00	484	425	0.90		

Table 4.2. Pairwise F_{ST} values for each *Montastraea cavernosa* (upper table) and *Porites astreoides* (lower table) population. Statistically significant values ($p < 0.05$) are highlighted in bold. UK = Upper Keys, LK = Lower Keys, DT = Dry Tortugas, FGB = Flower Garden Banks

Population	FGB	DT shallow	DT mid	DT deep	LK shallow	LK mid	LK deep	UK shallow	UK mid	UK deep
FGB	0.000									
DT shallow	0.015	0.000								
DT mid	0.025	0.017	0.000							
DT deep	0.017	0.013	0.009	0.000						
LK shallow	0.025	0.003	0.013	0.017	0.000					
LK mid	0.024	0.036	0.026	0.024	0.042	0.000				
LK deep	0.055	0.069	0.044	0.036	0.075	0.011	0.000			
UK shallow	0.012	0.000	0.022	0.013	0.007	0.034	0.067	0.000		
UK mid	0.010	0.021	0.006	0.005	0.026	0.008	0.023	0.018	0.000	
UK deep	0.031	0.040	0.027	0.008	0.046	0.015	0.015	0.035	0.005	

Population	FGB	DT shallow	DT mid	DT deep	LK shallow	LK mid	LK deep	UK shallow	UK mid	UK deep
FGB	0.000									
DT shallow	0.090	0.000								
DT mid	0.123	0.067	0.000							
DT deep	0.086	0.057	0.059	0.000						
LK shallow	0.076	0.050	0.038	0.029	0.000					
LK mid	0.091	0.069	0.056	0.005	0.019	0.000				
LK deep	0.102	0.086	0.078	0.019	0.033	0.019	0.000			
UK shallow	0.094	0.040	0.032	0.031	0.019	0.036	0.062	0.000		
UK mid	0.100	0.085	0.086	0.012	0.031	0.004	0.016	0.049	0.000	
UK deep	0.095	0.087	0.113	0.025	0.047	0.031	0.020	0.066	0.015	

Table 4.3. Average membership probability for each *Montastraea cavernosa* cluster (A) and potential migrants with inferred ancestry (B), regarded as an individual being an immigrant itself or as having a parent or grandparent from that population. Individuals were assigned to the cluster (1= shallow or 2= deep) with the highest probability of assignment in a previous STRUCTURE run (Figure 4.1A). Potential migrants were identified as having a ≥ 0.1 probability of being or having an ancestor from another population.

(A)

Pop	Inferred clusters	
	Cluster 1 (shallow)	Cluster 2 (deep)
1	0.98	0.02
2	0.02	0.98

(B)

Cluster	Potential migrants	Probability of being from assumed pop	Probabilities of other populations			
			Pop	Individual	Parent	Grandparent
1	KL1169	0.44	2	0.27	0.17	0.12
1	DT203	0.53	2	0.01	0.16	0.30
1	KL1092	0.62	2	0.19	0.10	0.10
1	KL861	0.62	2	0.00	0.05	0.33
1	WE7	0.65	2	0.11	0.12	0.13
1	WS9	0.67	2	0.10	0.13	0.11
1	DT254	0.71	2	0.04	0.11	0.15
1	KL1040	0.71	2	0.13	0.07	0.09
1	DT250	0.74	2	0.04	0.09	0.13
1	KL1130	0.75	2	0.01	0.11	0.14
1	DT105	0.76	2	0.01	0.11	0.12
1	DT231	0.78	2	0.02	0.08	0.13
1	LK027	0.78	2	0.02	0.07	0.13
1	KL1197	0.79	2	0.01	0.10	0.10
1	KL909	0.82	2	0.01	0.05	0.13
1	WS7	0.84	2	0.01	0.06	0.10
1	DT217	0.84	2	0.02	0.04	0.11
1	KL939	0.85	2	0.01	0.05	0.10
1	DT221	0.86	2	0.00	0.03	0.11
1	DT34	0.86	2	0.00	0.02	0.12
1	DT235	0.87	2	0.00	0.03	0.10
1	KL1361	0.88	2	0.00	0.02	0.10
1	FRM1186	0.89	2	0.00	0.01	0.10

2	LK110	0.23	1	0.16	0.42	0.19
2	LK145	0.73	1	0.00	0.08	0.19
2	LK78	0.78	1	0.00	0.10	0.12
2	KL1379	0.83	1	0.00	0.03	0.14
2	LK97	0.84	1	0.00	0.03	0.13
2	LK109	0.84	1	0.00	0.04	0.11
2	LK212	0.85	1	0.00	0.05	0.10

Table 4.4. Average membership probability for each *Porites astreoides* cluster (A) and potential migrants with inferred ancestry (B), regarded as an individual being an immigrant itself or as having a parent or grandparent from that population. Individuals were assigned to the cluster (1= shallow, 2= deep and 3= FGB) with the highest probability of assignment in a previous STRUCTURE run (Figure 4.1B). Potential migrants were identified as having a ≥ 0.1 probability of being or having an ancestor from another population. There are no potential migrants in cluster 3 (FGB). FGB= Flower Garden Banks, Pop= population

(A)

Pop	Inferred clusters		
	Cluster 1 (shallow)	Cluster 2 (deep)	Cluster 3 (FGB)
1	0.98	0.01	0.01
2	0.01	0.98	0.01
3	0.01	0.01	0.99

(B)

Cluster	Potential migrants	Probability of being from assumed pop	Probabilities of other populations			
			Pop	Individual	Parent	Grandparent
1	DT174	0.62	2	0.01	0.22	0.15
1	DT175	0.72	2	0.00	0.14	0.13
1	DT234	0.73	3	0.01	0.11	0.14
1	KL1058	0.75	3	0.03	0.10	0.11
1	KL1168	0.78	3	0.01	0.11	0.10
2	KL1016	0.38	3	0.00	0.18	0.40
2	FRP396	0.41	3	0.00	0.06	0.40
2	C497	0.55	3	0.00	0.25	0.16
2	KL908	0.74	3	0.00	0.09	0.11

Table 4.5. Direction of gene flow and number of migrants per generation for *Montastraea cavernosa* and *Porites astreoides*. (A) Comparison of log Bayes factors (marginal log-likelihood differences, LBF) approximated by thermodynamic integration for three different gene flow models (*M. cavernosa*: A= FGB to shallow, B= FGB to mid/deep and C= panmixia; *P. astreoides*: A= FGB to shallow, B= FGB to mid/deep and C= panmixia in the Upper Keys and Lower Keys and A= FGB to shallow/mid, B= FGB to deep and C= panmixia in the Dry Tortugas). (B) Estimated mutation-scaled population sizes (θ) between source and receiving populations for model best supported (C). Numbers in parenthesis indicate the 95% CI for parameter θ . UK = Upper Keys, LK = Lower Keys, DT = Dry Tortugas, FGB = Flower Garden Banks

(A)

Sub region	<i>M. cavernosa</i>						<i>P. astreoides</i>					
	LBF for model			Rank of model			LBF for model			Rank of model		
	A	B	C	A	B	C	A	B	C	A	B	C
Upper Keys	-92445	-344856	0	2	3	1	-21536	-301125	0	2	3	1
Lower Keys	-231421	-215540	0	3	2	1	-70264	-86534	0	2	3	1
Dry Tortugas	-277062	-310098	0	2	3	1	-88269	-202145	0	2	3	1

(B)

Source population	Receiving population	<i>M. cavernosa</i>	<i>P. astreoides</i>
		Parameter and 95% CI	Parameter and 95% CI
		θ	θ
FGB	UK shallow	21.89 (19.27-25.40)	13.98 (0.27-4.13)
FGB	LK shallow	7.026 (3.67-7.40)	6.01 (1.33-6.20)
FGB	DT shallow (<i>M. cavernosa</i>) DT shallow/mid (<i>P. astreoides</i>)	7.35 (3.07-8.73)	2.20 (0.47-3.87)

Figure 4.1. *Montastraea cavernosa* (A) and *Porites astreoides* (B) population structure across regions (Flower Garden Banks, Dry Tortugas, Lower Keys and Upper Keys) and depths [shallow (≤ 10 m), mid (15-20 m) and deep (≥ 25 m)]. Bar graphs show the average probability of membership (y-axis) of individuals (x-axis) in $K = 2$ (*M. cavernosa*) and $K = 3$ (*P. astreoides*) clusters as identified by STRUCTURE. Within regions, samples were arranged in order of increasing depth.

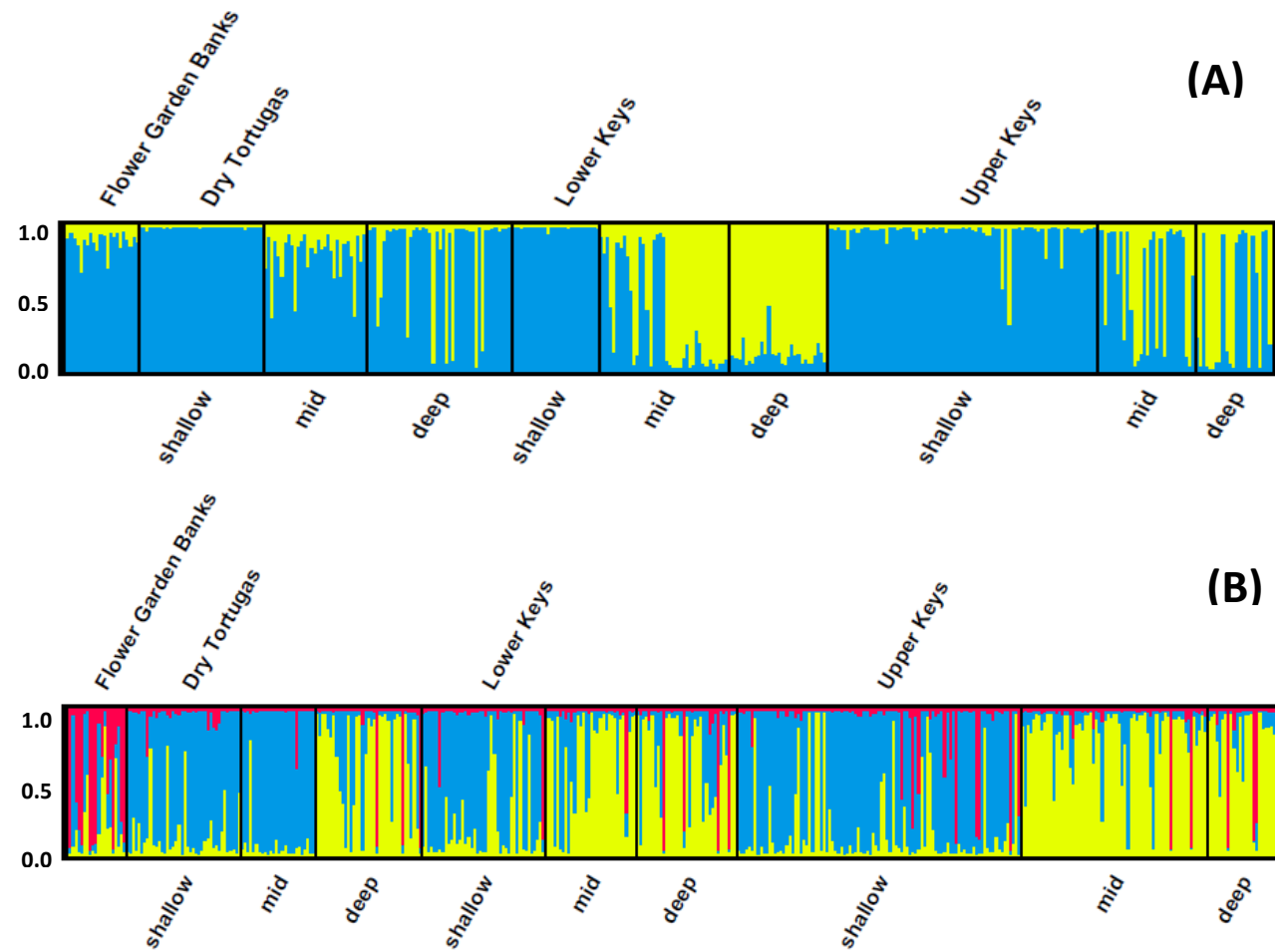


Figure 4.2. Principal Component Analysis (PCA) of allele frequency covariance in *Montastraea cavernosa* (A) and *Porites astreoides* (B) populations. For *M. cavernosa*, 9 of 163 axes were retained, explaining 100% of the cumulative variance. Plotted are the first and second axes explaining 42.36% ($P < 0.01$) and 15.76% ($P > 0.05$) of the variance, respectively. For *P. astreoides*, 9 of 72 axes were retained, explaining 100% of the cumulative variance. Plotted are the first and second axes explaining 35.50% ($P < 0.05$) and 26.35% ($P < 0.01$) of the variance, respectively. Axes cross at 0. The different shapes denote each of the 4 regions sampled in this study (Upper Keys, Lower Keys, Dry Tortugas and Flower Garden Banks), whereas the different colors denote each of the 3 depths under comparison [shallow (≤ 10 m), mid (15-20 m) and deep (≥ 25 m in Florida or 20-30 in Flower Garden Banks)]. UK= Upper Keys, LK= Lower Keys, DT= Dry Tortugas, FGB= Flower Garden Banks

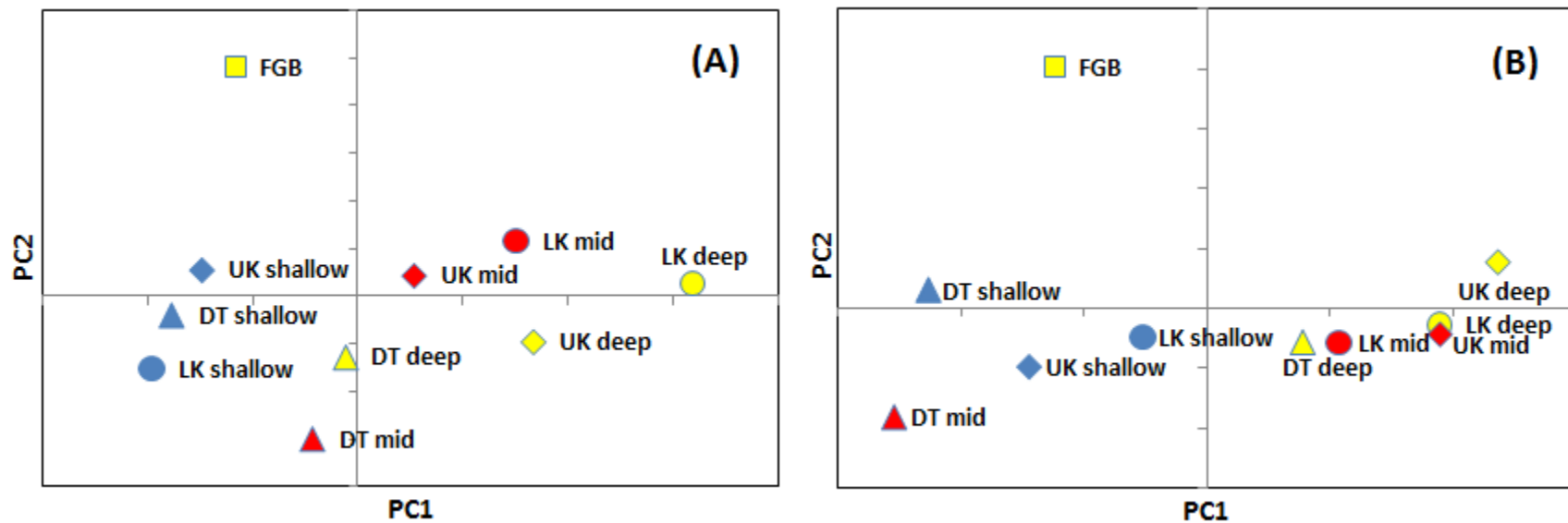


Figure 4.3. *Montastraea cavernosa* backtracking (depicted in blue) from the Upper Keys (A), Lower Keys (B) or Dry Tortugas (C) at shallow sites, and forward tracking (depicted in red) from Flower Garden Banks sites. Green areas show the overlap of backtracking and forward tracking. Sites are listed in Table 4.1. UK = Upper Keys, LK = Lower Keys, DT = Dry Tortugas, FGB = Flower Garden Banks

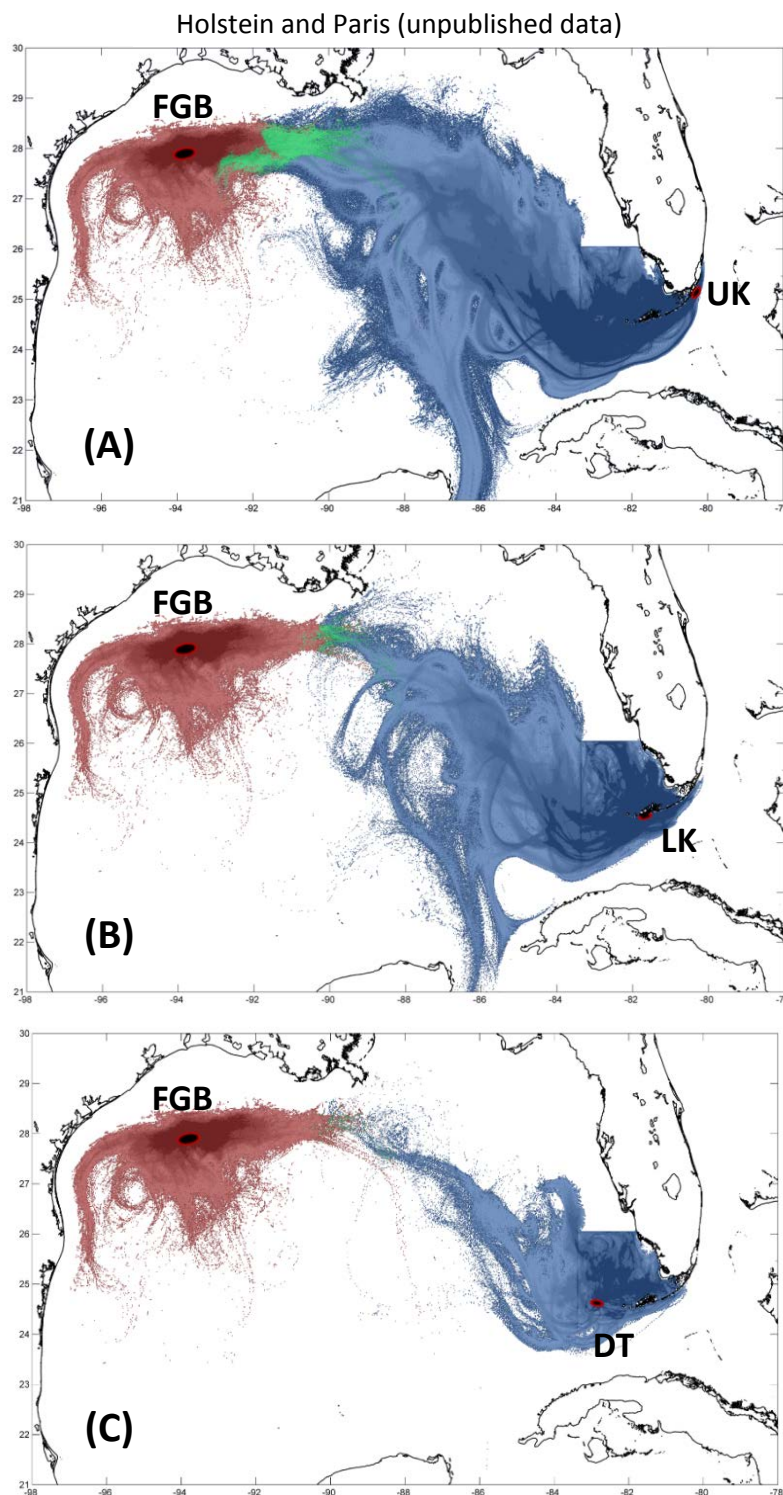


Figure 4.4. *Porites astreoides* backtracking (depicted in blue) from the Upper Keys (A), Lower Keys (B), or Dry Tortugas (C) at shallow sites, and forward tracking (depicted in red) from Flower Garden Banks sites. Sites are listed in Table 4.1. UK = Upper Keys, LK = Lower Keys, DT = Dry Tortugas, FGB = Flower Garden Banks

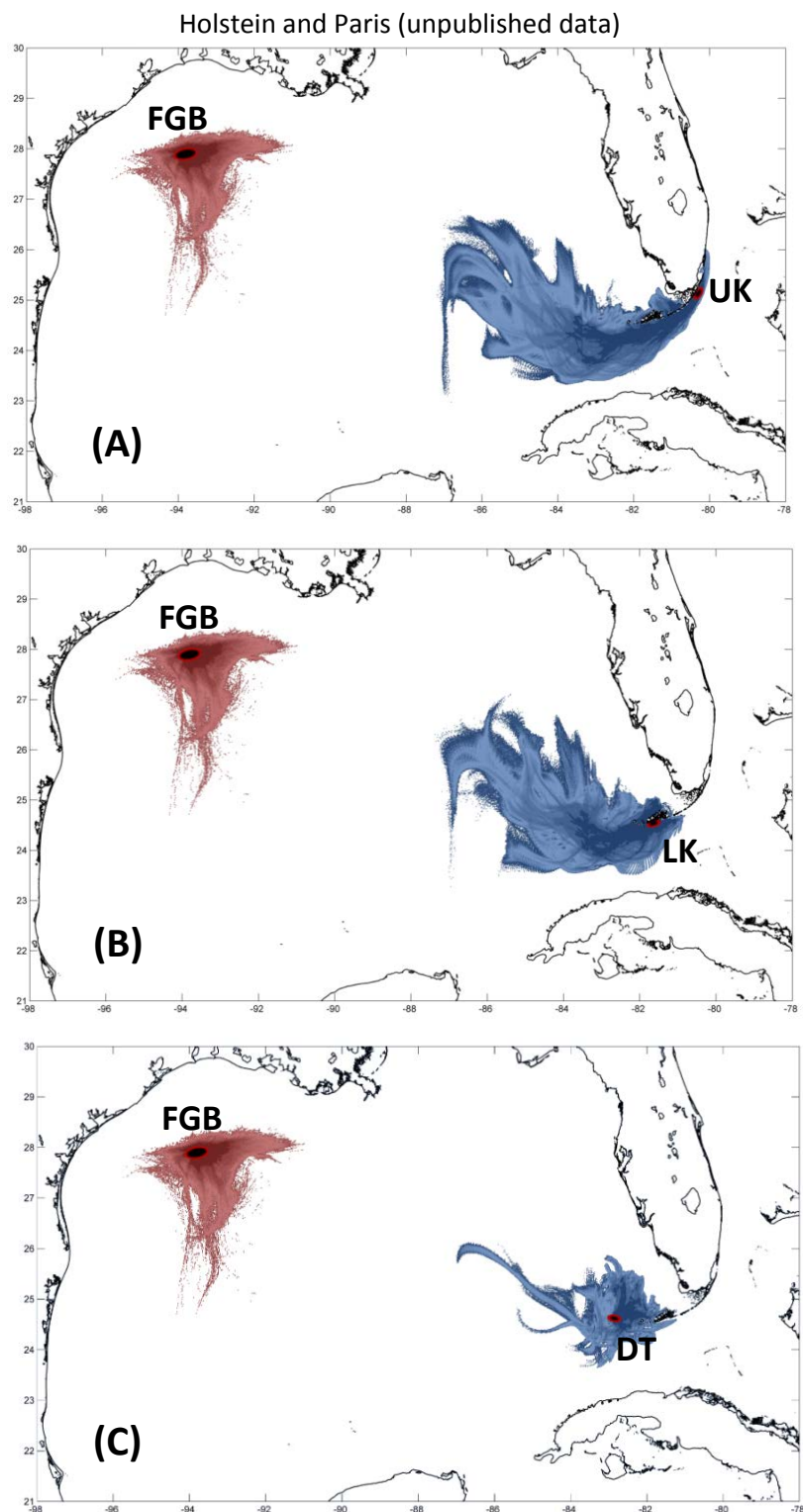


Figure 4.5. *Montastraea cavernosa* backtracking from shallow sites (≤ 10 m) in the Upper Keys. Sites are listed in Table 4.1. Colors represent the probability density function of particles after 30 days of release for five different depth layers (10, 20, 30, 40 and 50 m).

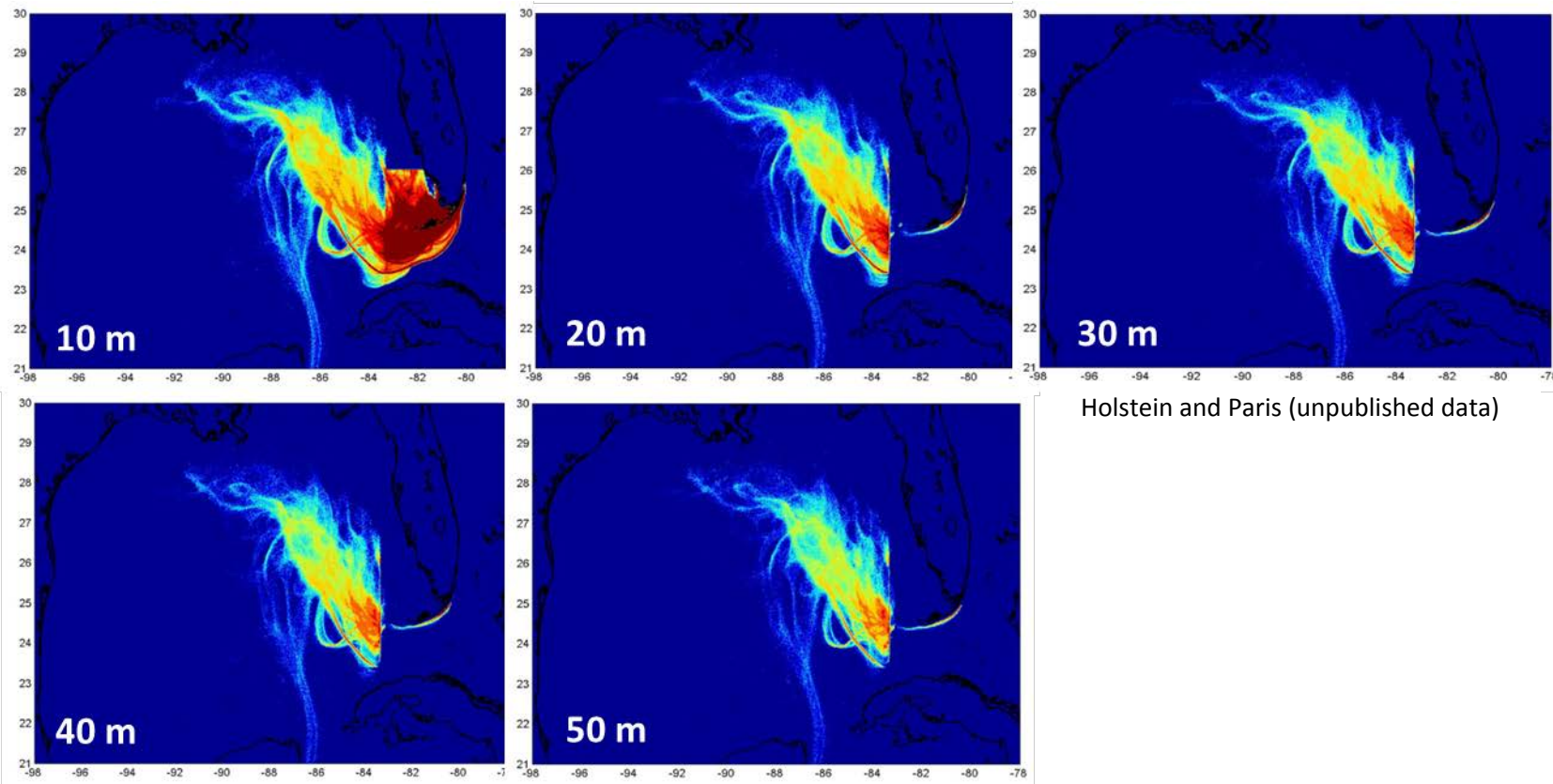


Figure 4.6. *Montastraea cavernosa* backtracking from intermediate (15-20 m) and deep sites (≥ 25 m) in the Upper Keys. Sites are listed in Table 4.1. Colors represent the probability density function of particles after 30 days of release for five different depth layers (10, 20, 30, 40 and 50 m).

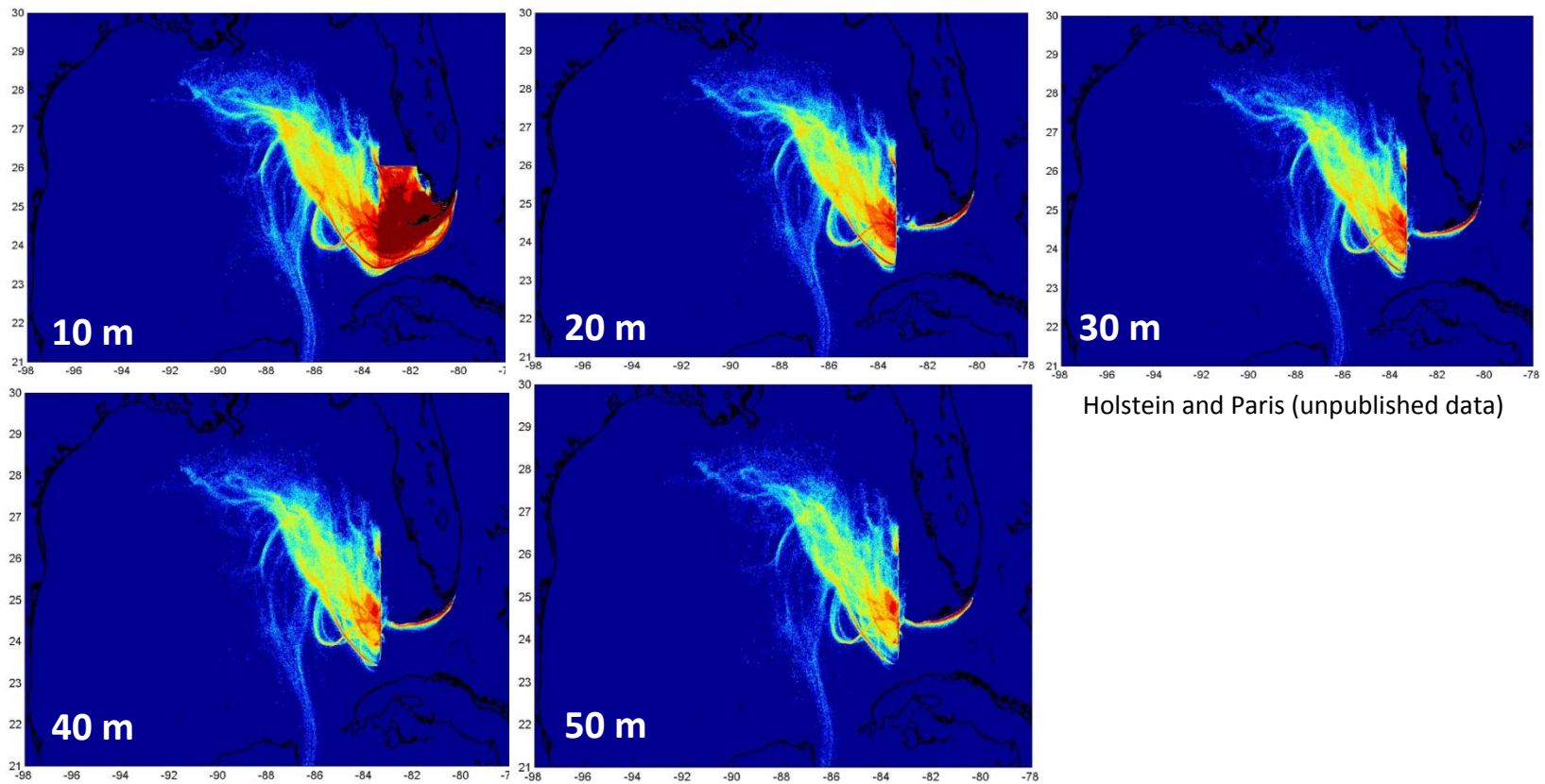


Figure 4.7. *Montastraea cavernosa* backtracking from shallow sites (≤ 10 m) in the Lower Keys. Sites are listed in Table 4.1. Colors represent the probability density function of particles after 30 days of release for five different depth layers (10, 20, 30, 40 and 50 m).

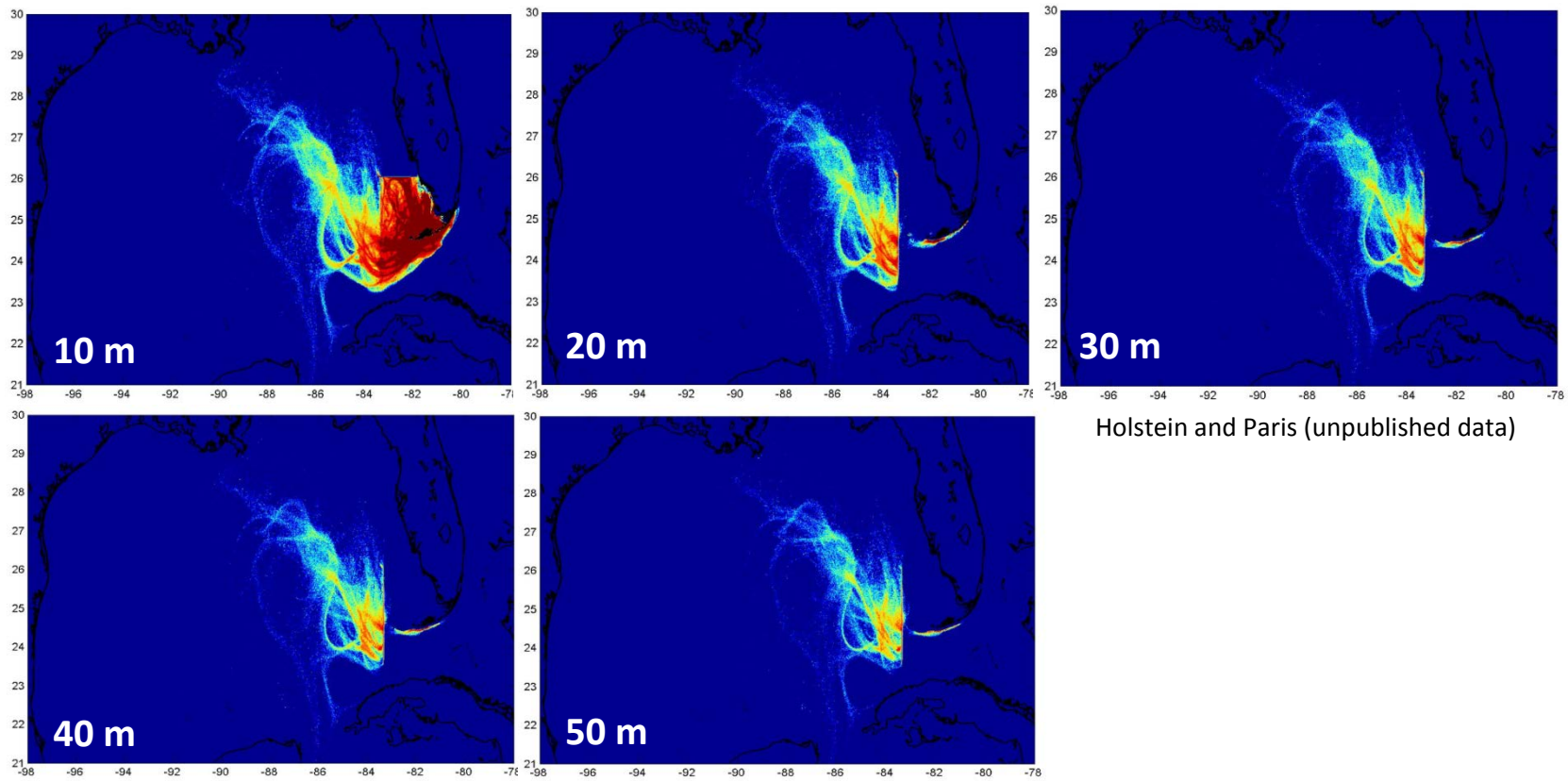


Figure 4.8. *Montastraea cavernosa* backtracking from intermediate (15-20 m) and deep sites (≥ 25 m) in the Lower Keys. Sites are listed in Table 4.1. Colors represent the probability density function of particles after 30 days of release for five different depth layers (10, 20, 30, 40 and 50 m).

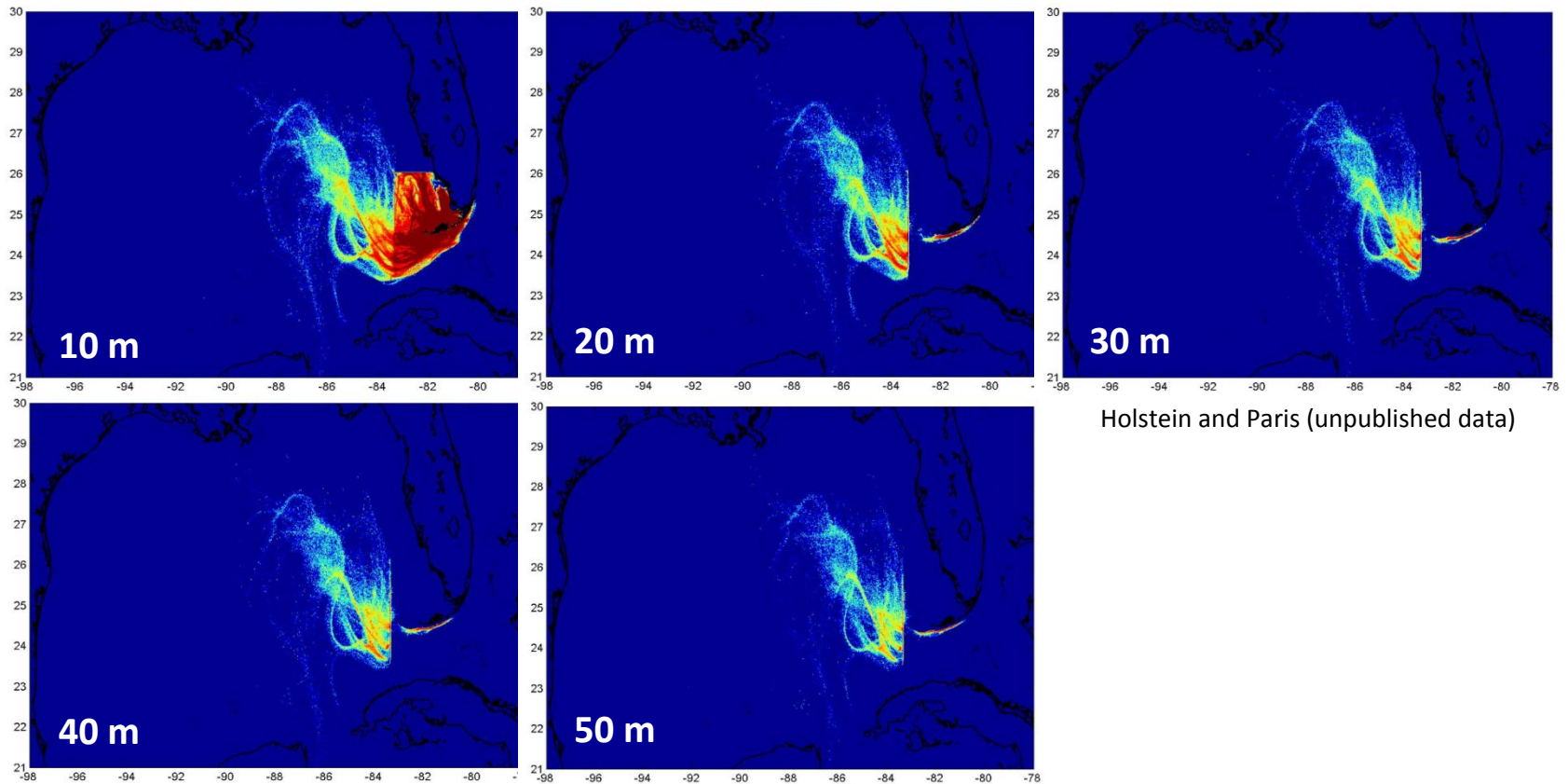


Figure 4.9. *Montastraea cavernosa* backtracking from shallow sites (≤ 10 m) in the Dry Tortugas. Sites are listed in Table 4.1. Colors represent the probability density function of particles after 30 days of release for five different depth layers (10, 20, 30, 40 and 50 m).

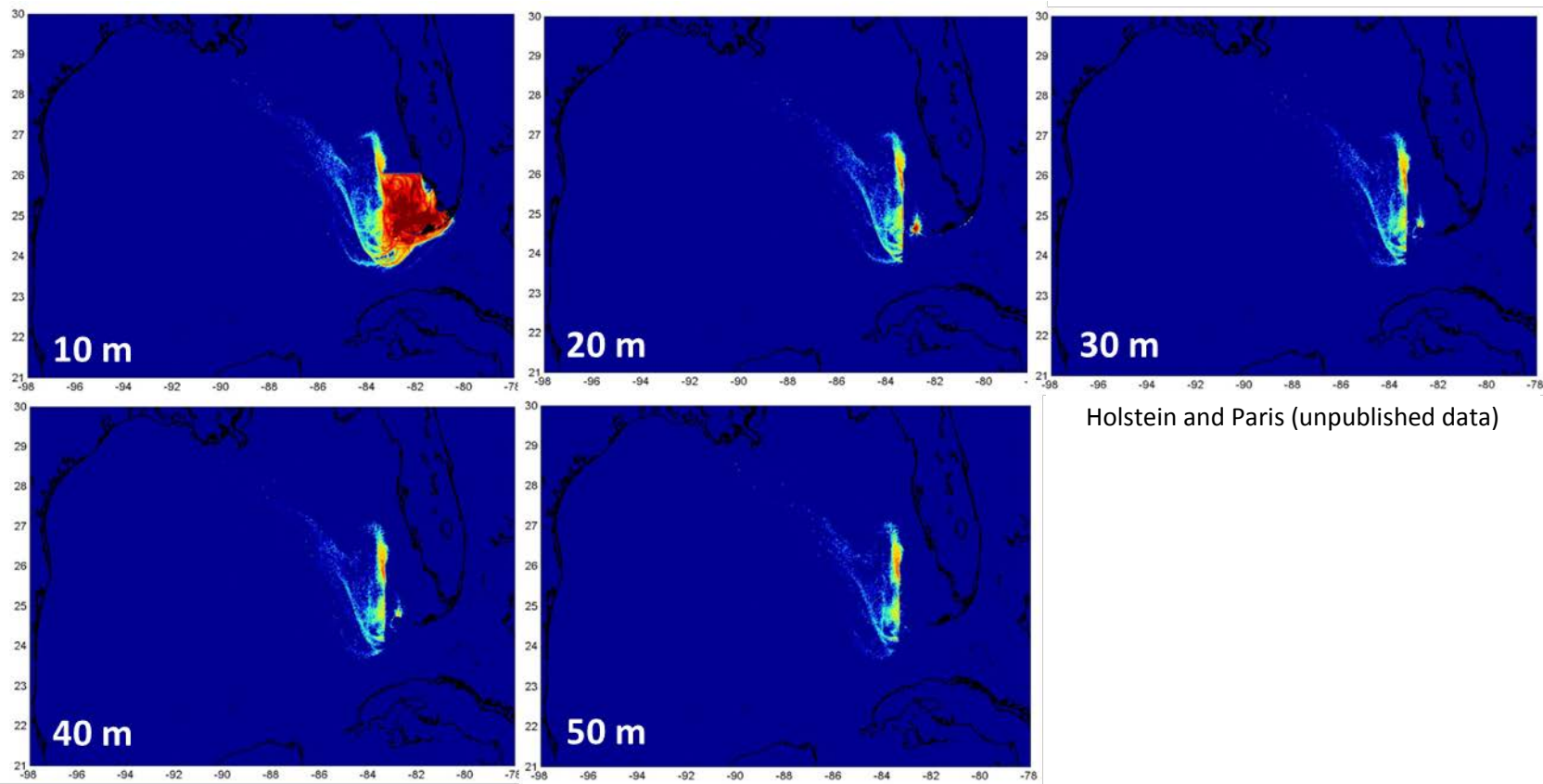


Figure 4.10. *Montastraea cavernosa* backtracking from intermediate (15-20 m) and deep sites (≥ 25 m) in the Dry Tortugas. Sites are listed in Table 4.1. Colors represent the probability density function of particles after 30 days of release for five different depth layers (10, 20, 30, 40 and 50 m).

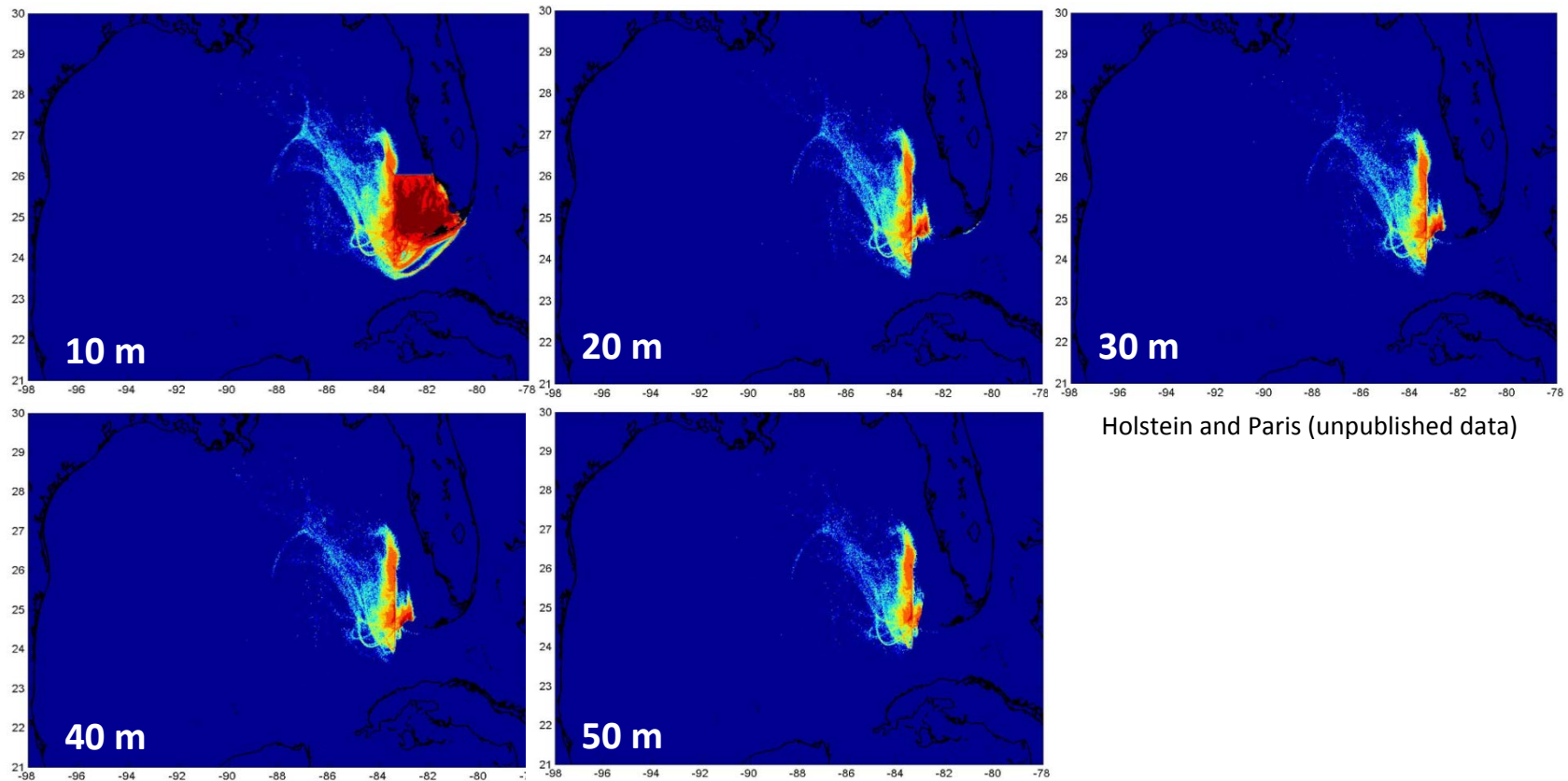


Figure 4.11. *Montastraea cavernosa* forward tracking from intermediate/deep sites (20-30 m) in the Flower Garden Banks. Sites are listed in Table 4.1. Colors represent the probability density function of particles after 30 days of release for five different depth layers (10, 20, 30, 40 and 50 m).

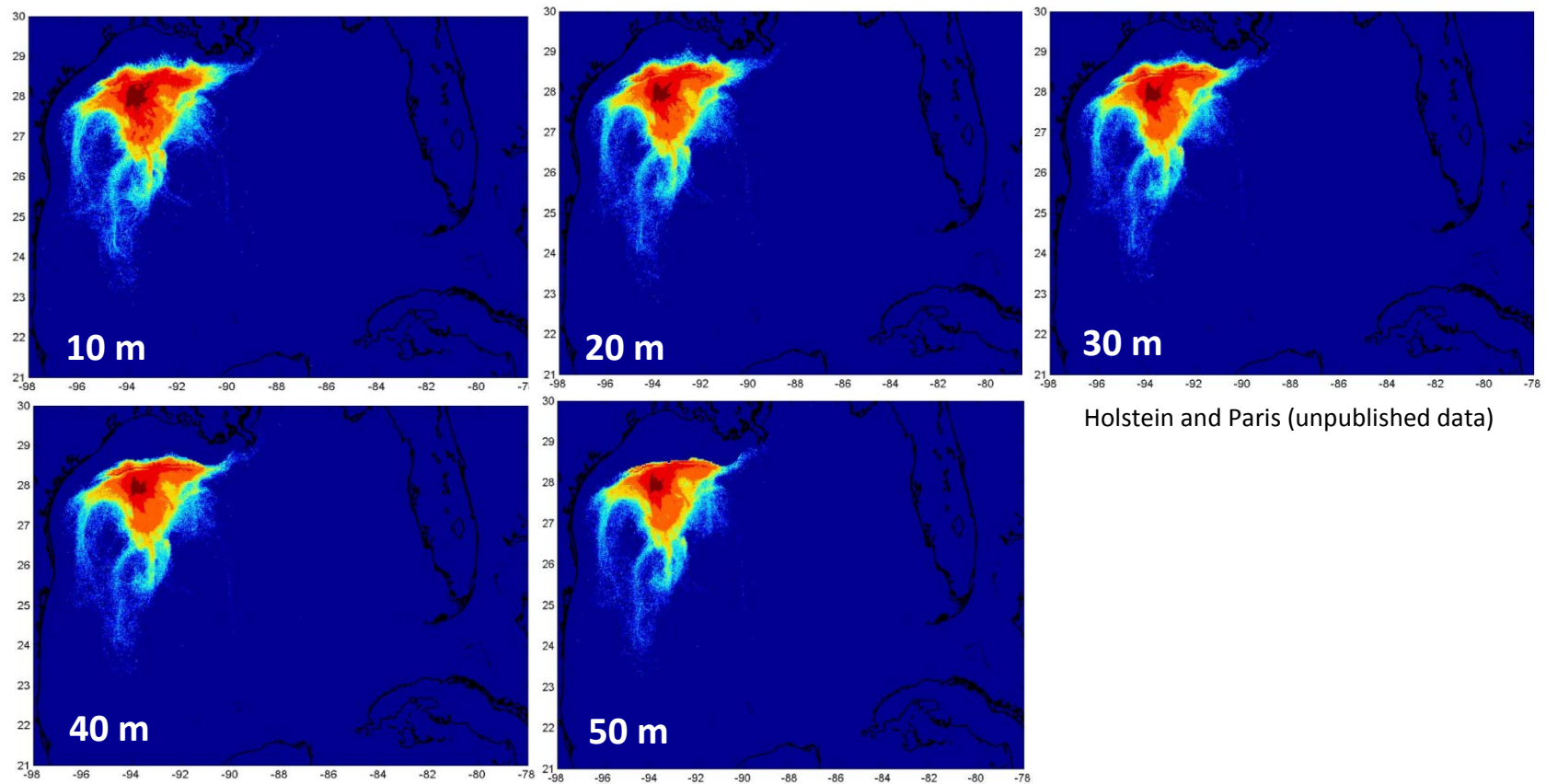


Figure 4.12. *Porites astreoides* backtracking from shallow sites (≤ 10 m) in the Upper Keys. Sites are listed in Table 4.1. Colors represent the probability density function of particles after 10 days of release for five different depth layers (10, 20, 30, 40 and 50 m).

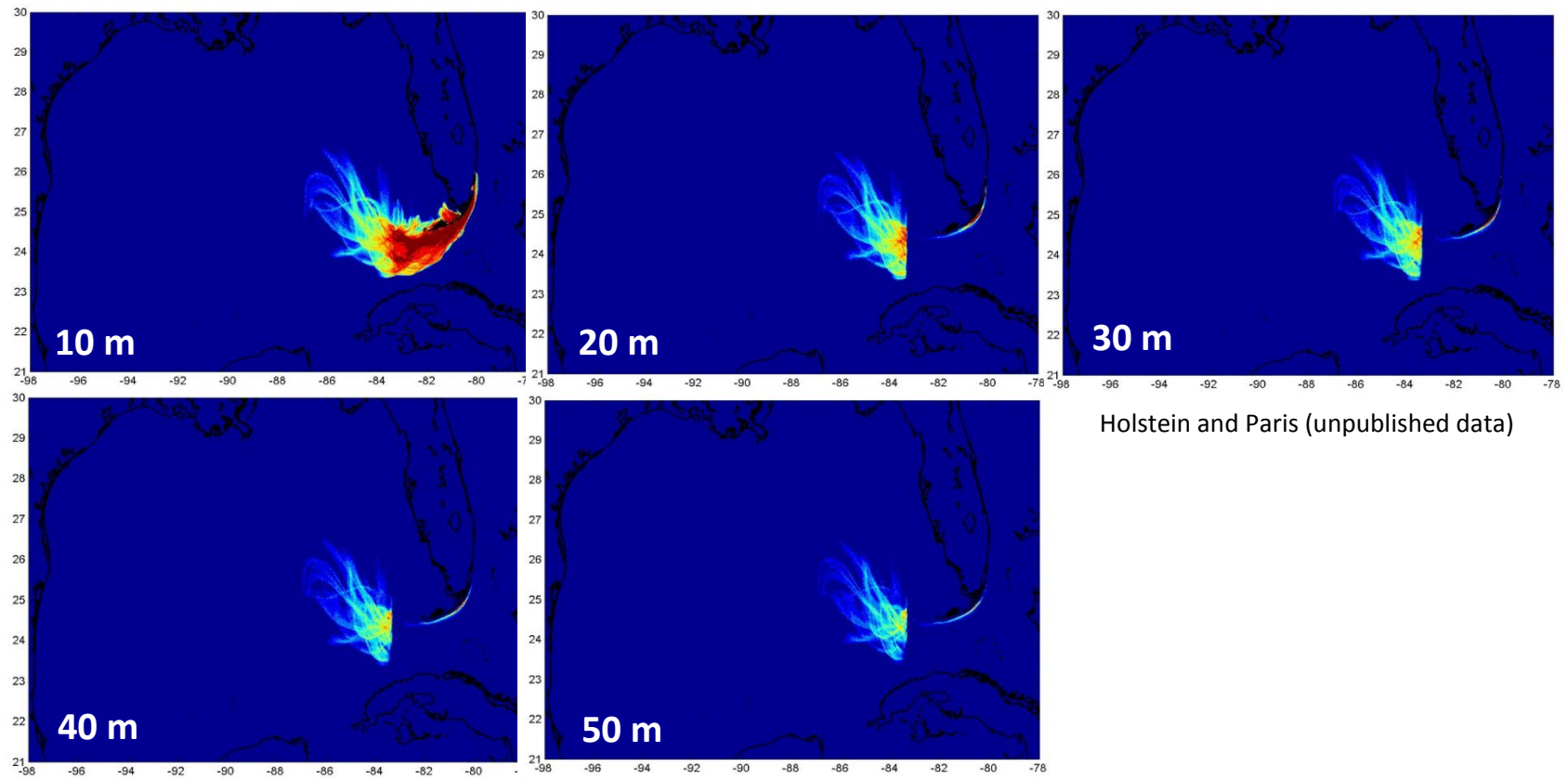


Figure 4.13. *Porites astreoides* backtracking from intermediate (15-20 m) and deep sites (≥ 25 m) in the Upper Keys. Sites are listed in Table 4.1. Colors represent the probability density function of particles after 10 days of release for five different depth layers (10, 20, 30, 40 and 50 m).

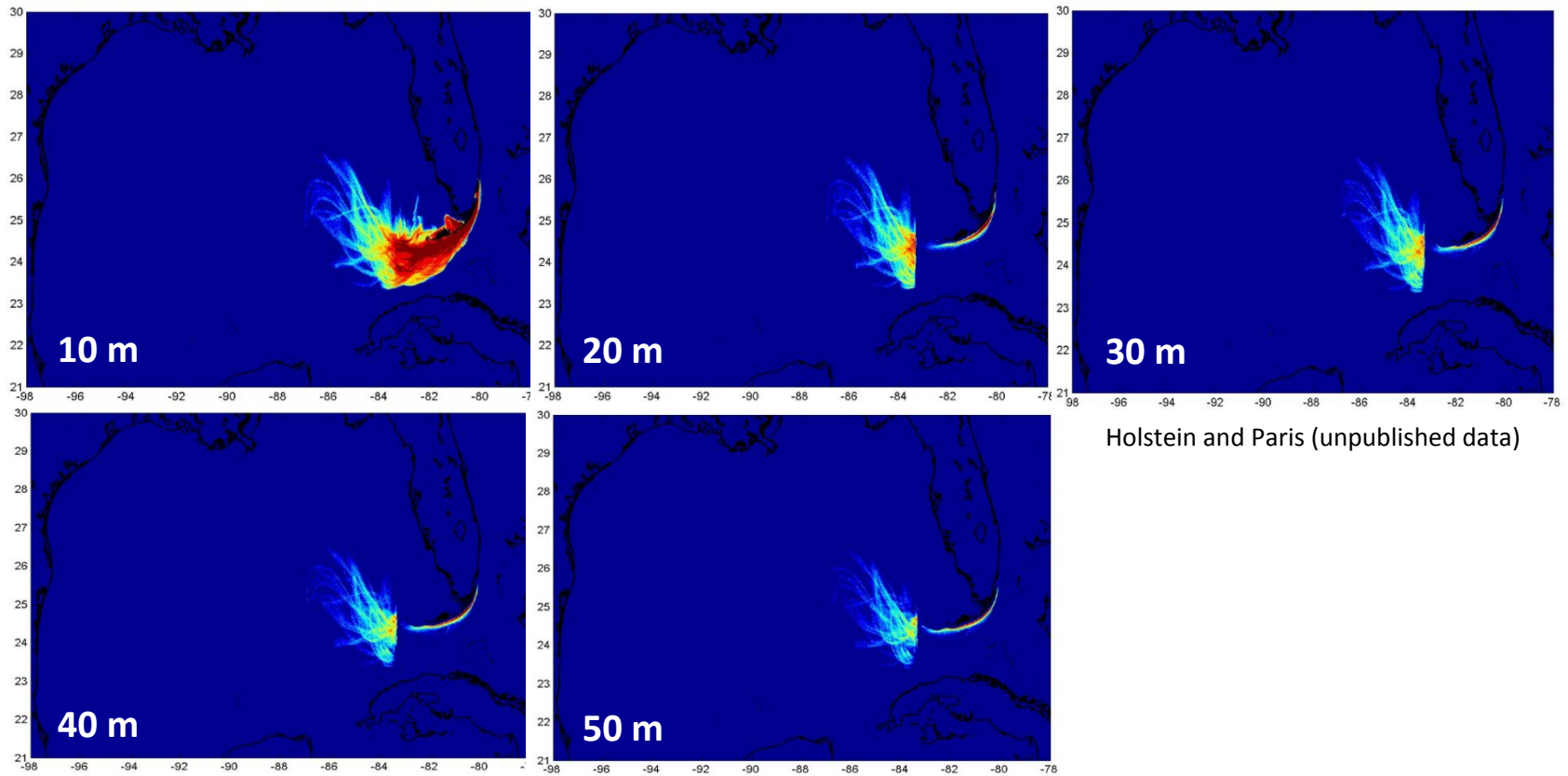


Figure 4.14. *Porites astreoides* backtracking from shallow sites (≤ 10 m) in the Lower Keys. Sites are listed in Table 4.1. Colors represent the probability density function of particles after 10 days of release for five different depth layers (10, 20, 30, 40 and 50 m).

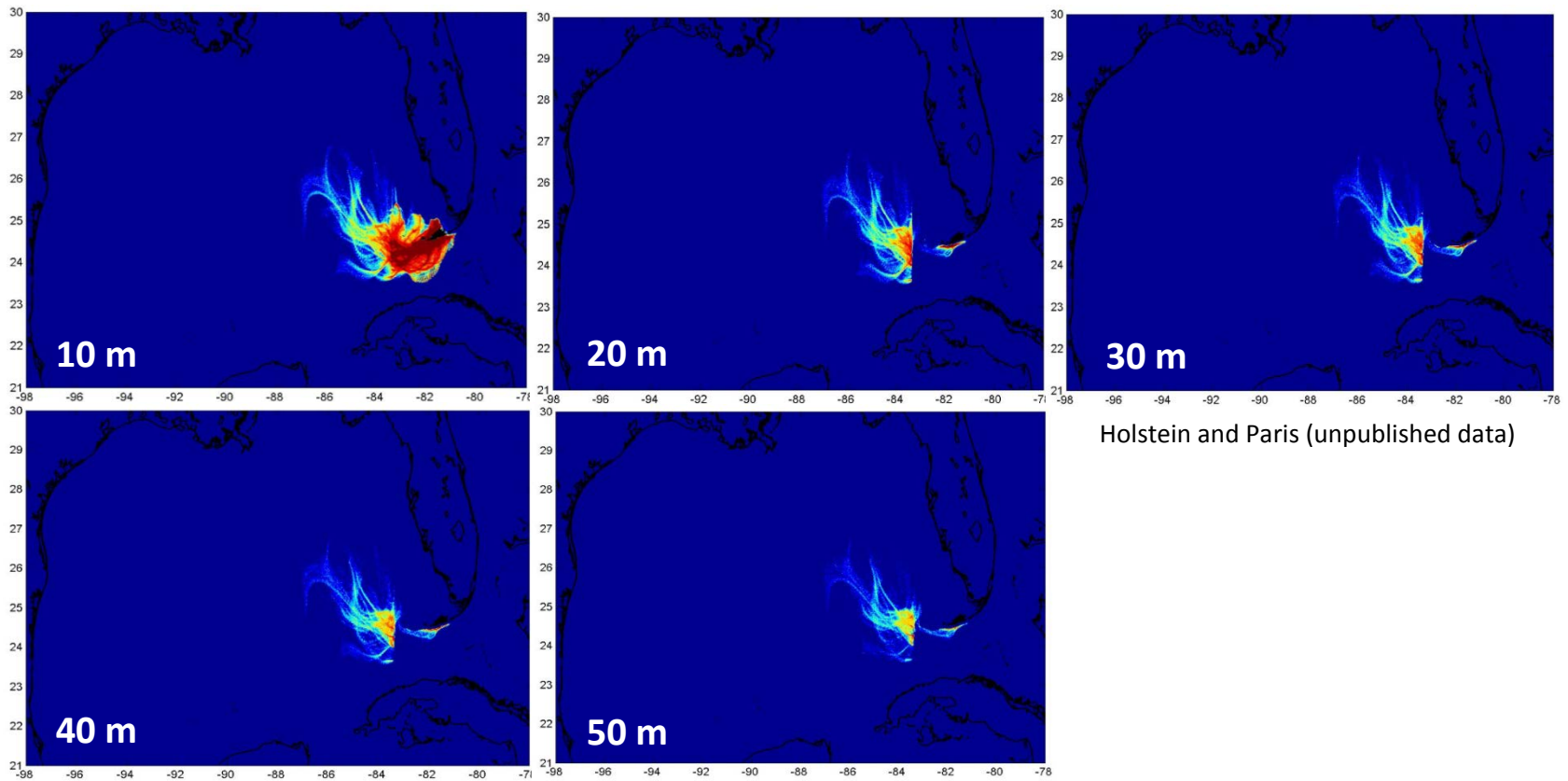


Figure 4.15. *Porites astreoides* backtracking from intermediate (15-20 m) and deep sites (≥ 25 m) in the Lower Keys. Sites are listed in Table 4.1. Colors represent the probability density function of particles after 10 days of release for five different depth layers (10, 20, 30, 40 and 50 m).

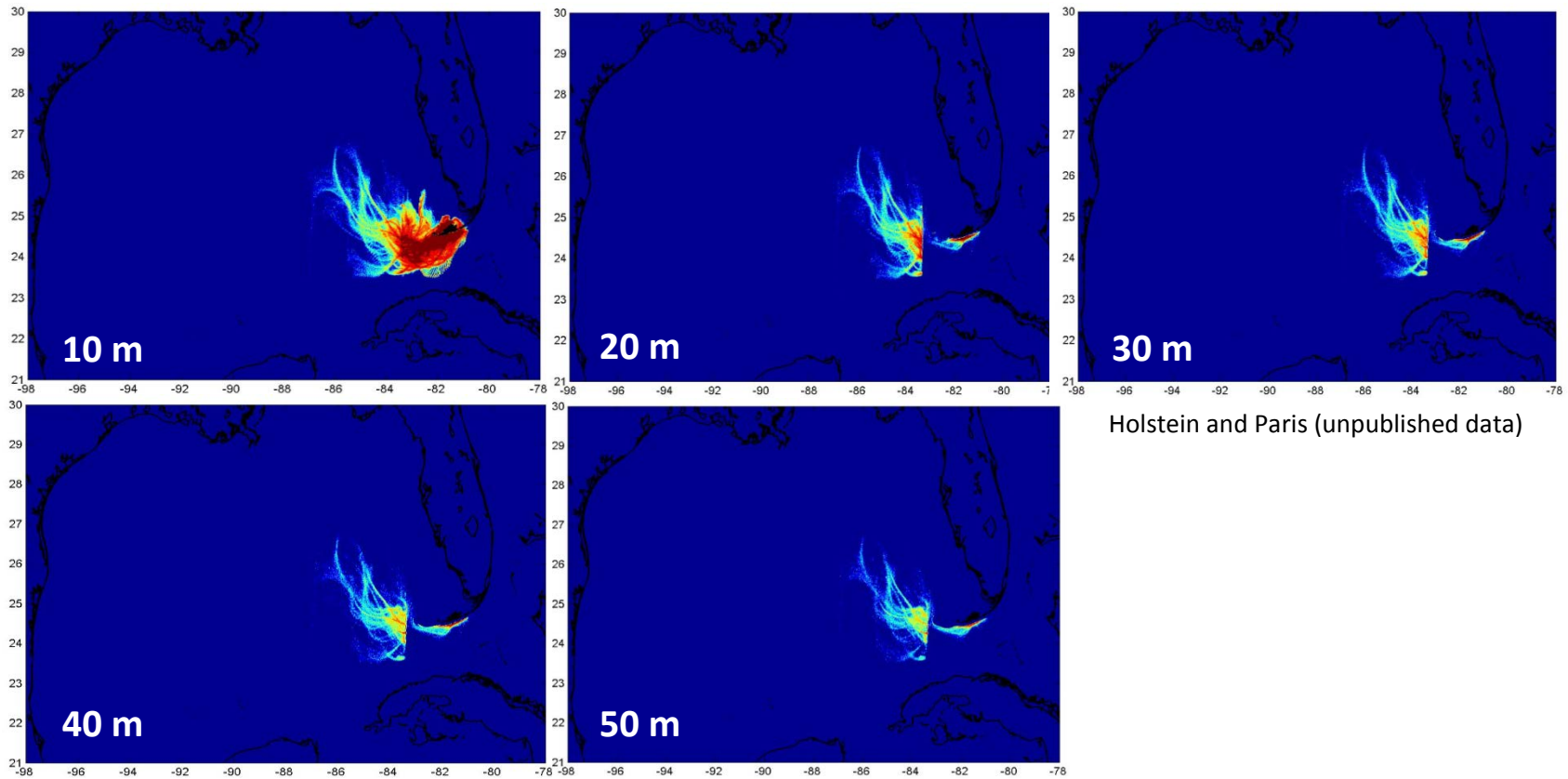


Figure 4.16. *Porites astreoides* backtracking from shallow sites (≤ 10 m) in the Dry Tortugas. Sites are listed in Table 4.1. Colors represent the probability density function of particles after 10 days of release for five different depth layers (10, 20, 30, 40 and 50 m).

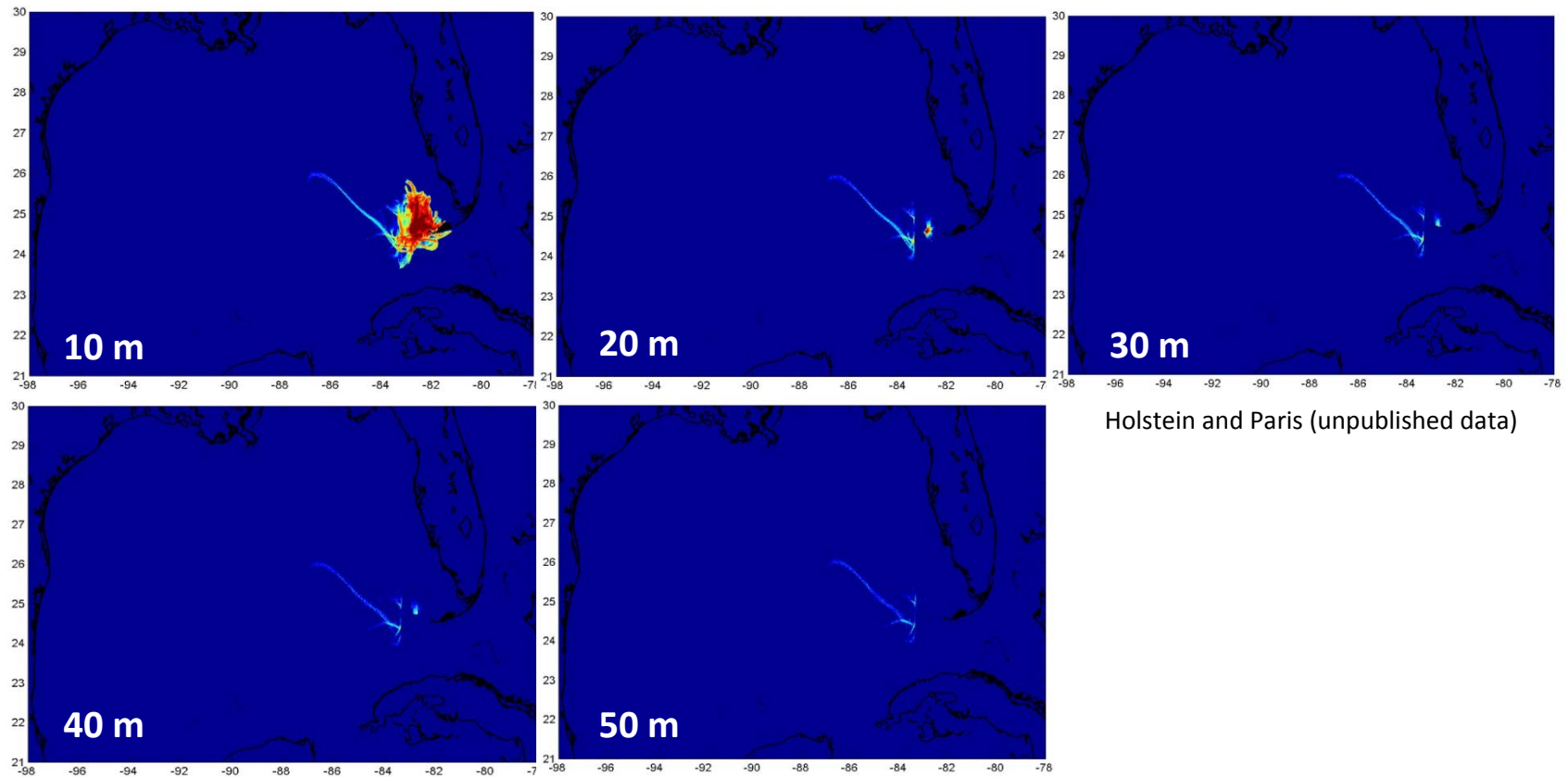


Figure 4.17. *Porites astreoides* backtracking from intermediate (15-20 m) and deep sites (≥ 25 m) in the Dry Tortugas. Sites are listed in Table 4.1. Colors represent the probability density function of particles after 10 days of release for five different depth layers (10, 20, 30, 40 and 50 m).

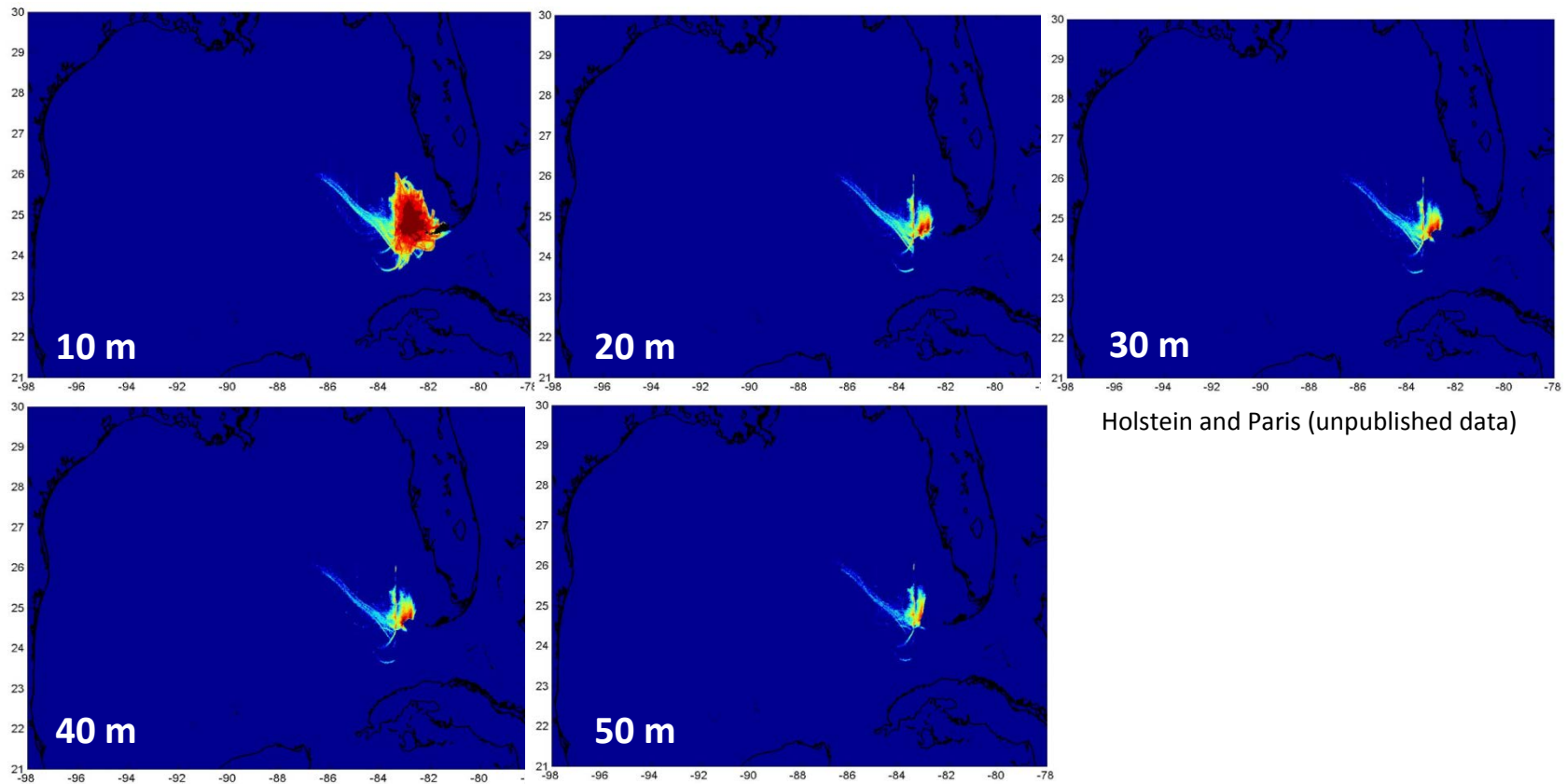
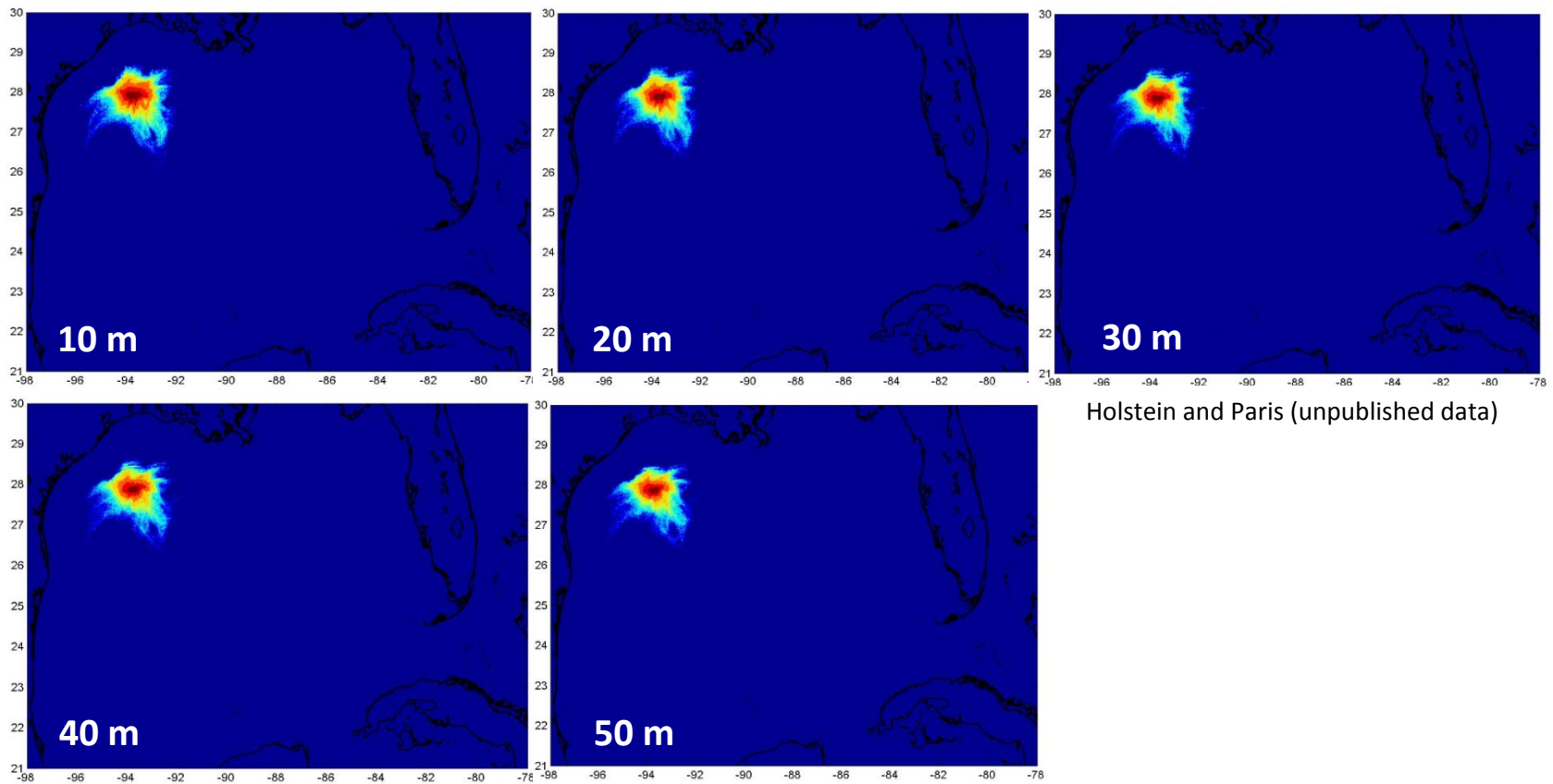


Figure 4.18. *Porites astreoides* forward tracking from intermediate/deep sites (23-25 m) in the Flower Garden Banks. Sites are listed in Table 4.1. Colors represent the probability density function of particles after 10 days of release for five different depth layers (10, 20, 30, 40 and 50 m).



CHAPTER 5

Summary, implications and recommendations

Dissertation summary

This dissertation used a multidisciplinary approach to investigate the connectivity of reef coral populations at select sites in the tropical western Atlantic, at both horizontal (long-distance dispersal) and vertical (depth) scales. The vertical component of this dissertation is unique, as it represents the first assessment of connectivity between shallow and deep coral communities for Caribbean reef-building species. I chose two depth-generalist coral species (*Montastraea cavernosa* and *Porites astreoides*) based on their documented abundance and distribution in target study sites, their differences in life-history characteristics (i.e., broadcast spawner vs. brooder), and their differences in algal symbiont transmission modes. The objectives of the dissertation were threefold: (1) Test the Deep Reef Refugia Hypothesis (*sensu* Bongaerts et al. 2010), which suggests that deep reefs can act as local recruitment sources for shallow reefs following disturbance (Chapter 2); (2) Test the hypothesis that reproductive mode correlates with dispersal ability (Chapter 3); and (3) Couple genetic results with high-resolution biophysical modeling to examine the degree of coral connectivity between sites in the Gulf of Mexico and Florida at different depth intervals (Chapter 4). The last of these objectives represents the first time a seascape genetics approach has been used to explore the mechanisms influencing connectivity at different depths. Overall, this dissertation has potential relevance for a variety of coral reef conservation applications, and will help inform management strategies to help protect critical reef resources.

The main challenge of this dissertation was generating molecular markers capable of detecting genetic differentiation over small spatial scales (<10 km). For coral species with algal symbionts this is particularly difficult, because DNA extraction protocols typically extract both host and symbiont DNA. Therefore, steps were taken to minimize contamination by symbiont DNA in the coral tissue used for microsatellite development. High throughput (454) sequencing was then used to develop 9 and 4 new microsatellite loci for *M. cavernosa* (Chapter 2) and *P. astreoides* (Chapter 3), respectively. These new markers (in combination with 4 existing loci for *P. astreoides*) were used to assess patterns of connectivity in >1,200 coral colonies as described in Chapters 2, 3 and 4. For Chapters 2 and 3, field activities were focused on shallow (≤ 10 m), intermediate (15-20 m) and deep (≥ 25 m) coral communities along the Florida Reef Tract (within the Upper Keys, Lower Keys and Dry Tortugas), Bermuda, and the USVI. For Chapter 4, additional samples were obtained from the Flower Garden Banks (the only major coral reefs in the northern Gulf of Mexico) to assess connectivity between this site and the Florida Reef Tract (FRT).

In Chapter 2, I aimed to determine the role of deep reefs in shallow reef recovery for the broadcast spawning scleractinian coral *Montastraea cavernosa*. The fact that this is one of the few Caribbean species that can inhabit extremely broad depth ranges (3-100 m) suggested that this species was an exceptional candidate for testing the Deep Reef Refugia Hypothesis in this region. In addition, gene flow in this species had already been shown to be high among shallow sites throughout the Caribbean, and between the Caribbean and Bermuda, suggesting that gene flow over much shorter vertical (depth) scales would also be high. However, analyses revealed significant genetic differentiation

by depth within <20 km in Florida, despite high levels of horizontal connectivity between shallow sites separated by >1,700 km. Even more importantly, regardless of the extent of vertical connectivity observed, migration always occurred asymmetrically from shallow to mid/deep habitats. Together, these findings strongly suggest that the potential for deep reefs to serve as larval sources for nearby shallow reefs (1) may be generally limited (since even the coral species with one of the broadest depth ranges showed structure by depth), and (2) varies among geographic locations, likely as a consequence of local hydrology. Based on the patterns of connectivity observed, I hypothesize that shallow reefs are more likely to rely on distant (unimpacted) shallow reefs, rather than nearby deep reefs, to provide a viable source of new recruits following disturbance.

In Chapter 3, I examined to what extent the contrasting life-history reproductive strategies of *P. astreoides* and *M. cavernosa* could influence larval dispersal and levels of gene flow at both horizontal and vertical scales. The general expectation is that brooding coral species, such as *P. astreoides*, exhibit limited dispersal capabilities and lower genetic connectivity compared to broadcast spawning species, presumably due to shorter pre-competency periods. Therefore, I assessed patterns of genetic connectivity for the Caribbean brooding coral *P. astreoides* and also tested whether depth zonation in algal symbionts could further limit effective connectivity by restricting the types of symbionts transferred from parent to offspring. Based on the results obtained in Chapter 2 with *M. cavernosa*, I had predicted low levels of horizontal and vertical connectivity for *P. astreoides*. However, *P. astreoides* exhibited high levels of horizontal gene flow between the USVI and Florida (but not between the Caribbean and Bermuda), as well as high levels of vertical gene flow in two of the three geographic locations examined (Bermuda

and the USVI). Furthermore, depth zonation in the algal symbionts of *P. astreoides* did not appear to limit effective connectivity. Instead, findings suggest that possessing or acquiring the appropriate algal symbionts (“high light” vs. “low light”) might be an important mechanism used to increase post-settlement survival across a wide range of habitats and depths. Together, these findings suggest that *P. astreoides* has similar or greater long-distance (horizontal) dispersal capabilities compared to other Caribbean broadcast spawning taxa, and potentially greater short-distance (vertical) dispersal capabilities compared to *M. cavernosa* (Chapter 2). Overall, these findings reinforce the notion that predicting patterns of connectivity based solely on reproductive mode and dispersal ability can be misleading. Instead, connectivity is likely the result of complex interactions between intrinsic and extrinsic factors (pre- or post-settlement) that are best studied using an integrated, multidisciplinary approach.

In Chapter 4, I led a collaborative seascape genetics effort to examine coral connectivity between the Flower Garden Banks (FGB, Gulf of Mexico) and the FRT at different depth intervals. The goal of this project was to determine whether, and how, the FGB might act as an important larval source for Florida’s coral populations. This is a timely and important investigation because the FGB are located close to many oil and gas platforms, including the Deepwater Horizon oil rig which exploded in 2010. By better understanding the processes that drive coral larval dispersal out of the Gulf of Mexico (GOM) and into the FRT, I hoped to identify whether (1) FGB could an important larval source for Florida’s shallow vs. deep coral populations, and (2) whether differences in reproductive season and pelagic larval duration of *M. cavernosa* and *P. astreoides* could affect connectivity between these two locations. Overall, genetic results revealed high

levels of gene flow between the FGB and the shallow Florida *M. cavernosa* population, but not for *P. astreoides*, suggesting limited gene flow among these regions. These patterns were in general agreement with modeled simulations of larval dispersal, suggesting that (1) FGB might be an important larval source for the shallow Florida population of *M. cavernosa*, and (2) differences in reproductive mode and season might be important drivers of reef coral connectivity within the GOM region. Furthermore, these findings suggest that an oil spill originating in the GOM (1) could have the potential to impact coral communities in Florida, (2) might have more important effects on broadcast spawning taxa like *M. cavernosa*, particularly if FGB is an important larval source for these species, and (3) is more likely to affect shallow habitats in Florida, likely sinks for coral larvae produced at FGB. These results also suggest that deep coral populations in Florida may constitute refugia due to their partial isolation from the shallow population, if these latter populations were to be impacted by oil or other stressors (see Chapters 2 and 3). However, they too might eventually be impacted in a stepping-stone fashion if shallow populations were slow, or unable to recover.

Implications and future directions

To get similar findings from two coral species with contrasting reproductive strategies is remarkable. Comparable levels of horizontal connectivity were observed between 2 of the 3 geographic locations examined (USVI and Florida) for both coral species, while in 4 of the 5 regions assessed (Upper Keys, Lower Keys, Bermuda and the USVI), similar patterns of genetic differentiation with depth were also observed. Even more remarkably, the gene flow model with migration from shallow to deep was ranked as the best model in all 5 regions, for both species.

Together these findings have important implications. First, they strongly suggest that long-distance horizontal connectivity is greater than vertical connectivity for both species, regardless of reproductive mode. Therefore, although the possibility that shallow reef recovery might be aided by deeper reefs cannot be ruled out, it is unlikely to be rapid. In fact, it is more likely that shallow reefs rely on more distant shallow reefs as sources of new recruits. However, in areas where panmixia was observed, such as Bermuda and the USVI, deep reefs may still be able to contribute to the resilience of shallow reefs nearby, even if it takes multiple generations due to low migration rates from deep to shallow water.

Second, patterns of vertical connectivity varied between and within geographic locations. Surprisingly, the largest genetic differentiation for *M. cavernosa* occurred between the Lower Keys shallow and deep sites, while the lowest degree of differentiation occurred in the Dry Tortugas, even though these regions are only ~130 km apart. Furthermore, for both species, Bermuda and the USVI appear highly panmictic. These findings strongly suggest that the potential for shallow reefs to recover from deep refugia may vary between sites as a consequence of local hydrology. Thus, while deep reefs in Florida appear unlikely to be able to rapidly re-seed their shallow water counterparts, it is possible that these reefs are acting as larval sources for other shallow reefs downstream. Future work should try to further elucidate the role of deep reefs as refugia for nearby vs. more distant, downstream shallow reefs.

Third, my findings suggest that reproductive mode does not necessarily correlate with realized dispersal ability. Although *P. astreoides* did exhibit lower levels of genetic connectivity between the Caribbean and Bermuda (Chapter 3) and between the FGB and

Florida (Chapter 4), evidence suggests that larvae occasionally disperse and settle in these locations. Further, the level of gene flow for *P. astreoides* between the USVI and Florida are similar to, or greater than, most Caribbean broadcast spawning taxa studied to date. In fact, I found no genetic evidence for an east/west Caribbean barrier for either of the two species I examined. In terms of management, I recommend avoiding predicting patterns of connectivity based solely on reproductive mode, as it might lead to wrong conclusions and might result in no observable marine reserve effects. Instead, a combination of factors – both intrinsic and extrinsic – should be taken into account when predicting connectivity for a species within a region of interest.

Fourth, findings from this study confirm new evidence suggesting that depth is an important population structuring factor in corals (Eytan et al. 2009; van Oppen et al. 2011; Prada and Hellberg, 2013; Brazeau et al. 2013). In fact, our findings support those from Caribbean broadcast spawners in the genus *Oculina* (Eytan et al. 2009), the Pacific brooding coral *S. hystrix* (van Oppen et al. 2011) and the Caribbean octocoral *E. flexuosa* (Prada and Hellberg, 2013), despite different study locations, coral species and reproductive strategies. The general lack of admixture observed between shallow and deep colonies for all these species suggests that there must be strong selective pressures in shallow vs. deep habitats, which ultimately prevents colonies from interbreeding. Further, it is possible that populations at different depths become so locally adapted, that immigration to other depths results in poor performance (immigrant inviability, *sensu* Prada and Hellberg, 2013). Therefore, even if impacted shallow reefs are re-colonized by larvae originating from deep water, strong selective forces might result in reduced or little post-settlement survival.

Remarkably, my findings suggest that regardless of reproductive mode and geographic location, migration is asymmetric, with greater downward migration from shallow to deep. Therefore, genetic mixing is likely maintained by supply of larvae down the slope, rather than migration in both directions. Fragmentation of shallow colonies and subsequent re-attachment in deeper habitats is unlikely to be the cause since all repeated multi-locus genotypes were confined to the same sampling location or depth interval. I hypothesize that this is the result of a higher gamete production in shallow environments, as a result of higher growth rates, coral cover, and faster growth to sexual maturity compared to deeper environments. Deeper reefs may also be less environmentally harsh than shallow reefs, promoting higher survivorship of migrants. Regardless, the number of migrants from deep to shallow may be insufficient to replenish shallow reefs in the event of catastrophic coral mortality, resulting in prolonged reef recovery. Further research should assess whether or not this trend applies to other coral species and regions.

Finally, contrary to expectations, the mode of algal symbiont transmission does not appear to limit effective vertical connectivity. I hypothesized that broadcast spawners such as *M. cavernosa* would be more capable of colonizing habitats over a broad depth range by acquiring the appropriate “high light” or “low light” symbionts from the environment. However, these expectations were not entirely met, as I found that *M. cavernosa* predominantly hosts a single *Symbiodinium* type (C3), even in areas where significant structure with depth was observed. Conversely, I had hypothesized that depth zonation in algal symbionts for *P. astreoides* would limit effective connectivity by restricting the availability of suitable symbionts. However, depth zonation of algal symbionts in *P. astreoides* did not affect its ability to disperse to different depths. Instead,

migrants either already possessed or were able to acquire the appropriate symbionts. This may be an important element in determining post-settlement survival, especially for deep migrants settling in shallow habitats, as acquisition of symbionts in clade A seemed to offer a competitive advantage in conditions of high irradiance.

Together, findings revealed lower levels of horizontal gene flow but higher levels of vertical gene flow for *P. astreoides* compared to *M. cavernosa*. Therefore, while reproductive mode may not be a reliable predictor of connectivity, broadcast spawning may be advantageous for increasing horizontal (long-distance) gene flow, while brooding may be advantageous for enhancing vertical (short-distance) gene flow due to higher survival regardless of depth. I hypothesize that reasons for the higher survival of brooding corals migrating to different depths may include their: (1) competitive advantage in high irradiance (shallow) habitats due to possession or acquisition of appropriate symbionts, (2) availability of maternal (energy) reserves, and/or (3) increased chances for genetic mixing due to multiple reproductive events per year. Whether or not these patterns apply to other brooding coral species merits further investigation.

Overall, the data presented here addresses a set of important questions concerning the larval dispersal, recruitment and connectivity of two important Caribbean reef corals, at both horizontal and vertical scales. Findings suggests that shallow water reefs (<15 m) are even more important than recognized, as they (1) are more likely to help re-colonize other distant shallow reefs following a disturbance compared to deep reefs, and (2) help maintain genetic diversity and a stable/productive community across the reef slope (via production of migrants that settle in deep habitats). As such, they deserve a high priority

for managers and measures should be taken to reduce local and global anthropogenic impacts that might further accelerate their loss rate.

LITERATURE CITED

- Addison JA, Hart MW (2005) Spawning, copulation and inbreeding coefficients in marine invertebrates. *Biology Letters* 1, 450-453.
- Atchison AD, Sammarco PW, Brazeau DA (2008) Genetic connectivity in corals on the Flower Garden Banks and surrounding oil/gas platforms, Gulf of Mexico. *Journal of Experimental Marine Biology and Ecology* 365, 1-12.
- Bak RP, Nieuwland G, Meesters EH (2005) Coral reef crisis in deep and shallow reefs: 30 years of constancy and change in reefs of Curacao and Bonaire. *Coral Reefs*, 24, 475-479.
- Baker (1999) The symbiosis ecology of reef-building corals. Ph.D. thesis. Marine Biology and Fisheries, University of Miami, Miami, Florida. 137 pp.
- Baker AC, Glynn PW, Riegl B (2008) Climate change and coral reef bleaching: An ecological assessment of long-term impacts, recovery trends and future outlook. *Estuarine Coastal and Shelf Science*, 80, 435-471.
- Baker AC, Romanski AM (2007) Multiple symbiotic partnerships are common in scleractinian corals, but not in octocorals: Comment on Goulet (2006). *Marine Ecology Progress Series* 335, 237-242.
- Baker AC, Rowan R (1997) Diversity of symbiotic dinoflagellates (zooxanthellae) in scleractinian corals of the Caribbean and eastern Pacific. *Proceedings of the Eight International Coral Reef Symposium*, 2, 1301-1305.
- Banaszak AT, LaJeunesse TC, Trench RK (2000) The synthesis of mycosporine-like amino acids (MAAs) by cultured, symbiotic dinoflagellates. *Journal of Experimental Marine Biology and Ecology* 249, 219-233.
- Baums IB (2008) A restoration genetics guide for coral reef conservation. *Molecular Ecology* 17, 2796-2811.
- Baums IB, Hughes CR, Hellberg ME (2005a) Mendelian microsatellite loci for the Caribbean coral *Acropora palmata*. *Marine Ecology Progress Series* 288, 115-127.
- Baums IB, Miller MW, Hellberg ME (2005b) Regionally isolated populations of an imperiled Caribbean coral, *Acropora palmata*. *Molecular Ecology* 14, 1377-1390.
- Baums IB, Paris CB, Cherubin LM (2006) A bio-oceanographic filter to larval dispersal in a reef-building coral. *Limnology and Oceanography* 51, 1969-1981.
- Berli P (2004) Effect of unsampled populations on the estimation of population sizes and migration rates between sampled populations. *Molecular Ecology* 13, 827-836.

- Beerli P, Felsenstein J (2001) Maximum likelihood estimation of a migration matrix and effective population sizes in n subpopulations by using a coalescent approach. *Proceedings of the National Academy of Sciences of the United States of America* 98, 4563-4568
- Beerli P, Palczewski M (2010) Unified framework to evaluate panmixia and migration direction among multiple sampling locations. *Genetics* 185, 313-U463.
- Billinghurst Z, Douglas AE, Trapido-Rosenthal HG (1997) On the genetic diversity of the symbiosis between the coral *Montastraea cavernosa* and zooxanthellae in Bermuda. *Proceedings of the Eight International Coral Reef Symposium*, 2, 1291-1294.
- Bongaerts P, Ridgway T, Sampayo EM, Hoegh-Guldberg O (2010) Assessing the 'deep reef refugia' hypothesis: focus on Caribbean reefs. *Coral Reefs* 29, 309-327.
- Bongaerts P, Riginos C, Hay KB, et al. (2011a) Adaptive divergence in a scleractinian coral: physiological adaptation of *Seriatopora hystrix* to shallow and deep reef habitats. *BMC Evolutionary Biology*, 11, 303.
- Bongaerts P, Sampayo EM, Bridge TCL, et al. (2011b) *Symbiodinium* diversity in mesophotic coral communities on the Great Barrier Reef: a first assessment. *Marine Ecology Progress Series*, 439, 117-126.
- Botsford LW, White JW, Coffroth MA, et al. (2009) Connectivity and resilience of coral reef metapopulations in marine protected areas: matching empirical efforts to predictive needs. *Coral Reefs* 28, 327-337.
- Brazeau DA, Lesser MP, Slattery M (2013) Genetic structure in the coral *Montastraea cavernosa*: assessing genetic differentiation among and within mesophotic reefs. *Plos One*, 8, 5, doi:10.1371/journal.pone.0065845
- Brazeau DA, Sammarco PW, Gleason DF (2005) A multi-locus genetic assignment technique to assess sources of *Agaricia agaricites* larvae on coral reefs. *Marine Biology* 147, 1141-1148.
- Bright TJ, Kraemer GP, Minnery GA, Viada ST (1984) Hermatypes of the Flower Garden Banks, northwestern Gulf of Mexico- A comparison to other western Atlantic reefs. *Bulletin of Marine Science* 34, 461-476.
- Budd AF, Nunes FLD, Weil E, Pandolfi JM (2012) Polymorphism in a common Atlantic reef coral (*Montastraea cavernosa*) and its long-term evolutionary implications. *Evolutionary Ecology*, 26, 265-290.
- Chornesky EA, Peters EC (1987) Sexual reproduction and colony growth in the scleractinian coral *Porites astreoides*. *Biological Bulletin* 172, 161-177.

Chybicki IJ, Burczyk J (2009) Simultaneous estimation of null alleles and inbreeding coefficients. *Journal of Heredity* 100, 106-113.

Coffroth MA, Santos SR, Goulet TL (2001) Early ontogenetic expression of specificity in a cnidarian-algal symbiosis. *Marine Ecology Progress Series* 222, 85-96.

Correa AMS, Brandt ME, Smith TB, Thornhill DJ, Baker AC (2009a) *Symbiodinium* associations with diseased and healthy scleractinian corals. *Coral Reefs*, 28, 437-448.

Correa AMS, McDonald MD, Baker AC (2009b) Development of clade-specific *Symbiodinium* primers for quantitative PCR (qPCR) and their application to detecting clade D symbionts in Caribbean corals. *Marine Biology*, 156, 2403-2411.

Cowen RK, Paris CB, Srinivasan A (2006) Scaling of connectivity in marine populations. *Science* 311, 522-527.

Cowen RK, Sponaugle S (2009) Larval dispersal and marine population connectivity. In: *Annual Review of Marine Science*, pp. 443-466.

Crone TJ, Tolstoy M (2010) Magnitude of the 2010 Gulf of Mexico oil leak. *Science* 330, 634-634.

Cunning R, Baker AC (2013) Excess algal symbionts increase the susceptibility of reef corals to bleaching. *Nature Climate Change*, DOI: 10.1038/nclimate1711

Dokken QR, MacDonald IR, Tunnell Jr. JW, Wade T, Beaver CR, Childs SA, Withers K, Bates TW (2002) Long-term monitoring at the East and West Flower Garden Banks National Marine Sanctuary, 1998-1999. U.S. Dept. of the Interior, Minerals Management Service, Gulf of Mexico OCS Region, New Orleans, LA. 119 pp.

Earl DA (2009) Structure Harvester v0.56.3 http://taylor0.biology.ucla.edu/struct_harvest

Evanno G, Regnaut S, Goudet J (2005) Detecting the number of clusters of individuals using the software STRUCTURE: a simulation study. *Molecular Ecology* 14, 2611-2620.

Eytan RI, Hayes M, Arbour-Reily P, Miller M, Hellberg ME (2009) Nuclear sequences reveal mid-range isolation of an imperiled deep-water coral population. *Molecular Ecology*, 18, 2375-2389.

Fadlallah YH (1983) Sexual reproduction, development and larval biology in scleractinian corals. A review. *Coral Reefs* 2, 129-150.

Falkowski PG, Jokiel PL, Kinzie RA, III (1990) Irradiance and corals. Ed. Dubinsky, Z. *Ecosystems of the world: 25. Coral reefs*. pp. 89-107

Flood VS, Pitt JM, Smith SR (2005) Historical and ecological analysis of coral communities in Castle Harbour (Bermuda) after more than a century of environmental perturbation. *Marine Pollution Bulletin* 51, 545-557.

Foster NL, Paris CB, Kool JT, et al. (2012) Connectivity of Caribbean coral populations: complementary insights from empirical and modelled gene flow. *Molecular Ecology* 21, 1143-1157.

Frade PR, Englebort N, Faria J, Visser PM, Bak RPM (2008) Distribution and photobiology of *Symbiodinium* types in different light environments for three colour morphs of the coral *Madracis pharensis*: is there more to it than total irradiance? *Coral Reefs*, 27, 913-925.

Gaines SD, Gaylord B, Gerber LR, Hastings A, Kinlan BP (2007) Connecting places: the ecological consequences of dispersal in the sea. *Oceanography* 20, 90-99.

Gardner TA, Cote IM, Gill JA, Grant A, Watkinson AR (2003) Long-term region-wide declines in Caribbean corals. *Science* 301, 958-960.

Gelfand Y, Rodriguez A, Benson G (2006) TRDB — the Tandem Repeats Database. *Nucleic Acids Research*, gkl1013.

Gittings SR, Boland GS, Deslarzes KJP, et al. (1992) Mass spawning and reproductive viability of reef corals at the East Flower Garden Bank, northwest Gulf of Mexico. *Bulletin of Marine Science* 51, 420-428.

Gleason DF (1993) Differential-effects of ultraviolet-radiation on green and brown morphs of the Caribbean coral *Porites astreoides*. *Limnology and Oceanography* 38, 1452-1463.

Glynn PW (1996) Coral reef bleaching: Facts, hypotheses and implications. *Global Change Biology*, 2, 495-509.

Glynn PW, Mate JL, Baker AC, Calderon MO (2001) Coral bleaching and mortality in panama and Ecuador during the 1997-1998 El Nino-Southern oscillation event: Spatial/temporal patterns and comparisons with the 1982-1983 event. *Bulletin of Marine Science*, 69, 79-109.

Goodbody-Gringley G, Wetzel DL, Gillon D, et al. (2013) Toxicity of Deepwater Horizon source oil and the chemical dispersant, Corexit (R) 9500, to coral larvae. *Plos One* 8.

Goodbody-Gringley G, Woollacott RM, Giribet G (2011) Population structure and connectivity in the Atlantic scleractinian coral *Montastraea cavernosa* (Linnaeus, 1767). *Marine Ecology*, 33, 32-48.

- Goodbody-Gringley, GE (2009) Reproduction and phylogeography of two scleractinian corals in the western Atlantic. Ph.D. thesis. Biology of Organismic and Evolutionary Biology, Harvard University, Cambridge, Massachusetts. 165 pp.
- Goreau TF (1959) The ecology of Jamaican coral reefs 1. Species composition and zonation. *Ecology* 40, 67-90.
- Goreau TF, Wells JW (1967) Shallow-water scleractinia of Jamaica- Revised list of species and their vertical distribution range. *Bulletin of Marine Science* 17, 442-453.
- Grigg RW (2006) Depth limit for reef building corals in the Au'au Channel, SE Hawaii. *Coral Reefs*, 25, 77-84.
- Harrison PL, Wallace CC (1990) Reproduction, dispersal and recruitment of scleractinian corals. Ed. Dubinsky, Z. *Ecosystems of the world: 25. Coral reefs*. pp. 133-207
- Hemond EM, Vollmer SV (2010) Genetic diversity and connectivity in the threatened staghorn coral (*Acropora cervicornis*) in Florida. *Plos One* 5.
- Hinderstein LM, Marr JCA, Martinez FA, et al. (2010) Theme section on "Mesophotic coral ecosystems: characterization, ecology, and management". *Coral Reefs* 29, 247-251.
- Hitchcock GL, Lee TN, Ortner PB, et al. (2005) Property fields in a Tortugas Eddy in the southern straits of Florida. *Deep-Sea Research Part I-Oceanographic Research Papers*, 52, 544 2195-2213.
- Hoegh-Guldberg O, Mumby PJ, Hooten AJ, et al. (2007) Coral reefs under rapid climate change and ocean acidification. *Science* 318, 1737-1742.
- Hubisz MJ, Falush D, Stephens M, Pritchard JK (2009) Inferring weak population structure with the assistance of sample group information. *Molecular Ecology Resources* 9, 1322-1332.
- Hughes TP, Baird AH, Bellwood DR, et al. (2003) Climate change, human impacts, and the resilience of coral reefs. *Science* 301, 929-933.
- Hughes TP, Bellwood DR, Folke C, Steneck RS, Wilson J (2005) New paradigms for supporting the resilience of marine ecosystems. *Trends in Ecology & Evolution* 20, 380-386.
- Iglesias-Prieto R, Beltran VH, LaJeunesse TC, Reyes-Bonilla H, Thome PE (2004) Different algal symbionts explain the vertical distribution of dominant reef corals in the eastern Pacific. *Proceedings of the Royal Society B-Biological Sciences* 271, 1757-1763.

- Jakobsson M, Rosenberg NA (2007) CLUMPP: a cluster matching and permutation program for dealing with label switching and multimodality in analysis of population structure. *Bioinformatics* 23, 1801-1806.
- Jones RJ (2004) Testing the 'photoinhibition' model of coral bleaching using chemical inhibitors. *Marine Ecology Progress Series* 284, 133-145.
- Jones GP, Russ GR, Sale PF, Steneck RS (2009) Theme section on "Larval connectivity, resilience and the future of coral reefs". *Coral Reefs* 28, 303-305.
- Jones GP, Srinivasan M, Almany GR (2007) Population connectivity and conservation of marine biodiversity. *Oceanography* 20, 100-111.
- Kahng SE, Garcia-Sais JR, Spalding HL, et al. (2010) Community ecology of mesophotic coral reef ecosystems. *Coral Reefs* 29, 255-275.
- Kenkel CD, Goodbody-Gringley G, Caillaud D, et al. (2013) Evidence for a host role in thermotolerance divergence between populations of the mustard hill coral (*Porites astreoides*) from different reef environments. *Molecular Ecology* 22, 4335-4348.
- Klemas V (2010) Tracking oil slicks and predicting their trajectories using remote sensors and models: Case studies of the Sea Princess and Deepwater Horizon oil spills. *Journal of Coastal Research* 26, 789-797.
- Kourafalou VH, Kang H (2012) Florida Current meandering and evolution of cyclonic eddies along the Florida Keys Reef Tract: Are they interconnected? *Journal of Geophysical Research-Oceans*, 117, C05028, doi:10.1029/2011JC007383
- LaJeunesse TC (2002) Diversity and community structure of symbiotic dinoflagellates from Caribbean coral reefs. *Marine Biology* 141, 387-400.
- LaJeunesse TC (2005) "Species" radiations of symbiotic dinoflagellates in the Atlantic and Indo-Pacific since the miocene-pliocene transition. *Molecular Biology and Evolution*, 22, 570-581.
- LaJeunesse TC, Bhagooli R, Hidaka M, et al. (2004) Closely related *Symbiodinium* spp. differ in relative dominance in coral reef host communities across environmental, latitudinal and biogeographical gradients. *Marine Ecology Progress Series*, 284, 147-161.
- LaJeunesse TC, Loh WKW, van Woesik R, et al. (2003) Low symbiont diversity in southern Great Barrier Reef corals, relative to those of the Caribbean. *Limnology and Oceanography*, 48, 2046-2054.
- LaJeunesse TC, Trench RK (2000) Biogeography of two species of *Symbiodinium* (Freudenthal) inhabiting the intertidal sea anemone *Anthopleura elegantissima* (Brandt). *Biological Bulletin* 199, 126-134.

- Le Henaff M, Kourafalou VH, Paris CB, et al. (2012) Surface evolution of the Deepwater Horizon oil spill patch: combined effects of circulation and wind-induced drift. *Environmental Science & Technology* 46, 7267-7273.
- Lesser MP, Slattery M, Stat M et al. (2010) Photoacclimatization by the coral *Montastraea cavernosa* in the mesophotic zone: light, food, and genetics. *Ecology*, 91, 990-1003.
- Leviton DR, Fukami H, Jara J et al. (2004) Mechanisms of reproductive isolation among sympatric broadcast-spawning corals of the *Montastraea annularis* species complex. *Evolution*, 58, 308-323.
- Lirman D, Manzello D (2009) Patterns of resistance and resilience of the stress-tolerant coral *Siderastrea radians* (Pallas) to sub-optimal salinity and sediment burial. *Journal of Experimental Marine Biology and Ecology* 369, 72-77.
- Lugo-Fernandez A, Deslarzes KJP, Price JM, Boland GS, Morin MV (2001) Inferring probable dispersal of Flower Garden Banks coral larvae (Gulf of Mexico) using observed and simulated drifter trajectories. *Continental Shelf Research* 21, 47-67.
- Lugo-Fernandez A, Gravois M (2010) Understanding impacts of tropical storms and hurricanes on submerged bank reefs and coral communities in the northwestern Gulf of Mexico. *Continental Shelf Research* 30, 1226-1240.
- Magalon H, Adjeroud M, Veuille M (2005) Patterns of genetic variation do not correlate with geographical distance in the reef-building coral *Pocillopora meandrina* in the South Pacific. *Molecular Ecology* 14, 1861-1868.
- Margulies M, Egholm M, Altman WE, et al. (2005) Genome sequencing in microfabricated high-density picolitre reactors. *Nature* 437, 376-380.
- Marshall P, Schuttenberg H (2006) *A Reef Manager's Guide to Coral Bleaching*. Great Barrier Reef Marine Park Authority, Townsville, Australia
- Mass T, Einbinder S, Brokovich E et al. (2007) Photoacclimation of *Stylophora pistillata* to light extremes: metabolism and calcification. *Marine Ecology Progress Series*, 334, 93-102.
- McGuire MP (1998) Timing of larval release by *Porites astreoides* in the northern Florida Keys. *Coral Reefs* 17, 369-375.
- Meirmans, PG, Van Tienderen PH (2004) GENOTYPE and GENODIVE: two programs for the analysis of genetic diversity of asexual organisms. *Molecular Ecology Notes*, 4, 792-794.

- Menza C, Kendall M, Hile S (2008) The deeper we go the less we know. *Revista De Biologia Tropical* 56, 11-24.
- Mieog, JC, Van Oppen, MJH, Berkelmans, R, et al. (2009) Quantification of algal endosymbionts (*Symbiodinium*) in coral tissue using real-time PCR. *Molecular Ecology Resources*, 9, 74-82.
- Miller KJ, Ayre DJ (2008) Population structure is not a simple function of reproductive mode and larval type: insights from tropical corals. *Journal of Animal Ecology* 77, 713-724.
- Miller KJ, Howard CG (2004) Isolation of microsatellites from two species of scleractinian coral. *Molecular Ecology Notes* 4, 11-13.
- Mundy CN, Babcock RC (1998) Role of light intensity and spectral quality in coral settlement: Implications for depth-dependent settlement? *Journal of Experimental Marine Biology and Ecology* 223, 235-255.
- Muscatine L (1990) The role of symbiotic algae in carbon and energy flux in reef corals. Ed. Dubinsky, Z. *Ecosystems of the world: 25. Coral reefs*. pp. 75-87
- Muscatine L, Porter JW, Kaplan IR (1989) Resource partitioning by reef corals as determined from stable isotope composition .1. Delta-C-13 of zooxanthellae and animal tissue vs depth. *Marine Biology* 100, 185-193.
- Nunes F, Norris RD, Knowlton N (2009) Implications of isolation and low genetic diversity in peripheral populations of an amphi-Atlantic coral. *Molecular Ecology* 18, 4283-4297.
- Nunes FLD, Norris RD, Knowlton N (2011) Long distance dispersal and connectivity in amphi-Atlantic corals at regional and basin Scales. *Plos One* 6.
- Nystrom M, Folke C (2001) Spatial resilience of coral reefs. *Ecosystems* 4, 406-417.
- Paris CB, Cherubin LM, Cowen RK (2007) Surfing, diving or spinning: effects on population connectivity. Theme Section: Advances in modeling physical-biological interactions in fish early life history. *Marine Ecology Progress Series* 347: 285-300
- Paris CB, Cowen RK, Claro R, Lindeman KC (2005) Larval transport pathways from Cuban snapper (Lutjanidae) spawning aggregations based on biophysical modeling. *Marine Ecology Progress Series* 296, 93-106.
- Peakall R, Smouse PE (2006) GENALEX 6: genetic analysis in Excel. Population genetic software for teaching and research. *Molecular Ecology Notes* 6, 288-295.

Pochon X, Gates RD (2010) A new *Symbiodinium* clade (Dinophyceae) from soritid foraminifera in Hawai'i. *Molecular Phylogenetics and Evolution* 56, 492-497.

Potts DC, Garthwaite RL (1991) Evolution of reef-building corals during periods of rapid global change. *Proceedings of the Fourth International Congress of Systematic and Evolutionary Biology* 1, 170-178.

Prada C, Hellberg ME (2013) Long prereproductive selection and divergence by depth in a Caribbean candelabrum coral. *Proceedings of the National Academy of Sciences of the United States of America* 110, 3961-3966.

Pritchard JK, Stephens M, Donnelly P (2000) Inference of population structure using multilocus genotype data. *Genetics* 155, 945-959.

Raymond M, Rousset F (1995) Genepop (Version-1.2) – Population genetics software for exact tests and ecumenicism. *Journal of Heredity*, 86, 248–249.

Reed JK (1985) Deepest distribution of Atlantic hermatypic corals discovered in the Bahamas. *Proceedings of the Fifth International Coral Reef Symposium* 6, 249–254

Rezak, R., Bright, T.J., McGrail, D.W., 1985. Reefs and banks of the northwestern Gulf of Mexico: Their geological, biological, and physical dynamics. John Wiley and Sons, Inc., New York, NY. 259 pp.

Richmond RH (1987) Energetics, competence, and long-distance dispersal of planula larvae of the coral *Pocillopora damicornis*. *Marine Biology* 93, 527-533.

Riegl B, Piller WE (2003) Possible refugia for reefs in times of environmental stress. *International Journal of Earth Sciences* 92, 520-531.

Rosenberg NA (2004) DISTRUCT: a program for the graphical display of population structure. *Molecular Ecology Notes* 4, 137-138.

Rousset F, Raymond M (1995) Testing heterozygote excess and deficiency. *Genetics* 140, 1413-1419.

Rowan R, Knowlton N (1995) Intraspecific diversity and ecological zonation in coral algal symbiosis. *Proceedings of the National Academy of Sciences of the United States of America* 92, 2850-2853.

Rowan R, Powers DA (1991) Molecular genetic identification of symbiotic dinoflagellates (zooxanthellae). *Marine Ecology Progress Series*, 71, 65-73.

Sale PF, Cowen RK, Danilowicz BS, et al. (2005) Critical science gaps impede use of no-take fishery reserves. *Trends in Ecology & Evolution* 20, 74-80.

- Sampayo EM, Franceschinis L, Hoegh-Guldberg O, Dove S (2007) Niche partitioning of closely related symbiotic dinoflagellates. *Molecular Ecology*, 16, 3721-3733.
- Selkoe KA, Henzler CM, Gaines SD (2008) Seascape genetics and the spatial ecology of marine populations. *Fish and Fisheries* 9, 363-377.
- Severance EG, Karl SA (2006) Contrasting population genetic structures of sympatric, mass-spawning Caribbean corals. *Marine Biology* 150, 57-68.
- Shearer TL, Coffroth MA (2004) Isolation of microsatellite loci from the scleractinian corals, *Montastraea cavernosa* and *Porites astreoides*. *Molecular Ecology Notes* 4, 435-437.
- Shearer TL, Gutierrez-Rodriguez C, Coffroth MA (2005) Generating molecular markers from zooxanthellate cnidarians. *Coral Reefs* 24, 57-66.
- Slatkin M (2005) Seeing ghosts: the effect of unsampled populations on migration rates estimated for sampled populations. *Molecular Ecology* 14, 67-73.
- Slattery M, Lesser MP, Brazeau D, Stokes MD, Leichter JJ (2011) Connectivity and stability of mesophotic coral reefs. *Journal of Experimental Marine Biology and Ecology* 408, 32-41.
- Silverstein RN, Correa AMS, Baker AC (2012) Specificity is rarely absolute in coral-algal symbiosis: implications for coral response to climate change. *Proceedings of the Royal Society B-Biological Sciences* 279, 2609-2618.
- Smith TB, Blondeau J, Nemeth RS et al. (2010) Benthic structure and cryptic mortality in a Caribbean mesophotic coral reef bank system, the Hind Bank Marine Conservation District, US Virgin Islands. *Coral Reefs*, 29, 289-308.
- Strimmer K (2008) fdrtool: a versatile R package for estimating local and tail area-based false discovery rates. *Bioinformatics* 24, 1461-1462.
- Szmant AM (1986) Reproductive ecology of Caribbean reef corals. *Coral Reefs* 5, 43-53.
- Untergrasser A, Cutcutache I, Koressaar T, Ye J, Faircloth BC, Remm M, Rozen SG (2012) Primer3 - new capabilities and interfaces. *Nucleic Acids Research*, 40(15):e115
- van Oppen MJH, Bongaerts P, Underwood JN, Peplow LM, Cooper TF (2011) The role of deep reefs in shallow reef recovery: an assessment of vertical connectivity in a brooding coral from west and east Australia. *Molecular Ecology* 20, 1647-1660.
- van Oppen MJH, Woerheide G, Takabayashi M (2000) Nuclear markers in evolutionary and population genetic studies of scleractinian corals and sponges. *Proceedings 9th International Coral Reef Symposium 1*: 131-138

- Vera JC, Wheat CW, Fescemyer HW, et al. (2008) Rapid transcriptome characterization for a nonmodel organism using 454 pyrosequencing. *Molecular Ecology* 17, 1636-1647.
- Vermeij MJA (2005) Substrate composition and adult distribution determine recruitment patterns in a Caribbean brooding coral. *Marine Ecology Progress Series* 295, 123-133.
- Veron JEN (2000) Corals of the world. Volume 3. Australian Institute of Marine Science, Townsville.
- Villinski JT (2003) Depth-independent reproductive characteristics for the Caribbean reef-building coral *Montastraea faveolata*. *Marine Biology*, 142, 1043-1053.
- Vize PD (2006) Deepwater broadcast spawning by *Montastraea cavernosa*, *Montastraea franksi*, and *Diploria strigosa* at the Flower Garden Banks, Gulf of Mexico. *Coral Reefs* 25, 169-171.
- Vollmer SV, Palumbi SR (2007) Restricted gene flow in the Caribbean staghorn coral *Acropora cervicomis*: implications for the recovery of endangered reefs. *Journal of Heredity* 98, 40-50.
- Warner ME, LaJeunesse TC, Robison JD, Thur RM (2006) The ecological distribution and comparative photobiology of symbiotic dinoflagellates from reef corals in Belize: potential implications for coral bleaching. *Limnology and Oceanography* 51, 1887-1897.
- Waser PM, Strobeck C (1998) Genetic signatures of interpopulation dispersal. *Trends in Ecology & Evolution* 13, 43-44.
- Weil E (1993) Genetic and morphological variation in Caribbean and eastern Pacific Porites (Anthozoa, Scleractinia). Preliminary results. *Proceedings of the Seventh International Coral Reef Symposium* 2, 643-656.
- Werner FE, Cowen RK, Paris CB (2007) Coupled biological and physical models present capabilities and necessary developments for future studies of population connectivity. *Oceanography* 20, 54-69.
- West JM, Salm RV (2003) Resistance and resilience to coral bleaching: implications for coral reef conservation and management. *Conservation Biology*, 17, 956-967.
- Wheat C (2008) Rapidly developing functional genomics in ecological model systems via 454 transcriptome sequencing. *Genetica* doi 0.1007/s10709-008-9326-y
- Wilson JR, Harrison PL (1998) Settlement-competency periods of larvae of three species of scleractinian corals. *Marine Biology* 131, 339-345.

Appendices

Appendix 2.1. Summary of statistics per locus and population for *Montastraea cavernosa*. N = number of samples genotyped, N_a = number of alleles, H_o = observed heterozygosity, H_e = expected heterozygosity, P_{hwe} = p value for tests of Hardy Weinberg Equilibrium. Five out of 135 comparisons are significant after FDR-correction (highlighted in bold). USVI= U.S. Virgin Islands

Region	Sub region	Depth		Locus								
				MC4	MC18	MC29	MC41	MC46	MC49	MC65	MC97	MC114
Florida	Upper Keys	shallow	N	71	76	73	73	68	63	76	76	75
			Na	29	11	9	11	3	11	5	7	16
			Ho	0.922	0.817	0.747	0.684	0.375	0.594	0.402	0.707	0.889
			He	0.925	0.866	0.765	0.769	0.413	0.590	0.390	0.669	0.906
			Phwe	0.310	0.447	0.598	0.009	0.147	0.202	0.238	0.574	0.044
		mid	N	29	29	30	29	29	22	30	30	27
			Na	16	10	9	7	3	10	3	5	12
			Ho	0.793	0.586	0.700	0.448	0.138	0.636	0.267	0.633	0.926
			He	0.915	0.879	0.697	0.714	0.132	0.836	0.442	0.606	0.867
			Phwe	0.010	0.001	0.097	0.000	1.000	0.079	0.016	0.232	0.527
	deep	N	22	22	22	21	22	22	22	23	23	
		Na	20	9	8	5	2	15	4	6	11	
		Ho	0.818	0.636	0.591	0.619	0.091	0.727	0.045	0.739	0.739	
		He	0.937	0.838	0.723	0.692	0.169	0.918	0.215	0.739	0.862	
		Phwe	0.143	0.033	0.004	0.083	0.138	0.003	0.001	0.014	0.033	
	Lower Keys	shallow	N	27	27	27	26	27	19	22	27	27
			Na	18	9	7	9	4	7	4	6	15
			Ho	0.926	0.889	0.667	0.731	0.407	0.737	0.636	0.704	0.926
			He	0.917	0.853	0.779	0.764	0.470	0.640	0.538	0.676	0.917
			Phwe	0.776	0.998	0.038	0.157	0.574	1.000	0.017	0.095	0.948
mid		N	39	35	38	38	38	31	38	38	39	

		Na	27	7	8	8	4	13	4	5	16
		Ho	0.923	0.514	0.868	0.474	0.211	0.677	0.421	0.579	0.846
		He	0.951	0.834	0.807	0.584	0.238	0.853	0.416	0.642	0.869
		Phwe	0.804	0.000	0.587	0.029	0.496	0.002	1.000	0.318	0.647
	deep	N	30	30	30	28	26	28	30	29	30
		Na	21	8	8	4	4	10	4	6	12
		Ho	0.933	0.600	0.867	0.464	0.269	0.929	0.500	0.724	0.933
		He	0.934	0.840	0.831	0.440	0.250	0.843	0.397	0.683	0.873
		Phwe	0.015	0.004	0.293	0.579	1.000	0.622	0.581	0.358	0.863
	shallow	N	37	38	37	28	36	25	38	37	38
		Na	21	9	8	9	3	7	5	6	15
		Ho	0.919	0.816	0.757	0.786	0.444	0.680	0.500	0.649	0.895
		He	0.932	0.862	0.787	0.830	0.487	0.682	0.451	0.622	0.914
		Phwe	0.295	0.333	0.293	0.129	0.623	0.442	0.842	0.914	0.760
	mid	N	31	31	31	26	30	25	29	31	31
		Na	23	11	9	6	4	11	5	6	15
		Ho	0.935	0.742	0.742	0.615	0.233	0.680	0.828	0.548	0.968
		He	0.941	0.874	0.759	0.754	0.268	0.856	0.578	0.695	0.921
		Phwe	0.879	0.052	0.794	0.606	0.510	0.050	0.028	0.081	0.514
	deep	N	42	43	44	44	44	44	44	44	43
		Na	26	10	7	9	5	16	6	6	15
		Ho	0.786	0.767	0.614	0.682	0.341	0.864	0.455	0.773	0.907
		He	0.928	0.868	0.760	0.759	0.348	0.830	0.440	0.726	0.901
		Phwe	0.026	0.287	0.111	0.046	0.409	0.129	0.649	0.967	0.632
Bermuda	shallow	N	42	42	47	45	48	42	48	38	48
		Na	20	9	7	7	4	7	3	5	16
		Ho	0.857	0.810	0.638	0.644	0.375	0.690	0.063	0.500	0.854

USVI	mid	He	0.932	0.849	0.653	0.801	0.321	0.669	0.062	0.526	0.907
		Phwe	0.329	0.497	0.876	0.275	0.789	0.841	1.000	0.497	0.053
		N	39	43	43	42	43	39	43	41	41
		Na	20	11	8	6	4	8	2	5	13
	deep	Ho	0.949	0.791	0.698	0.714	0.465	0.590	0.023	0.512	0.951
		He	0.914	0.874	0.636	0.792	0.388	0.689	0.023	0.565	0.879
		Phwe	0.939	0.026	0.907	0.536	0.649	0.389	1.000	0.052	0.451
		N	41	44	45	40	44	38	45	43	44
	shallow	Na	21	10	8	6	6	10	2	5	14
		Ho	0.951	0.841	0.556	0.575	0.318	0.632	0.200	0.512	0.909
		He	0.927	0.858	0.641	0.787	0.323	0.698	0.217	0.555	0.896
		Phwe	0.721	0.297	0.199	0.037	0.423	0.179	0.499	0.164	0.194
	mid	N	39	39	42	42	40	41	42	41	39
		Na	29	12	7	9	3	9	2	5	16
		Ho	0.795	0.692	0.714	0.738	0.425	0.488	0.310	0.634	0.846
		He	0.939	0.867	0.736	0.706	0.404	0.621	0.327	0.662	0.876
	deep	Phwe	0.045	0.014	0.732	0.425	1.000	0.039	0.658	0.653	0.348
		N	11	12	12	10	11	11	12	12	5
		Na	13	8	6	4	3	8	3	5	8
		Ho	0.909	0.500	0.750	0.900	0.455	0.545	0.333	0.667	1.000
	deep	He	0.948	0.862	0.743	0.700	0.498	0.818	0.301	0.547	0.956
		Phwe	0.603	0.029	0.769	0.672	1.000	0.055	1.000	1.000	1.000
		N	47	49	49	49	48	48	49	48	49
		Na	30	12	9	9	4	12	4	6	15
deep	Ho	0.894	0.735	0.633	0.694	0.417	0.625	0.347	0.604	0.878	
	He	0.955	0.881	0.750	0.797	0.393	0.688	0.350	0.654	0.900	
	Phwe	0.161	0.035	0.142	0.760	1.000	0.092	0.797	0.424	0.111	

Appendix 2.2. Mean null alleles and inbreeding coefficient per locus and population for *Montastraea cavernosa*. USVI= U.S. Virgin Islands

Region	Sub region	Depth	Mean null allele frequency									Fi		
			MC4	MC18	MC29	MC41	MC46	MC49	MC65	MC97	MC114	Mean	Lower CI	Upper CI
Florida	Upper Keys	shallow	0.01	0.03	0.03	0.07	0.09	0.03	0.03	0.02	0.03	0.00	0.00	0.03
		mid	0.09	0.19	0.05	0.20	0.15	0.20	0.15	0.06	0.03	0.01	0.00	0.09
		deep	0.09	0.15	0.10	0.13	0.22	0.13	0.27	0.07	0.06	0.04	0.00	0.21
	Lower Keys	shallow	0.03	0.03	0.08	0.08	0.09	0.05	0.10	0.05	0.03	0.01	0.00	0.05
		mid	0.03	0.27	0.03	0.13	0.13	0.13	0.09	0.10	0.03	0.01	0.00	0.07
		deep	0.03	0.14	0.03	0.12	0.19	0.03	0.04	0.06	0.03	0.01	0.00	0.05
	Dry Tortugas	shallow	0.04	0.04	0.05	0.07	0.13	0.06	0.04	0.05	0.03	0.01	0.00	0.08
		mid	0.03	0.08	0.04	0.17	0.15	0.18	0.03	0.10	0.02	0.01	0.00	0.05
		deep	0.10	0.09	0.09	0.05	0.06	0.02	0.04	0.03	0.03	0.01	0.00	0.05
Bermuda	shallow	0.05	0.04	0.05	0.12	0.04	0.04	0.08	0.09	0.04	0.01	0.00	0.06	
	mid	0.02	0.06	0.03	0.07	0.03	0.12	0.09	0.12	0.02	0.01	0.00	0.04	
	deep	0.02	0.04	0.06	0.19	0.09	0.08	0.07	0.08	0.03	0.01	0.00	0.06	
USVI	shallow	0.11	0.15	0.04	0.03	0.09	0.12	0.07	0.06	0.05	0.01	0.00	0.06	
	mid	0.10	0.21	0.07	0.09	0.20	0.23	0.11	0.07	0.14	0.02	0.00	0.09	
	deep	0.05	0.07	0.07	0.06	0.07	0.06	0.05	0.07	0.03	0.00	0.00	0.03	

Appendix 2.3. *Symbiodinium* types identified in figure 5 and corresponding GenBank accession numbers for the ITS-2 marker.

<i>Symbiodinium</i> taxa	GenBank accession number
C3	FN298467
D1a	AF499802
B1	FJ811928

Appendix 3.1. Summary of statistics per locus and population for *Porites astreoides*. N = number of samples genotyped, N_a = number of alleles, H_o = observed heterozygosity, H_e = expected heterozygosity, P_{hwe} = p value for tests of Hardy Weinberg Equilibrium. Seven out of 120 comparisons are significant after FDR-correction (highlighted in bold). USVI= U.S. Virgin Islands

Region	Sub region	Depth		Locus									
				PA3	PA7	PA13	PA69	Past_3	Past_16	Past_17	Past_21		
Florida	Upper Keys	shallow	N	67	98	81	89	80	99	93	93		
			Na	8	6	11	16	4	3	5	7		
			Ho	0.808	0.692	0.862	0.853	0.512	0.524	0.570	0.420		
					He	0.799	0.767	0.877	0.867	0.461	0.407	0.551	0.397
					Phwe	0.033	0.003	0.003	0.000	0.210	0.000	0.042	0.726
			mid	N	50	64	60	65	55	64	56	64	
		Na		9	5	10	12	4	2	4	6		
		Ho		0.765	0.662	0.967	0.909	0.536	0.169	0.825	0.492		
				He	0.798	0.679	0.875	0.879	0.530	0.156	0.703	0.460	
				Phwe	0.636	0.497	0.010	0.012	1.000	1.000	0.029	0.286	
		deep	N	19	24	24	24	22	24	19	24		
	Na		7	4	9	13	2	2	4	5			
	Ho		0.850	0.800	0.720	0.840	0.652	0.160	0.800	0.600			
				He	0.728	0.722	0.845	0.863	0.449	0.216	0.632	0.519	
				Phwe	0.224	0.503	0.003	0.063	0.050	0.287	0.078	0.649	
		Lower Keys	shallow	N	39	43	42	43	39	44	43	40	
	Na			6	5	11	15	3	2	6	6		
Ho	0.744			0.767	0.810	0.930	0.487	0.432	0.535	0.475			
				He	0.771	0.720	0.768	0.906	0.541	0.342	0.594	0.428	
				Phwe	0.259	0.484	0.692	0.690	0.250	0.170	0.001	0.843	
	mid		N	27	32	28	27	31	32	32	30		
Na		7	4	10	9	3	2	6	5				

		Ho	0.815	0.469	0.643	0.889	0.581	0.250	0.719	0.567
		He	0.797	0.613	0.863	0.863	0.497	0.222	0.736	0.499
		Phwe	0.466	0.129	0.019	0.135	0.493	1.000	0.269	0.944
	deep	N	34	33	31	32	32	35	33	30
		Na	7	5	11	14	2	3	5	5
		Ho	0.882	0.727	0.742	0.969	0.406	0.286	0.667	0.533
		He	0.729	0.613	0.879	0.905	0.484	0.252	0.592	0.531
		Phwe	0.989	0.730	0.002	0.418	0.463	1.000	0.820	0.562
Dry Tortugas	shallow	N	35	39	38	25	39	40	28	39
		Na	6	5	11	13	3	2	4	5
		Ho	0.730	0.683	0.825	0.963	0.610	0.595	0.767	0.561
		He	0.722	0.784	0.803	0.882	0.554	0.506	0.661	0.450
		Phwe	0.259	0.002	0.000	0.000	0.887	0.353	0.171	0.026
	mid	N	26	25	23	26	25	25	22	22
		Na	6	5	8	11	3	2	3	5
		Ho	0.815	0.808	0.500	0.963	0.538	0.462	0.304	0.522
		He	0.788	0.711	0.798	0.832	0.480	0.434	0.329	0.466
		Phwe	0.062	0.482	0.000	0.085	0.594	1.000	0.618	0.510
	deep	N	36	38	38	36	37	39	37	39
		Na	8	5	11	13	3	2	4	5
		Ho	0.972	0.895	0.842	0.861	0.514	0.410	0.730	0.641
		He	0.829	0.726	0.859	0.874	0.505	0.330	0.690	0.566
		Phwe	0.437	0.191	0.001	0.001	1.000	0.314	0.306	0.881
Bermuda	shallow	N	31	31	31	35	40	41	40	34
		Na	6	5	8	13	2	2	3	5
		Ho	0.939	0.788	0.879	0.838	0.452	0.209	0.476	0.722
		He	0.777	0.721	0.715	0.864	0.441	0.226	0.373	0.641
		Phwe	0.005	0.044	0.083	0.000	1.000	0.519	0.150	0.161

USVI	mid	N	27	30	26	26	28	30	29	24
		Na	6	5	6	5	3	2	3	5
		Ho	0.892	0.725	0.833	0.889	0.632	0.450	0.051	0.647
		He	0.765	0.704	0.766	0.716	0.525	0.353	0.051	0.660
		Phwe	0.030	0.242	0.043	0.329	0.190	0.164	1.000	0.583
	deep	N	15	18	17	16	14	17	18	17
		Na	5	4	4	5	2	2	4	4
		Ho	0.824	0.700	0.789	0.722	0.500	0.368	0.150	0.737
		He	0.759	0.619	0.721	0.703	0.444	0.309	0.146	0.706
		Phwe	0.669	0.087	0.203	0.914	1.000	1.000	1.000	0.518
	shallow	N	38	40	40	40	35	39	35	35
		Na	9	5	10	17	3	3	5	6
		Ho	0.925	0.762	0.810	0.881	0.351	0.293	0.730	0.568
		He	0.814	0.680	0.838	0.894	0.378	0.338	0.699	0.586
		Phwe	0.445	0.446	0.001	0.102	0.550	0.143	0.369	0.685
	mid	N	12	12	10	12	12	12	11	12
		Na	7	4	6	8	3	2	5	3
		Ho	0.750	0.833	0.900	0.750	0.333	0.667	0.636	0.500
		He	0.804	0.634	0.842	0.841	0.598	0.464	0.615	0.453
		Phwe	0.391	0.478	0.252	0.101	0.100	0.216	0.241	0.341
deep	N	40	38	39	35	41	43	39	41	
	Na	9	5	9	14	3	3	6	5	
	Ho	0.875	0.526	0.795	0.829	0.561	0.395	0.590	0.341	
	He	0.762	0.552	0.854	0.925	0.539	0.353	0.654	0.304	
	Phwe	0.140	0.159	0.002	0.000	1.000	0.729	0.221	1.000	

Appendix 3.2. Mean null alleles and inbreeding coefficient per locus and population for *Porites astreoides*. USVI= U.S. Virgin Islands

Region	Sub region	Depth	Mean null allele frequency								Fi		
			PA3	PA7	PA13	PA69	Past_3	Past_16	Past_17	Past_21	Mean	Lower CI	Upper CI
Florida	Upper Keys	shallow	0.03	0.02	0.02	0.02	0.02	0.04	0.02	0.03	0.00	0.00	0.02
		mid	0.04	0.05	0.02	0.03	0.03	0.04	0.01	0.01	0.00	0.00	0.02
		deep	0.04	0.14	0.04	0.04	0.04	0.04	0.08	0.04	0.01	0.00	0.04
	Lower Keys	shallow	0.07	0.04	0.07	0.04	0.05	0.04	0.03	0.02	0.01	0.00	0.05
		mid	0.05	0.07	0.04	0.04	0.04	0.10	0.12	0.04	0.01	0.00	0.06
		deep	0.09	0.06	0.03	0.06	0.02	0.03	0.09	0.02	0.01	0.00	0.04
	Dry Tortugas	shallow	0.03	0.04	0.03	0.03	0.04	0.08	0.05	0.03	0.01	0.00	0.03
		mid	0.06	0.07	0.10	0.05	0.06	0.04	0.18	0.02	0.01	0.00	0.04
		deep	0.06	0.04	0.04	0.04	0.02	0.02	0.04	0.03	0.01	0.00	0.03
Bermuda	shallow	0.05	0.08	0.04	0.03	0.02	0.05	0.02	0.03	0.01	0.00	0.04	
	mid	0.00	0.00	0.00	0.00	0.00	0.01	0.00	0.00	0.00	0.00	0.03	
	deep	0.09	0.08	0.11	0.06	0.05	0.05	0.05	0.07	0.01	0.00	0.06	
USVI	shallow	0.02	0.03	0.00	0.00	0.00	0.00	0.00	0.00	0.01	0.00	0.03	
	mid	0.19	0.07	0.09	0.10	0.09	0.06	0.07	0.08	0.01	0.00	0.08	
	deep	0.05	0.05	0.07	0.05	0.02	0.06	0.06	0.06	0.01	0.00	0.05	

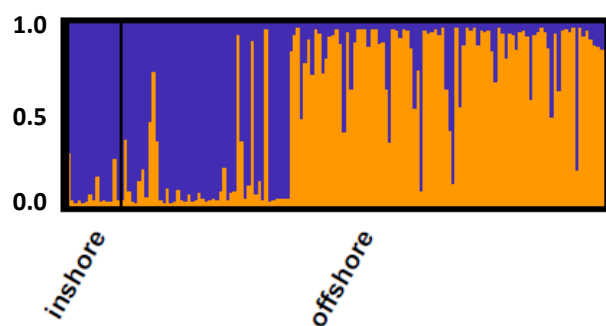
Appendix 3.3. *Porites astreoides* pairwise F_{ST} values of sites from the Upper Keys (Florida), designated as either inshore [shallow (≤ 10 m)] or offshore [shallow (≤ 10 m), mid (15-20 m) or deep (≥ 25 m)]. Sites UK6 and UK7 were considered inshore sites, whereas sites UK3, UK5, UK9 and UK10-16 were considered offshore sites (site names and GPS locations are given in Table 3.2). Statistically significant values ($p = 0.05$) after FDR correction are highlighted in bold.

Designation	Site	UK6	UK7	UK3	UK5	UK9	UK10	UK11	UK12	UK13	UK14	UK16
inshore shallow	UK6	0.000										
inshore shallow	UK7	0.035	0.000									
offshore shallow	UK3	0.000	0.067	0.000								
offshore shallow	UK5	0.046	0.034	0.017	0.000							
offshore shallow	UK9	0.041	0.030	0.037	0.007	0.000						
offshore mid	UK10	0.133	0.111	0.093	0.068	0.036	0.000					
offshore mid	UK11	0.084	0.101	0.046	0.048	0.027	0.016	0.000				
offshore mid	UK12	0.101	0.115	0.080	0.073	0.040	0.019	0.000	0.000			
offshore deep	UK13	0.137	0.123	0.100	0.086	0.051	0.022	0.005	0.008	0.000		
offshore deep	UK14	0.036	0.084	0.020	0.028	0.008	0.000	0.000	0.000	0.000	0.000	
offshore deep	UK16	0.236	0.237	0.171	0.181	0.145	0.116	0.123	0.096	0.112	0.111	0.000

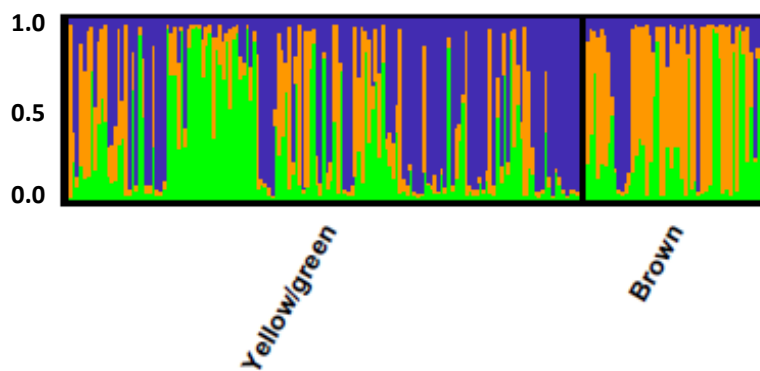
Appendix 3.4. *Symbiodinium* types identified in figure 3.6A and corresponding GenBank accession numbers for the ITS-2 marker.

<i>Symbiodinium</i> taxa	GenBank accession numbers
A4/A4a	EU449033/EU449040
C1	JQ180021
D1a	AF499802
B1	FJ811928

Appendix 3.5. *Porites astreoides* population structure of individuals from the Upper Keys (Florida), designated as either inshore [shallow (≤ 10 m)] or offshore [shallow (≤ 10 m), mid (15-20 m) or deep (≥ 25 m)]. Sites UK6 and UK7 were considered inshore sites, whereas sites UK3, UK5, UK9 and UK10-16 were considered offshore sites (site names and GPS locations are given in Table 3.2). Bar graphs show the average probability of membership (y-axis) of individuals ($n = 152$, x-axis) in $K = 2$ clusters as identified by STRUCTURE.



Appendix 3.6. *Porites astreoides* population structure by color morph (yellow/green or brown). Bar graphs show the average probability of membership (y-axis) of individuals ($n = 200$, x-axis) in $K = 3$ clusters as identified by STRUCTURE.



Appendix 4.1. Summary of statistics per locus and population for *Montastraea cavernosa*. N = number of samples genotyped, N_a = number of alleles, H_o = observed heterozygosity, H_e = expected heterozygosity, P_{hwe} = p value for tests of Hardy Weinberg Equilibrium. Seven out of 90 comparisons are significant after FDR-correction (highlighted in bold). FGB = Flower Garden Banks

Region	Sub region	Depth		Locus								
				MC4	MC18	MC29	MC41	MC46	MC49	MC65	MC97	MC114
FL	Upper Keys	shallow	N	71	76	73	73	68	63	76	76	75
			Na	29	11	9	11	3	11	5	7	16
			Ho	0.922	0.817	0.747	0.684	0.375	0.594	0.402	0.707	0.889
			He	0.925	0.866	0.765	0.769	0.413	0.590	0.390	0.669	0.906
			Phwe	0.310	0.447	0.598	0.009	0.147	0.202	0.238	0.574	0.044
		mid	N	29	29	30	29	29	22	30	30	27
			Na	16	10	9	7	3	10	3	5	12
			Ho	0.793	0.586	0.700	0.448	0.138	0.636	0.267	0.633	0.926
			He	0.915	0.879	0.697	0.714	0.132	0.836	0.442	0.606	0.867
			Phwe	0.010	0.001	0.097	0.000	1.000	0.079	0.016	0.232	0.527
	deep	N	22	22	22	21	22	22	22	23	23	
		Na	20	9	8	5	2	15	4	6	11	
		Ho	0.818	0.636	0.591	0.619	0.091	0.727	0.045	0.739	0.739	
		He	0.937	0.838	0.723	0.692	0.169	0.918	0.215	0.739	0.862	
		Phwe	0.143	0.033	0.004	0.083	0.138	0.003	0.001	0.014	0.033	
	Lower Keys	shallow	N	27	27	27	26	27	19	22	27	27
			Na	18	9	7	9	4	7	4	6	15
			Ho	0.926	0.889	0.667	0.731	0.407	0.737	0.636	0.704	0.926
			He	0.917	0.853	0.779	0.764	0.470	0.640	0.538	0.676	0.917
			Phwe	0.776	0.998	0.038	0.157	0.574	1.000	0.017	0.095	0.948
mid		N	39	35	38	38	38	31	38	38	39	
		Na	27	7	8	8	4	13	4	5	16	
		Ho	0.923	0.514	0.868	0.474	0.211	0.677	0.421	0.579	0.846	

		He	0.951	0.834	0.807	0.584	0.238	0.853	0.416	0.642	0.869
		Phwe	0.804	0.000	0.587	0.029	0.496	0.002	1.000	0.318	0.647
	deep	N	30	30	30	28	26	28	30	29	30
		Na	21	8	8	4	4	10	4	6	12
		Ho	0.933	0.600	0.867	0.464	0.269	0.929	0.500	0.724	0.933
		He	0.934	0.840	0.831	0.440	0.250	0.843	0.397	0.683	0.873
		Phwe	0.015	0.004	0.293	0.579	1.000	0.622	0.581	0.358	0.863
Dry Tortugas	shallow	N	37	38	37	28	36	25	38	37	38
		Na	21	9	8	9	3	7	5	6	15
		Ho	0.919	0.816	0.757	0.786	0.444	0.680	0.500	0.649	0.895
		He	0.932	0.862	0.787	0.830	0.487	0.682	0.451	0.622	0.914
		Phwe	0.295	0.333	0.293	0.129	0.623	0.442	0.842	0.914	0.760
	mid	N	31	31	31	26	30	25	29	31	31
		Na	23	11	9	6	4	11	5	6	15
		Ho	0.935	0.742	0.742	0.615	0.233	0.680	0.828	0.548	0.968
		He	0.941	0.874	0.759	0.754	0.268	0.856	0.578	0.695	0.921
		Phwe	0.879	0.052	0.794	0.606	0.510	0.050	0.028	0.081	0.514
	deep	N	42	43	44	44	44	44	44	44	43
		Na	26	10	7	9	5	16	6	6	15
		Ho	0.786	0.767	0.614	0.682	0.341	0.864	0.455	0.773	0.907
		He	0.928	0.868	0.760	0.759	0.348	0.830	0.440	0.726	0.901
		Phwe	0.026	0.287	0.111	0.046	0.409	0.129	0.649	0.967	0.632
FGB	deep	N	22	22	21	16	21	5	23	21	23
		Na	14	7	6	5	4	3	4	4	11
		Ho	0.773	0.409	0.476	0.438	0.476	0.200	0.391	0.381	0.739
		He	0.900	0.752	0.681	0.700	0.408	0.600	0.370	0.575	0.871
		Phwe	0.211	0.001	0.105	0.002	1.000	0.048	0.497	0.024	0.019

Appendix 4.2. Summary of statistics per locus and population for *Porites astreoides*. N = number of samples genotyped, N_a = number of alleles, H_o = observed heterozygosity, H_e = expected heterozygosity, P_{hwe} = p value for tests of Hardy Weinberg Equilibrium. Five out of 80 comparisons are significant after FDR-correction (highlighted in bold). FGB = Flower Garden Banks

Region	Sub region	Depth		Locus							
				PA3	PA7	PA13	PA69	Past_3	Past_16	Past_17	Past_21
Florida	Upper Keys	shallow	N	67	98	81	89	80	99	93	93
			Na	8	6	11	16	4	3	5	7
			Ho	0.808	0.692	0.862	0.853	0.512	0.524	0.570	0.420
			He	0.799	0.767	0.877	0.867	0.461	0.407	0.551	0.397
		Phwe	0.033	0.003	0.003	0.000	0.210	0.000	0.042	0.726	
		mid	N	50	64	60	65	55	64	56	64
			Na	9	5	10	12	4	2	4	6
			Ho	0.765	0.662	0.967	0.909	0.536	0.169	0.825	0.492
			He	0.798	0.679	0.875	0.879	0.530	0.156	0.703	0.460
		Phwe	0.636	0.497	0.010	0.012	1.000	1.000	0.029	0.286	
		deep	N	19	24	24	24	22	24	19	24
			Na	7	4	9	13	2	2	4	5
	Ho		0.850	0.800	0.720	0.840	0.652	0.160	0.800	0.600	
	He		0.728	0.722	0.845	0.863	0.449	0.216	0.632	0.519	
	Phwe	0.224	0.503	0.003	0.063	0.050	0.287	0.078	0.649		
	Lower Keys	shallow	N	39	43	42	43	39	44	43	40
			Na	6	5	11	15	3	2	6	6
			Ho	0.744	0.767	0.810	0.930	0.487	0.432	0.535	0.475
			He	0.771	0.720	0.768	0.906	0.541	0.342	0.594	0.428
		Phwe	0.259	0.484	0.692	0.690	0.250	0.170	0.001	0.843	
mid		N	27	32	28	27	31	32	32	30	
		Na	7	4	10	9	3	2	6	5	
		Ho	0.815	0.469	0.643	0.889	0.581	0.250	0.719	0.567	
	He	0.797	0.613	0.863	0.863	0.497	0.222	0.736	0.499		

		Phwe	0.466	0.129	0.019	0.135	0.493	1.000	0.269	0.944	
	deep	N	34	33	31	32	32	35	33	30	
		Na	7	5	11	14	2	3	5	5	
		Ho	0.882	0.727	0.742	0.969	0.406	0.286	0.667	0.533	
		He	0.729	0.613	0.879	0.905	0.484	0.252	0.592	0.531	
		Phwe	0.989	0.730	0.002	0.418	0.463	1.000	0.820	0.562	
	Dry Tortugas	shallow	N	35	39	38	25	39	40	28	39
		Na	6	5	11	13	3	2	4	5	
		Ho	0.730	0.683	0.825	0.963	0.610	0.595	0.767	0.561	
		He	0.722	0.784	0.803	0.882	0.554	0.506	0.661	0.450	
		Phwe	0.259	0.002	0.000	0.000	0.887	0.353	0.171	0.026	
		mid	N	26	25	23	26	25	25	22	22
		Na	6	5	8	11	3	2	3	5	
		Ho	0.815	0.808	0.500	0.963	0.538	0.462	0.304	0.522	
		He	0.788	0.711	0.798	0.832	0.480	0.434	0.329	0.466	
		Phwe	0.062	0.482	0.000	0.085	0.594	1.000	0.618	0.510	
		deep	N	36	38	38	36	37	39	37	39
		Na	8	5	11	13	3	2	4	5	
		Ho	0.972	0.895	0.842	0.861	0.514	0.410	0.730	0.641	
		He	0.829	0.726	0.859	0.874	0.505	0.330	0.690	0.566	
		Phwe	0.437	0.191	0.001	0.001	1.000	0.314	0.306	0.881	
FGB		deep	N	19	20	19	14	20	21	20	18
		Na	5	3	5	7	3	2	4	4	
		Ho	0.684	0.950	0.895	0.857	0.900	0.810	0.800	0.611	
		He	0.595	0.617	0.630	0.728	0.559	0.512	0.568	0.640	
		Phwe	0.964	0.003	0.077	0.009	0.001	0.010	0.101	0.387	